Development of a consistent geochemical modelling approach for leaching and reactive transport processes in contaminated materials

Promotoren:

Prof. Dr. R. N. J. Comans

Hoogleraar Milieugeochemie, Wageningen Universiteit

Prof. Dr. W. H. van Riemsdijk

Hoogleraar Bodemscheikunde en Chemische Bodemkwaliteit, Wageningen Universiteit

Promotiecommissie:

Prof. Dr. T. H. Christensen (*Technical University of Denmark*)

Dr. C. A. Johnson (*EAWAG, Switzerland*)

Prof. Dr. A. A. Koelmans (*Wageningen Universiteit*)

Prof. Dr. P. C. de Ruiter (*Universiteit Utrecht*)

Dit onderzoek is uitgevoerd binnen de onderzoeksschool SENSE.

Development of a consistent geochemical modelling approach for leaching and reactive transport processes in contaminated materials

Joris J. Dijkstra

Contents

Chapter 1

General introduction

Background

Waste materials are increasingly being recycled as construction products instead of being landfilled. The recycling of waste materials into functional applications is beneficial from both an economical and environmental perspective, as it reduces the use of costly primary materials, while the need for space-consuming landfills and the associated long-term monitoring and aftercare is reduced. However, waste materials often contain increased levels of potentially toxic trace elements compared to natural materials such as soils. The potential environmental risk associated with the application of such waste materials in the environment (e.g., the application of incineration ashes in road bases or sound barriers) depends on many physical and chemical factors such as the application scenario (e.g., whether the material is exposed to rain- or groundwater), the contaminant concentration, its chemical form, toxicity, and ability to migrate towards vulnerable compartments such as soil and groundwater.

In many countries, the application of waste materials is regulated by environmental criteria that aim to ensure long-term environmental protection. These criteria are increasingly being based on the potential "leaching" of contaminants, i.e. the release of contaminants from the solid phase to the water phase with which the material may be in contact (e.g., percolating rainwater). The extent to which contaminants are susceptible for leaching processes depends strongly on the specific chemical form of the contaminant. Chemical "speciation" refers to the different chemical forms in which an element may be present, such as dissolved complexes, a mineral phase, or bound to reactive surfaces and colloids (e.g., (hydr)oxide surfaces, dissolved and particulate organic matter, clay minerals). In addition to chemical speciation, the mobility of contaminants in the environment is also a function of transport processes (convection, diffusion) and time-dependent processes such as reaction kinetics and slow changes of the geochemical properties of materials (weathering reactions). Therefore, in order to better understand the environmental risks associated with the application of waste materials in the environment, as well as to further develop environmental criteria and associated test methods, it is important to gain a fundamental understanding of the underlying chemical and physical processes that

control the leaching of contaminants as well as the fate of these contaminants in soil and groundwater.

The complexity of speciation and transport processes make that the identification of the major controlling processes responsible for observed leaching phenomena is generally not straightforward. However, hypotheses with respect to possibly involved processes can often be translated in (computer) models that simulate these processes. The verification of predictions made by such models against experimental data may lead to either confirmation or rejection of the underlying hypotheses. The latter may result in modification and/or expansion of the model, until the system is sufficiently understood and adequate model predictions are obtained. Used in this way, models form valuable instruments in the scientific process of gaining knowledge, and contribute to the identification of the dominant processes that control the behaviour of contaminants in the situation under study. Once a model incorporates the major identified processes, it may be used to make predictions on the (long-term) leaching behaviour of contaminated materials in specific environments.

Models to be used for the above described purposes may be either of a more empirical or more fundamental (mechanistic) nature. Although empirical models may satisfactorily describe a specific situation, e.g., by polynomial functions fitted to measurements, these models tend to become unreliable when they are applied to conditions beyond the measurement range. However, since fundamental processes on a molecular scale have a general validity across the wide variety in contaminated materials, application scenarios and environmental conditions, models that are based on these processes (hereafter referred to as "mechanistic" models) have a much wider applicability than empirical models.

Studying chemical processes that take place in the earth 's natural environment is part of the field of geochemistry, hence the term geochemical models refer to models that are constructed to simulate these processes. During the past decades, mechanistic geochemical models describing the different chemical interactions that elements may undergo in the natural environment (including soils, sediments, and the aquatic environment) have strongly developed. This development particularly includes models describing sorption processes to reactive surfaces that are commonly found in soils, such as natural organic matter and hydrous ferric oxides. For a number of these models, "generic" parameter sets have been derived that allow a general application of

these models with respect to different systems and/or conditions. The applicability of these mechanistic models therefore also extends to anthropogenically influenced materials/environments, such as contaminated (waste) materials.

Research over the past decades has shown that sorption processes to reactive surfaces have an important influence on the mobility of contaminants in various types of environments. An important challenge is therefore to investigate the possibility to combine the recently developed mechanistic (sub-) models and associated generic parameter sets to a more complete "multi-surface" geochemical model, capable of describing the dominant interactions that contaminants undergo in both natural and waste environments. These interactions include the formation of mineral phases, aqueous complexes, and interactions of elements with multiple reactive surfaces (e.g., metal (hydr)oxides, dissolved and particulate natural organic matter). Coupling such a comprehensive geochemical model with a model for transport processes (also referred to as "reactive transport") forms a potentially valuable instrument to describe the time- dependent leaching of contaminants from waste materials as well as their further rate of transport in soil and groundwater.

Due to the process- based character and expected wide applicability, a mechanistic geochemical modelling approach is believed to be a suitable instrument to address different important topics that relate to the application of waste materials in the environment. Among these are [i)] identification of the processes that control the leaching of contaminants from widely different materials under a variety of conditions; [ii)] prediction of contaminant leaching in (long-term field) leaching scenarios and the effect of soil and groundwater quality; [iii)] improved interpretation and further development of generally applicable regulatory leaching test methods; [iv)] development of technologies to improve the environmental quality of waste materials; [v)] development of realistic regulatory limits for the safe application of waste materials in the environment.

Aim and approach

The aim of this thesis is to develop a generally applicable, mechanistic geochemical modelling approach with which dynamic leaching and reactive transport processes in "contaminated materials" can be predicted. The term "contaminated materials"

ultimately refers to any natural or waste material that may potentially release contaminants by leaching. In this thesis, Municipal Solid Waste Incinerator (MSWI) bottom ash (see text box) and contaminated soils are studied as relevant and representative cases of such materials. This thesis focuses on the leaching of inorganic contaminants, although the principles of the approach do also apply to organic contaminants that fall beyond the scope of this work.

The approach consists of a number of successive steps. The first step consists of the identification of the (major) processes that control the leaching of contaminants from the material under study. In this step, geochemical model calculations are performed and compared to experimental data in order to verify hypotheses on the underlying leaching processes. As leached concentrations of elements generally vary by orders of magnitude as a function of pH, data generated by batch pH-static leaching experiments over a wide range of pH (e.g., pH 2 to pH 12) provide a sensitive verification of such hypotheses. Depending on the outcome of the verification, the model may need to be modified and/or further expanded with additional relevant processes, until the model calculations provide an adequate representation of the measurements. In the next step, the resulting geochemical model is coupled with a model for transport processes. Based on the processes identified in the previous step, the time- dependent leaching of contaminants in dynamic (reactive transport) systems is predicted and verified against experimental data from column experiments. Similar to the previous step, the verification of model predictions may lead to modification and/or further expansion of the reactive transport model. The ultimate goal of the approach is to use the resulting reactive transport model as the basis for predictions on contaminant leaching and transport in long-term field scenarios. The latter forms an indispensable step towards the assessment of the impact that contaminated materials may have on the environment, as well as towards the development of corresponding regulatory limits. Field-scale modelling and model verification is, however, beyond the scope of the present study.

The (long- term) predictive value of geochemical models strongly depends on the way the model is parameterized, i.e. with respect to the used thermodynamic parameters and estimates of material- specific properties/input parameters, such as the amount of reactive surfaces. The approach described in this thesis is, therefore, aiming for consistency between the hypothesized processes, the chosen (sorption)

Municipal Solid Waste Incinerator (MSWI) bottom ash

The bulk of the residue that remains after the incineration of municipal solid waste is generally referred to as "bottom ash", but is also called slag, grate ash or clinkers. The material is produced world-wide in very large and ever- increasing quantities. During incineration, the volume and weight of the parent material is reduced by about 90 and 60%, respectively, while at the same time electricity is produced from the heat generated by the incineration process. The bulk chemical composition of MSWI bottom ash is very different from that of a natural soil, as is illustrated by the figure below that compares the average elemental composition of both materials. For instance, bottom ash may contain about two to three orders of magnitude higher levels of heavy metals such as copper, cadmium, lead, and zinc. Other elements, such as silicon, are relatively depleted in MSWI bottom ash.
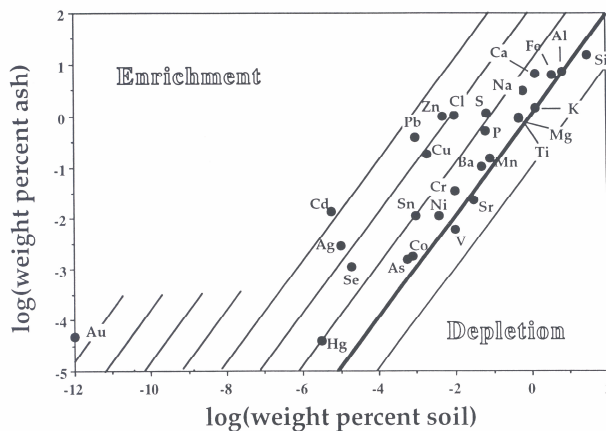

Figure: Double-log plot comparing weight percent of elements in an average soil and in MSWI bottom ash. The heavy line represents equal concentrations in both materials; upper lines represent order of magnitude enrichments. The more abundant the element, the closer the points are to the upper right corner. (Figure from Kirby & Rimstidt, 1993. Reprinted with permission, copyright 1993 American Chemical Society).

In many countries, utilization of MSWI bottom ash in construction works has emerged as a viable option as an alternative to landfilling. In the Netherlands, about 1,2 million tons of MSWI bottom ash was produced in 2004, which is almost completely re-used in construction works such as road embankments and sound barriers.

References and further reading:

Chandler, A.J., Eighmy, T.T., Hartlen, J., Hjelmar, O., Kosson, D.S., Sawell, S.E., Van der Sloot, H.A., Vehlow, J., 1997. Municipal solid waste incinerator residues. Elsevier Science B.V., Amsterdam, The Netherlands .

Vereniging Afvalbedrijven (http://www.verenigingafvalbedrijven.nl/)

Kirby, C. S., Rimstidt, J. D. Mineralogy and surface properties of municipal solid waste ash. *Environ. Sci. Technol*. 1993, 27, 652-660.

model to simulate these processes, necessary model input parameters and experimental methods to determine these parameters. Wherever sorption to a reactive surface is suspected to be an important process, mechanistic sorption models are selected, with a preference for models for which "generic" parameter sets have been derived. Although such generic parameter sets may not provide the best description of measurements for a particular system, these parameter sets are internally consistent and are therefore of a more general validity. In addition, when the purpose is to model complex (natural and waste) systems, there is a need for parameter sets that cover a broad range of major and trace elements in order to account for multi- component interactions. Examples of such interactions are competition between different elements for the (limited) sorption "sites" on reactive surfaces, as well as the formation of precipitates and soluble complexes.

In order to achieve a general validity of the modelling approach, the selected models and associated parameter sets are applied without modification, and only published thermodynamic and binding parameters are used (i.e. without parameter fitting). In this respect, it is important to note that not for all potentially important sorption processes, mechanistic sorption models and associated generic parameter sets are available. In those cases, it is attempted to derive the necessary sorption characteristics from those of similar reactive surfaces, for which this type of information is available. Whenever sorption models are taken into account for such reactive surfaces, information is needed on the amount of these surfaces present in the sample under study. To maintain consistency between the models and parameter sets, this information is collected using independent, carefully selected experimental procedures that aim to estimate the concentrations of the specific type of reactive surface of interest. Important reactive surfaces that are treated in this way include amorphous and crystalline iron- and aluminium (hydr)oxides, clays, and reactive fractions of dissolved and particulate organic matter (humic and fulvic acids).

Model predictions that aim to predict contaminant leaching over a range of relevant conditions (such as a certain range of pH values that can be met in field scenarios) require input of concentrations of contaminants that are active in mineral dissolution/precipitation and sorption processes. These concentrations are referred to in this thesis by the term "availability". The availability of an element of interest does not necessarily equate to the total concentration present in the sample, as part of the

total concentration of an element may be present in, for instance, inert glass phases or in solid phases that show extremely slow dissolution kinetics. Hence, assuming the total concentrations in the sample to be fully available may lead to overestimates of the leaching potential of materials. The approach followed in this thesis is, therefore, to estimate the availabilities of elements at conditions unfavourable for sorption (by low and/or high pH extracts for cations and anions, respectively) and/or when dissolution of common mineral phases is assumed complete. The conditions at which the "availability" is best estimated in different materials is critically evaluated throughout this thesis.

Outline of this thesis

The successive steps of the modelling approach as outlined above are reflected in the different chapters. The point of departure is described in **chapter 2**. For the case of weathered MSWI bottom ash, the at that time available knowledge of processes that control the leaching of contaminants in batch systems is used to predict experimental leaching data obtained from (dynamic) column experiments. This evaluation leads to the identification of potentially important processes on the basis of which the modelling approach can be further improved in the forthcoming chapters.

In **chapter 3**, it is investigated to what extent the batch modelling approach followed in the preceding chapter is also applicable to identify and describe the processes that control the pH-dependent leaching of the metals Ni, Cu, Zn, Cd and Pb from contaminated soils. As soils contain relatively high amounts of natural organic matter compared to MSWI bottom ash, the modelling approach used in the preceding chapter is extended with a model for the adsorption of ions to dissolved and particulate organic matter. The approach is also extended with a model for the non-specific sorption to clay surfaces.

In **chapter 4**, the leaching of a wide range of major and trace elements from MSWI bottom ash is studied as a function of equilibration time, over a wide range of pH under pH-controlled conditions. Based on recent insights and assumptions on the composition of dissolved organic carbon (DOC) in MSWI bottom ash leachates, a similar "multi-surface" geochemical modelling approach as developed in the preceding chapter for contaminated soils is used to improve the interpretation of MSWI bottom

ash leaching test results, and to investigate whether "equilibrium" is attained during the time scale of the batch pH-static leaching experiments.

Chapter 5 aims to provide a mechanistic insight into the beneficial effects of accelerated aging of MSWI bottom ash on the leaching of copper and molybdenum using the "multi-surface" geochemical modelling approach developed in the preceding chapters. Experimental observations and model calculations in literature and in the previous chapters have shown that the leaching of DOC is likely to be the key process responsible for the generally observed enhanced leaching of copper and possibly other metals. Therefore, a novel experimental method is used to characterize DOC quantitatively in terms of humic, fulvic and hydrophilic acids over a wide pH range in order to identify the processes controlling the solid/liquid partitioning of these reactive ligands and their role in the effects of aging on contaminant leaching. Based on the experimental and model results, a new approach is developed to model the pH-dependent leaching of fulvic acids from MSWI bottom ash.

In the final **chapter 6**, the insights and model developments of the preceding chapters are combined into a novel predictive modelling approach in which the leaching of a broad range of major and trace elements from MSWI bottom ash is predicted simultaneously, based on a single set of model input parameters. The approach is applicable to both batch and dynamic systems, as verified experimentally with data from pH-static and dynamic (column) experiments. To address the possible influence of non-equilibrium processes, the column experiments are operated at different flow velocities and with flow interruption periods. Novel aspects of this final chapter compared to the initial chapter 2 include the characterization of DOC in terms of its reactive components humic and fulvic acids as a function of liquid-to-solid ratio (L/S) and pH, the inclusion of mechanistic models that predict the binding of metals to these substances, the inclusion of a surface complexation model that predicts concentrations of fulvic acids, and the combination of these geochemical models with a model for non-equilibrium processes. Although the model predictions have strongly improved compared to those shown in chapter 2, a number of recommendations are made for further research and improvement of the modelling approach.

Chapter 2

Process identification and model development of contaminant transport in MSWI bottom ash

Abstract

In this work we investigate to what extent we are able to predict experimental data on column leaching of heavy metals from Municipal Solid Waste Incinerator (MSWI) bottom ash, using the current knowledge on processes controlling aqueous heavy metal concentrations in combination with a multicomponent reactive transport computer model. Heavy metal concentrations were modelled with a surface complexation model for metal sorption to (hydr)oxide minerals in the bottom ash matrix. For transport modelling it was necessary to simplify the sorption modelling approach. Therefore, we determined a minimal set of components and species that still provided an adequate description of the pH dependent heavy metal behaviour. The concentration levels of the heavy metals are generally predicted to within one order of magnitude. Discrepancies between the model and the data are caused by uncertainty in modelling parameters and a still insufficient description of the dynamics of macroelement leaching and pH. In general, the simulated leaching curves show much more abrupt changes than the measurements. This observation might be an indication of non-equilibrium. Processes that have to be taken into account for further model development are the influence of non-equilibrium effects and the facilitated transport of heavy metals by dissolved organic matter.

Introduction

MSWI Bottom ashes are considerably enriched in potentially toxic trace elements compared to average soils. The material, either re-used or disposed, can be qualified as a potential risk to the environment, depending on the availability of the contaminants for leaching. Modelling processes governing availability and transport of contaminants in waste materials is of importance for long-term environmental risk assessment and for improvement of waste management techniques.

Geochemical modelling has proven to be a useful tool to estimate the leaching potential of contaminants from waste materials (*1-5*). Leaching of major elements, such as Ca and S, is shown to be often controlled by the dissolution of common minerals (*1*), whereas in weathered materials, heavy metals such as Cd and Pb are presumably controlled by sorption to neoformed iron- and aluminium (hydr)oxides (*2, 3*). However, in field situations, the distribution of contaminants is both a function of the controlling geochemical process and physical transport processes. Therefore, the application of reactive transport modelling to natural and waste environments can be a valuable instrument in assessing the time dependent leaching potential of waste materials as well as the fate of contaminants in the environment after leaching.

In this work, we use a multicomponent reactive transport computer model to investigate to what extent we are able to predict experimental data on column leaching of heavy metals from MSWI bottom ash, using current knowledge on processes controlling heavy metal concentrations obtained from batch experiments (e.g*.,* Meima and Comans (*1-4*)). We use weathered and fresh MSWI bottom ash samples with stable pH values of around 8, which made our modelling problem less complex than it would be for highly alkaline materials.

We use batch pH-stat leaching data to verify that heavy metal concentrations as a function of pH can be described adequately with a surface complexation model for sorption to hydrous ferric oxide (HFO) and amorphous Al- (hydr)oxides, according to the approach of Meima and Comans (*2*). Some modification of this batch modelling approach was needed before it could be incorporated in a transport model. The modelling approach of Meima and Comans (*2*) requires the input of many (major) elements and transport numerical calculation times tend to become excessively large

the more components and species are involved in the transport calculation. Therefore, the next step in our approach was to determine the minimal set of components and species that would still provide an adequate description of the heavy metal behaviour. Also, such an analysis provides insight in the relative importance of the components and species considered. This resulted in a relatively simple model for the solution and surface chemistry, with which we could describe the pH dependent leaching of the heavy metals reasonably well. With this set of components and reactions we performed transport simulations and tested the model predictions with data from high-resolution column experiments.

Materials and methods

Used MSWI Bottom ash

MSWI bottom ash samples were collected from two different major MSWI plants in the Netherlands. Bottom ash sample 1 (BA1) was collected in 1994 and had been in open storage for 1.5 years. Leaching data (pH-stat) and modelling results of this sample have been described in previous publications (*1-4*) in which it was referred to as "1.5YR". Bottom ash sample 2 (BA2) was freshly produced and had been collected in 1996. This sample is atypical for a freshly produced MSWI bottom ash with respect to its low natural pH (7.8) and high redox potential (344 mV). The samples had been dried and sieved (not ground) and stored in closed vessels until usage. All experiments were conducted with < 2 mm sieved fractions.

X-ray diffraction analysis was performed using a Guinier de Wolff camera, using CuKα radiation, on finely ground sub samples of BA1 and BA2 to obtain independent information on the bulk mineralogical composition. Detected in both samples were quartz (SiO_2), calcite ($CaCO_3$) and Fe-oxide, probably magnetite (Fe_3O_4) and hematite (Fe_2O_3). Although Meima and Comans (*1*) found anhydrite ($CaSO_4$) in BA1 using a diffractometer, we could only detect the presence of anhydrite in the BA2 sample. Total concentrations of elements in the samples were determined on 300 mg subsamples (ground in an agate mortar) which were digested with concentrated $HNO_3/HClO_4$ (at 190 °C for 10 hours). The resulting solution was diluted and

stabilized with HF; residual material was further digested with $HNO_3/HClO_4/HF$. Element concentrations were measured by ICP-AES. Total element concentrations and bulk chemical characteristics are shown in Table 1.

Table 1. Bulk chemical characteristics of the MSWI bottom ash samples used in this study (amounts in g/kg bottom ash)[a].

BA 1				BA 2			
pH	8.53	Calcite	96	pH	7.8	Calcite	90
E_H (mV)	301	Gypsum	3.5	E_H (mV)	344	Gypsum	22.2
Si	232.55	Zn	3.55	Si	210.83	Zn	2.37
Ca	71.71	Mn	0.90	Ca	78.45	Mn	1.85
Fe	86.67	Ba	3.72	Fe	76.88	Ba	1.68
Al	38.03	Cu	2.19	Al	38.15	Cu	1.64
Na	12.99	Pb	1.95	Na	18.54	Pb	1.27
Mg	11.65	Ni	0.65	Mg	13.43	Ni	0.28
K	8.67	Sr	0.26	K	10.75	Sr	0.26
S	3.70	Mo	0.02	S	6.32	Mo	0.03
P	3.49	Cd	0.01	P	3.93	Cd	0.01
Cl	1.56			Cl	n.m.		

[a] Gypsum was determined by aqueous extraction at a high liquid to solid (L/S = 25) ratio and measurement of SO_4. Calcite was measured by acidification with concentrated HNO_3 and determination of the gas volume developed. "n.m" = not measured.

pH-stat leaching experiments

The pH-stat leaching procedure has been described in detail elsewhere (*1*). In short, the samples were subjected for 24 h to batch leaching in acid-cleaned 300 mL PTFE vessels at various pH values between 2 and 12, using a computerised pH-stat system and a liquid to solid (L/S) ratio of 5 L/kg. Suspensions were kept in contact with the atmosphere. Solutions of 1 M HNO_3 and NaOH (analytical grade) were used to adjust the pH of the suspensions. After the 24 h equilibration period, the suspensions were filtered through 0.2 μm membrane filters. The filters were pre-cleaned with nanopure water, and the first approximately 2 mL of the filtrate was discarded. The clear filtrates were acidified with concentrated HNO_3 (suprapure) and analysed by ICP-AES and GFAAS (only in BA1, for Cd and Pb) to obtain total concentrations of Na, K, Ca, Mg, Mn, Al, Si, Fe, Ba, Sr, Zn, Cu, Mo, Cd, Ni, Pb, S and P. A carbon analyser (Shimadzu) was used to determine CO_3 and dissolved

organic carbon (DOC) in unacidified fractions. Chloride was determined with an ion selective electrode (ISE). Concentrations of S and P measured with ICP-AES are assumed to represent SO_4 and PO_4, as was checked with ion chromatography for the BA1 sample.

High-resolution column experiments

High-resolution column experiments were performed using borosilicate glass columns (Omnifit) with an inner diameter of 25 mm and an (adjustable) length of 400 mm. The columns were equipped with PTFE endpieces and PTFE filters with a pore size of 10 μm at the inlet and outlet of the column. Dry bottom ash was added to the columns in layers of a few cm and packed by manual shaking and knocking on the outside of the column up to a height of 30 and 30.7 cm, resulting in dry bulk densities of 1.18 g/cm^3 and 1.01 g/cm^3, respectively for BA1 and BA2. Nanopure demineralised water of natural pH stored in a container open to the atmosphere was pumped with a peristaltic pump in upflow direction through the column. Before the start of the experiments, the column, filters and tubing (PTFE) were pre-rinsed with acid and nanopure water.

The pH of the effluent was measured online using a flow-through gel-electrode (Broadley James Inc.). Effluent was collected with a fraction collector containing acid-cleaned 10 mL PE test tubes in fractions of about 6 mL. The columns were kept at a constant temperature of 21 °C with a thermostatic jacket (Omnifit). Flow velocity was chosen such that leachant residence times were comparable to that of a seperate study, in which we investigated at which flow velocity column experiments should be operated to approach local equilibrium as best as possible within workable time periods (Dijkstra, unpublished results). Flow velocities were determined by weighing the effluent fractions in the fraction collector and were 3.64 and 3.92 mL/h for BA1 and BA2, respectively. Weight differences between the dry column and the water-saturated column (i.e. the gravimetrically determined pore volume) appeared to increase during the experiments by about 10 grams, to end values of 82 grams for both BA1 and BA2. This may be the net result of physical changes of the bottom ash matrix in the column (due to processes such as removal of salts, increased wetting over time, etcetera).

A continuous stream of moistened Ar or N_2 gas, flowing through a cap placed over the fraction collector, protected the column effluent against contamination, carbonation and evaporation. Effluent fractions (around 6 mL per vial of 10 mL) were collected daily from the fraction collector and kept in a refrigerator under a N_2 or Ar atmosphere until further treatment. Effluent fractions were filtered through 0.2 μm membrane filters and diluted 1:2 to obtain sufficient sample volume for chemical analysis. Filtration, further treatment and chemical analysis was performed in the same way as for the pH stat-leachates (previous section).

At the end of the leaching experiments, pore volumes and dispersivities of the columns were estimated from pulse and breakthrough experiments with 0.015 M NaCl, which was assumed to behave like a chemically inert tracer. The tracer experiments were performed at different flow velocities (the flow velocities mentioned above and approximately twice as high). Concentrations of Cl^- present in the eluate fractions (3-4 mL) were measured with an ion-selective electrode. The pore volumes of BA1 and BA2 determined from the breakthrough curves of the tracers (60 mL and 87 mL, respectively, see below) did not correspond to the gravimetrically determined pore volumes (82 mL each, see above). For BA1, the discrepancy suggests that part of the percolate is relatively immobile (stagnant zones). However, the results for BA2 question the presumed conservativeness of the tracer used (chloride) or are biased by an experimental artifact (such as a weighing error). For these reasons, the tracer test does, unfortunately, not allow for adequate parameter estimation in terms of mass transfer processes between a mobile and an immobile domain. Therefore, these processes were not further considered in the present study, and front spreading is assumed to be solely caused by hydrodynamic dispersion and interparticle diffusion. The "effective" pore volumes and hydrodynamic dispersivities were fit to the advection-dispersion equation manually with PHREEQC (*6*) by applying "flux-type" boundary conditions at the inlet and the outlet of the column. The fitted values of the "effective" pore volumes were 60.23 $\pm$ 0.11 mL and 87.02 $\pm$ 0.06 mL; fitted dispersivities were 2.38 $\pm$ 0.13 cm and 0.44 $\pm$ 0.02 cm, respectively for BA1 and BA2.

Geochemical modelling

Mineral dissolution, solution speciation and sorption modelling was performed with the hydrogeochemical computer model PHREEQC for Windows (an extended version of PHREEQC-2 (*6*)). The thermodynamic database of the geochemical speciation code MINTEQA2, version 3.11 (*7*) was used for all calculations. Amendments made to this database for our calculations are summarised in Table 2.

Saturation indices were calculated using the measured concentrations of the elements listed in the section "pHstat leaching experiments" as input in the model. The pH was fixed to the measured value and solid precipitation was suppressed. PHREEQC-2 incorporates the Generalized Two Layer Model (GTLM) of Dzombak and Morel (*17*) for modelling surface complexation and surface precipitation reactions on hydrous ferric oxide (HFO). We refer to Dzombak and Morel (*17*) for a description of the model. For the determination of sorption parameters required for this model we followed the approach of Meima and Comans (*2*). In short, the amount of sorbent mineral needed as input in the model was estimated by selective chemical extractions. The HFO-content of the bottom ash samples was estimated by ascorbate extraction according to Ferdelman (*18*), described in Kostka and Luther (*19*), and will be referred to as Fe (ASC). The amorphous Al-(hydr)oxide content was estimated by oxalate extraction according to Blakemore et al. (*20*) and is referred to as Al (OX). The extracted amount of HFO (referred to as Fe (ASC)) apparently represented a too low amount of surface area in the model to explain the heavy metal concentrations measured. Therefore, amorphous Al-(hydr)oxides were considered as additional sorbent minerals, for which HFO was taken as a surrogate sorbent in the model. The reason for this approach is the absence of a complete and systematic database for sorption reactions on amorphous Al-oxides and hydroxides. Meima and Comans (*2*) have treated the extracted Al-(hydr)oxides and HFO equally in the model assuming 1 mol Fe (ASC) $\approx$ 1 mol Al (OX). The obtained sorbent mineral concentration is referred to as Fe (ASC) + Al (OX). For a justification of this approach we refer to Meima and Comans (*2*). Availabilities of sorbates were estimated from leached concentrations at pH values unfavourable for sorption (pH 2–4 for heavy metal cations, pH 10.5 for MoO_4). The sorption parameters determined for our study are summarised in Table 3.

Table 2. Additional or modified equilibrium formation constants (Log K) in the MINTEQA2 database.

Species / mineral	Log K	Ref.	Species / mineral	Log K	Ref.
$Cu(OH)_2^0$	-16.20	(8)	Ettringite	-57.06	(13)
$HMoO_4^-$	4.24	(9)	$Pb(H_2PO_4)_2$ (c)	48.95	(14)
$H_2MoO_4^0$	8.24	(9)	$Pb_4O(PO_4)_2$ (c)	36.86	(14)
$CaNO_3^+$	2.57	(10)	$CuMoO_4$ (c)	6.48	(14)
$Fe(NO_3)_3^0$	1.00	(10)	$Cu_4(OH)_6SO_4.1.3H_2O$ (c)	-17.27	(14)
$SrCO_3^0$	2.81	(10)	$ZnFe_2O_4$ (c)	-9.85	(14)
$SrHCO_3^+$	11.539	(10)	$PbSO_4.PbO$ (c)	0.19	(14)
$SrNO_3^+$	0.60	(10)	MCP	40.25	(14)
$SrSO_4^0$	2.30	(10)	Brushite	18.92	(14)
$BaCO_3^0$	2.71	(10)	Monetite	19.25	(14)
$BaHCO_3^+$	11.309	(10)	OCP	46.89	(14)
$BaNO_3^+$	0.70	(10)	α-$Ca_3(PO_4)_2$	25.49	(14)
$BaSO_4^0$	2.13	(10)	β-$Ca3(PO_4)_2$	28.92	(14)
$CuNO_3^+$	0.50	(10)	Newberryite	18.17	(14)
$Cu(NO_3)_2^0$	-0.40	(10)	$MgKPO_4.6H_2O$	10.62	(14)
$ZnNO_3^+$	0.40	(10)	Struvite	13.15	(14)
$Zn(NO_3)_2^0$	-0.30	(10)	$Mg_3(PO_4)_2$	14.59	(14)
$Cd(NO_3)_2^0$	0.20	(10)	Bobierite	25.00	(14)
$Pb(NO_3)_2^0$	1.40	(10)	$Mg_3(PO_4)_2.22H_2O$	23.09	(14)
$CaMoO_4^0$	2.57	(11)	$Zn_5(OH)_6(CO_3)_2$ (c)	-9.65	(15)
$MgMoO_4^0$	3.03	(11)	Illite	-12.22	(16)
$CaSO_4.2H_2O$ (c)	4.62	(8)	Hfo_sOHSr^{2+}	5.01	(17)
Mo (c)	19.73	(9)	Hfo_wOSr^+	-6.58	(17)
MoO_2 (c)	30.02	(9)	Hfo_wSrOH^0	-17.60	(17)
MoO_3 (c)	12.1	(9)	Hfo_wOMg^+	-4.60	(17)
H_2MoO_4 (c)	13.37	(9)	Hfo_sOMn^+	-0.40	(17)
$CaMoO_4$ (c)	7.94	(9)	Hfo_wOMn^+	-3.50	(17)
$FeMoO_4$ (c)	7.70	(9)	$Hfo\_sMoO_4^-$	9.50	(17)
$Fe_2(MoO_4)_3$ (c)	-38.82	(9)	$Hfo\_wMoO_4^-$	9.50	(17)
$MgMoO_4$ (c)	0.62	(9)	$Hfo\_sOHMoO_4^{2-}$	2.40	(17)
$PbMoO_4$ (c)	15.80	(9)	$Hfo\_wOHMoO_4^{2-}$	2.40	(17)
$ZnMoO_4$ (c)	4.4	(9)	$=Fe(OH)_3$(s)	-2.50	(17)
$CdCO_3$ (c)	12.1	(12)	$=Zn(OH)_2$(s)	-11.70	(17)

Surface precipitation is a term for the process that at very high surface coverages, a surface phase may be formed whose composition varies continuously between that of the original sorbent metal (hydr)oxide and a pure precipitate of the sorbing cation (21). Dzombak and Morel (17) recommend to consider surface precipitation in the model when [1] the dissolved sorbate concentration exceeds half the total amount of

surface sites or [2] the sorbate concentration exceeds one tenth of its solubility. Zn and Cu in our leachates are close to compliance with these criteria. Taking surface precipitation of Zn and Cu into account results in a strongly improved description of the leaching of Zn, which has been shown earlier by Meima and Comans (*2*), and a slightly better description of the leaching of Cu (this study). It has also an effect on the modelled behaviour of the other metals, for the reason that a large part of the available Zn and Cu is now bound in a surface precipitate and does not compete with other metals for surface complexation sites. Other metals that do not take part in the surface precipitate, will therefore show an increased sorption and lower leaching.

Note that surface precipitation, although an integral part of the GTLM of Dzombak and Morel (*17*), is not a standard option in PHREEQC-2. However, the formation of the surface precipitate can be modelled by implementing additional reactions (*17*) in combination with the "solid solution" option. Ferrihydrite (HFO) and the respective metal cation hydroxides (e.g., $=Zn(OH)_2(s)$ from Table 2) were used as the end members of an ideal solid solution.

Recently, Meima et al. (*4*) studied the complexation of Cu with dissolved organic ligands (DOC) in leachates from fresh and weathered samples of bottom ash, using a competitive ligand-exchange solvent extraction procedure (CLE-SE). We applied the conditional stability constants and sites densities from their study for modelling the leaching of Cu from the batch and column studies. Although it is likely that complexation with DOC enhances the leaching of many metals from bottom ash, only the site densities and conditional stability constants for the binding of Cu to DOC determined by Meima et al. (*4*) are available at present.

Reactive transport modelling

PHREEQC-2 has the capability to model equilibrium and kinetic chemical reactions in combination with one-dimensional transport processes. Dispersion was simulated using the measured dispersivities as input parameters in the model. The default PHREEQC value for the effective diffusion coefficient of aqueous species (0.3e-9 m²/s) was used in all transport calculations. Batch adsorption parameters were recalculated for the column system using the "effective" pore volumes and known material densities in the columns (Table 3).

Table 3. Parameters used for sorption modelling (see text for explanation of the abbreviations used)[a].

		pH stat		*Column*	
		BA1	BA2	BA1	BA2
L/S	L/kg	5	5	0.35	0.57
Fe (ASC)	g/L	0.512	0.92	7.40	8.07
Fe (ASC) + Al (OX)	g/L	5.24	7.88	75.74	69.14
Sorbate availability:					
Ni (pH 4)	mol/L	5.07E-5	5.27E-5	7.33E-4	4.62E-4
Cu (pH 2)	mol/L	2.20E-3	2.27E-3	3.18E-2	1.99E-2
Zn (pH 4)	mol/L	3.00E-3	2.66E-3	4.34E-2	2.33E-2
MoO_4 (pH 10.5)	mol/L	2.80E-6	2.03E-6	4.05E-5	1.78E-5
Cd (pH 4)	mol/L	4.60E-6	4.99E-6	6.65E-5	4.38E-5
Pb (pH 2)	mol/L	4.00E-4	8.40E-4	5.78E-3	7.37E-3

[a] Values for the column were calculated from the values measured in batch (pH-stat) experiments and the initial L/S ratio of the columns (see text)

Results and discussion

pH-stat data and modelling results

The pH-stat data of the leaching of Ni, Cu, Zn, MoO_4, Cd and Pb from BA1 and BA2 are shown in Figure 1. The leaching of major and minor elements appears to be very similar for BA1 and BA2, except for the leaching of DOC and Cu. The higher leaching of Cu in BA2 can probably be explained by the higher leaching of DOC, for which Cu has a high affinity (*4*). In qualitative terms, the behaviour of the metals of both samples is in agreement with the hypothesis that their leachate concentrations are controlled by sorption to (hydr)oxide minerals. Cations tend to sorb more strongly with increasing pH resulting in lower solution concentrations. In contrast, the sorption affinity of anions such as MoO_4 for the surface decreases with increasing pH, resulting in a higher solution concentration. At very high pH, hydrolysis and carbonate complexation of cations generally causes an elevated solution concentration. The opposite is generally valid for anions: at very low pH, increased protonation causes a lower affinity for the surface, resulting in an increased solution concentration.

Two modelling scenarios are shown in Figure 1 (for clarity, only the modelling results for BA1 are shown, but the results for BA2 are similar). Scenario 1 is the "point of departure"- model with concentrations of all elements listed in the section "pH-static leaching experiments" serving as input in the model, in addition to the

parameters listed in Table 3. The approach differs from the approach of Meima and Comans (*2*) in that sorption of major elements has been taken into account in a different way. Namely, the input of the measured concentrations of Ca, Mg, Mn, Ba, Sr, PO_4 and SO_4 in the model causes depletion of these components from solution due to sorption on the hydroxide surface, which in turn affects the sorption of the heavy metals due to competition for sorption sites. A better approach is therefore to pre-equilibrate the HFO- surface sites with the initial solution containing the major elements. After this, the "available" heavy metal concentrations (Table 3) are introduced in the solution and the final sorption equilibrium is calculated. This way, initial concentrations of the major elements are largely retained and an improved model prediction of the pH-dependent leaching of most heavy metals is obtained.

The leaching of Ni is largely overestimated, especially in the higher pH regions where sorption of cations is generally strongest. Cu is described accurately within the pH window (pH 7.5 – 10.5) for which complexation parameters with DOC have been determined (*4*), but outside of this pH window, Cu is strongly underestimated (not shown). Taking surface precipitation into account, in combination with DOC/Cu complexation, slightly improves the model prediction in comparison with the situation where only surface complexation is considered (Figure 1). Qualitatively, Zn leaching is predicted rather well over a wide pH range, but is overestimated between pH 8-10. $MoO4$ is predicted accurately at neutral to high pH in BA1 as well as BA2. Leached concentrations of Pb and Cd follow the measured leaching patterns up to high pH in BA1 and BA2, but are overestimated more than one order of magnitude in BA2 at very alkaline pH values (pH 10 – 12).

In agreement with Meima and Comans (*2*), the calculation of saturation indices indicated that none of the minerals listed in the MINTEQA2 database and Table 2 lead to a better description of the batch pH-static leaching data of Ni, Cu, Zn, MoO_4, Cd and Pb than the sorption model. For these reasons we have chosen the sorption model for the description of the solid/liquid partitioning of the heavy metals in the transport model.

When the above sorption processes are incorporated in a transport model, a reduction of the amount of components and species is necessary (see next section). Therefore, the next step in our approach was to determine the minimal set of
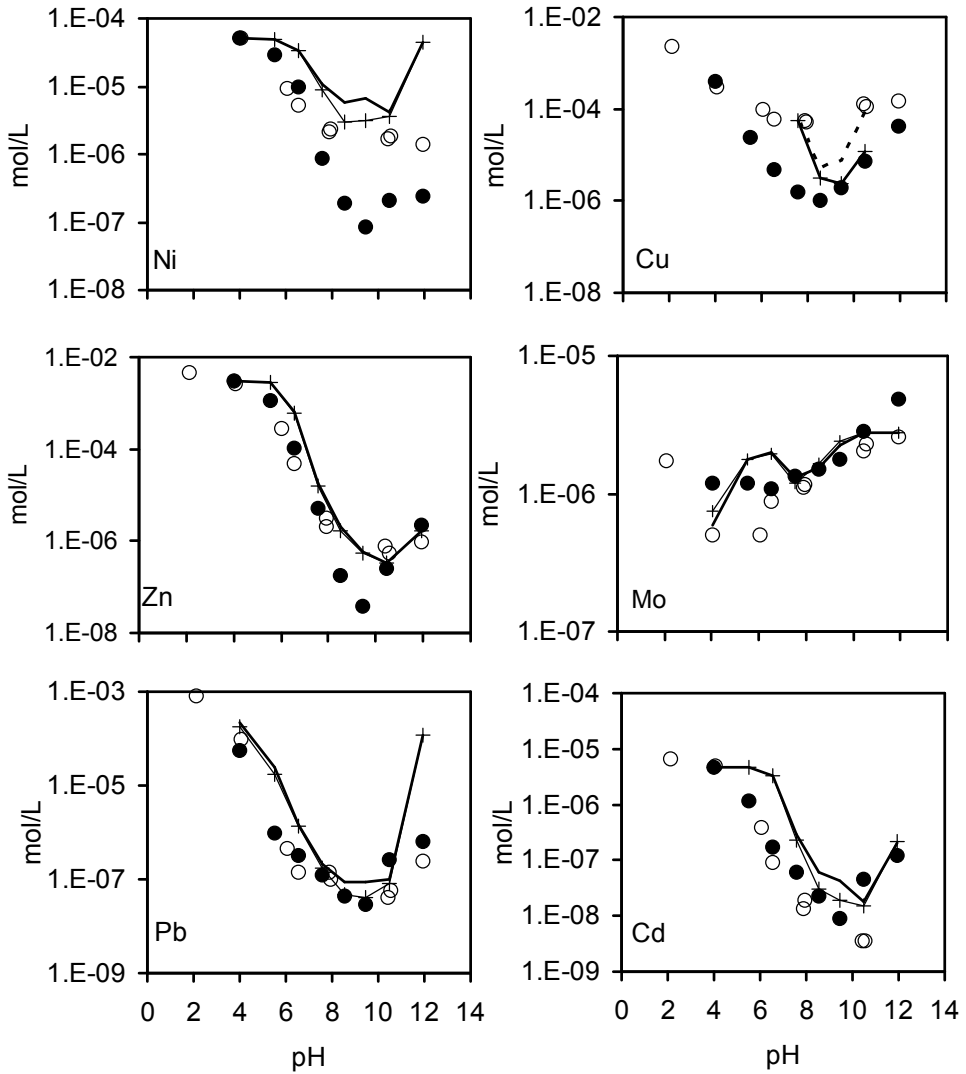
Figure 1. Leached concentrations as a function of pH of Ni, Cu, Zn, Mo, Pb and Cd from MSWI bottom ash BA1 (with symbol ●) and BA2 (with symbol ○). The black lines represent model scenario 1. The black lines marked with + represent model scenario 2 (simplified version of scenario 1). The dashed line in the graph for Cu represents the result where surface precipitation of Cu has not been taken into account.

components and species that would still provide an adequate description of the heavy metal behaviour. Scenario 2 represents the "simplified" model without the input of the components Na, Mg, Mn, Ba, Sr, Al, Si, Cl, K, NO_3 and Cl. The components Ca, PO_4 and (less important) SO_4 were found to be essential for an adequate description of the heavy metal behaviour. The result is shown in Figure 1, where the lines of scenario 1 and 2 almost coincide. The small differences between the model curves of scenario 1 and 2 are mainly caused by the absence of the competitive influence that the omitted elements have on the sorption of the heavy metals. The competitive influence among the heavy metals and between the metals and the major elements is currently being investigated in more detail (*22*).

Column transport data and modelling results

Preliminary transport calculations have shown that taking processes into account for all elements listed in the section "pH-static leaching experiments" increased the calculation times extensively and sometimes caused convergence problems. Therefore, our multicomponent reactive transport model is based on the approach of scenario 2 (see previous section). To be able to simulate dynamic changes in pH and mineral amounts, we chose to model pH, Ca, CO_3 and SO_4 with the system $CaCO_3$-$CaSO_4.2H_2O$-H_2O in equilibrium with atmospheric CO_2 ($pCO_2 = 10^{-3.5}$ bar). We used the measured amounts of these minerals listed in Table 1 as the input value for the initially present amounts in the column. Based on an evaluation of saturation indices in the batch experiments, we chose to model PO_4 solubility in BA1 on the basis of equilibrium with b-TCP (b-$Ca_3(PO_4)_2$) and in BA2 with OCP ($Ca_4H(PO_4)_3.2.5H_2O$), although this might not be mechanistically correct (particularly for OCP in BA2), as will be discussed below. Both minerals are precursor phases of HAP (hydroxylapatite, $Ca_5(PO_4)_3OH$) which is a common mineral in soils (*14*). However, X-ray diffraction on our samples did neither confirm the presence of b-TCP and OCP, nor the presence of other phosphates like a-TCP, HAP or FAP ($Ca_5(PO_4)_3F$). The amounts initially present were chosen to be large enough to prevent mineral exhaustion in the simulations.Ionic strength effects were modelled by adding amounts of NaCl to the model columns resulting in ionic strengths that were close to the values calculated for

the first leachate fractions. The sorption parameters and sorbate availabilities of Table 3 were used for sorption modelling. The feed solution was defined as H_2O in equilibrium with atmospheric CO_2 and, as a result, had a pH of 5.66. The results of the high-resolution column experiments and the model predictions are shown in the Figures 2 and 3.

pH

The pH of the leachates varies between 7.9 and 8.4 for both BA1 and BA2 and, except for the first few pore volumes, remains rather constant towards the end of the experiments (Figure 2a and 2b). These values are in agreement with earlier values determined in batch studies for weathered MSWI bottom ash ([1]). The pH values measured are close to the pH of calcite ($CaCO_3$) in equilibrium with atmospheric CO_2, which is around 8.3, but the presence of gypsum ($CaSO_4.2H_2O$) decreases this value to around 7.8. This is in agreement with pH stat leaching data of Ca, CO_3 and SO_4 for BA1 and BA2, which are described rather well with the system $CaCO_3$-$CaSO_4.2H_2O$. However, calcite is oversaturated by up to one order of magnitude, which is a common phenomenon in leachates of waste materials ([1, 5, 23-25]). The prediction of the pH in BA1 and BA2 is rather close to the measured pH (Fig 2a and 2b). However, the predicted sharp increase in pH at about 3 npv in BA1 and 14 npv in BA2, caused by the complete dissolution of gypsum, is hardly visible in the data.

Major elements

Concentrations of Ca and SO_4 gradually decrease from the start of the experiment in BA1, while in BA2 a plateau is reached between approximately 1 and 10 pore volumes (Fig. 2c and 2d). Throughout the experiment, leachate fractions of BA1 gradually become more undersaturated with respect to gypsum (saturation indices not shown). In BA2, however, leachates are very close to equilibrium with gypsum between 1 and 10 pore volumes but become increasingly undersaturated towards the end of the experiment. These results suggest exhaustion of the gypsum content in the columns, which happens later in BA2 than in BA1. This is consistent with the independently determined gypsum content in the samples (Table 1) which is in turn
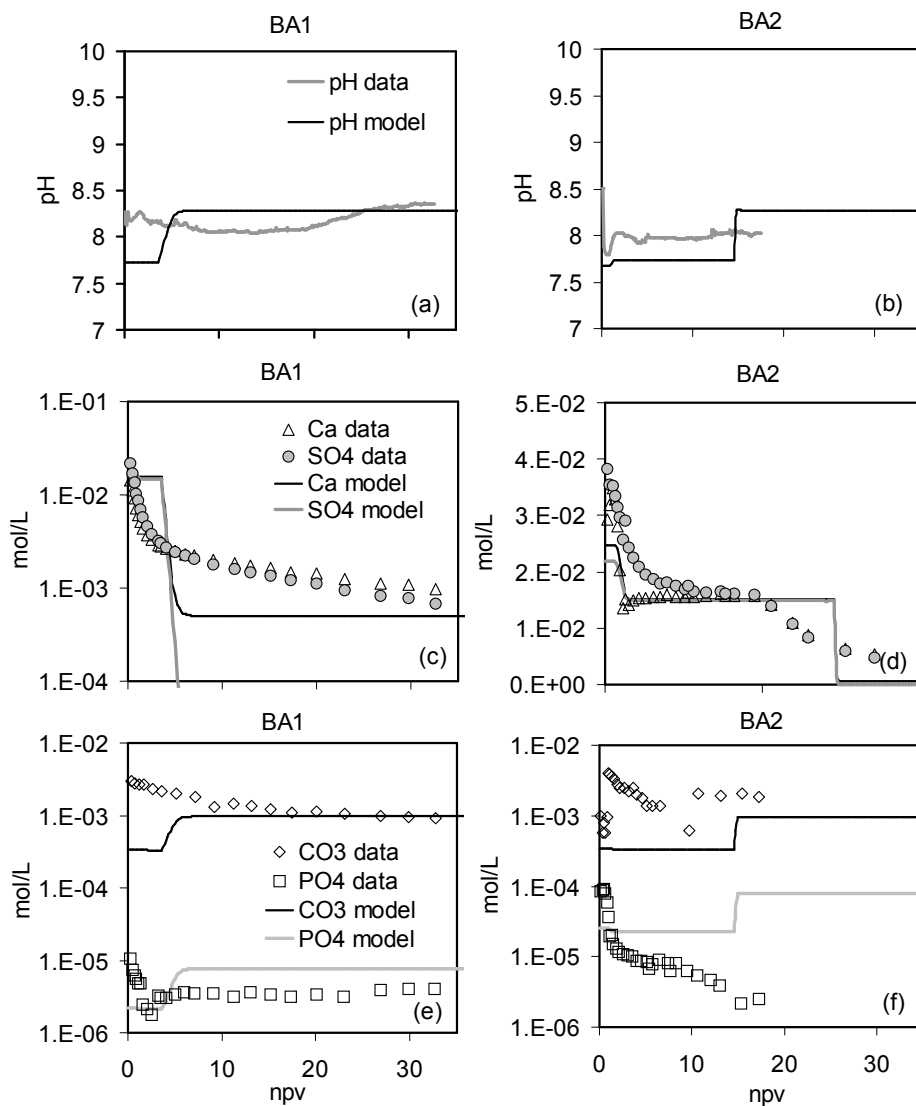
Figure 2. Results of the high-resolution column experiments on MSWI bottom ash samples BA1 and BA2. Measured and simulated pH (a and b); measured leachate concentrations and modelling curves of Ca and SO_4 (c and d); CO_3 and PO_4 (e and f). Data are expressed as a function of number of pore volumes (npv).

consistent with the higher age of BA1, which was stored in the open for 1.5 years while BA2 had not been stored in the open. Calcite becomes less oversaturated at later pore volumes for both BA1 and BA2 (saturation indices 0.26 and 0.76 at the end of the experiments, respectively).

Elevated concentrations of Ca, CO_3 and SO_4 in the first few pore volumes may be explained by the high ionic strength (low activity coefficients), caused by soluble salts that readily wash out of the column (Fig. 2c and 2d). The low activity coefficients cause solution concentrations of ions in equilibrium with minerals to be higher. This effect is particularly visible in BA2, of which the leachates in the first pore volume contained much higher concentrations of soluble salts than the leachates of BA1. At later pore volumes, the gypsum and calcite equilibria are described reasonably well (especially in BA2).

After the first pore volumes, PO_4 concentrations in the column leachates of BA1 remain fairly constant up to the end of the experiments, in contrast with BA2, where PO_4 has not reached a plateau even at the end of the experiments (Fig. 2e and 2f). The behaviour in BA1 suggests that PO_4 is solubility-controlled, while the continuing decrease of PO_4 concentrations in BA2 suggest that other processes are governing the release from this bottom ash (e.g. sorption to (hydr)oxides). Qualitatively, the behaviour of PO_4 is described rather well in the BA1 leachates, except for the initial pore volumes where PO_4 is underestimated. In BA2, predicted PO_4 concentrations using OCP as PO_4-controlling mineral do not match with the data, even in a qualitative way. As PO_4 is a strong sorbate (*17*), and therefore a strong competitor for oxyanions such as MoO_4, it is important to identify the processes controlling PO_4 in bottom ash.

Heavy metal cations and MoO4

In general, metal cation concentrations are higher in the first few pore volumes in comparison with the pore volumes thereafter (Fig. 3a – 3f). We interpret this behaviour as a combination of the changing pH, the competitive influence of the major elements Ca, SO_4 and PO_4, and the complexation with complexing ligands of which the most important is probably DOC. The facilitated transport effect that DOC can have on heavy metals is noticeable for Cu, when the leaching of DOC and Cu
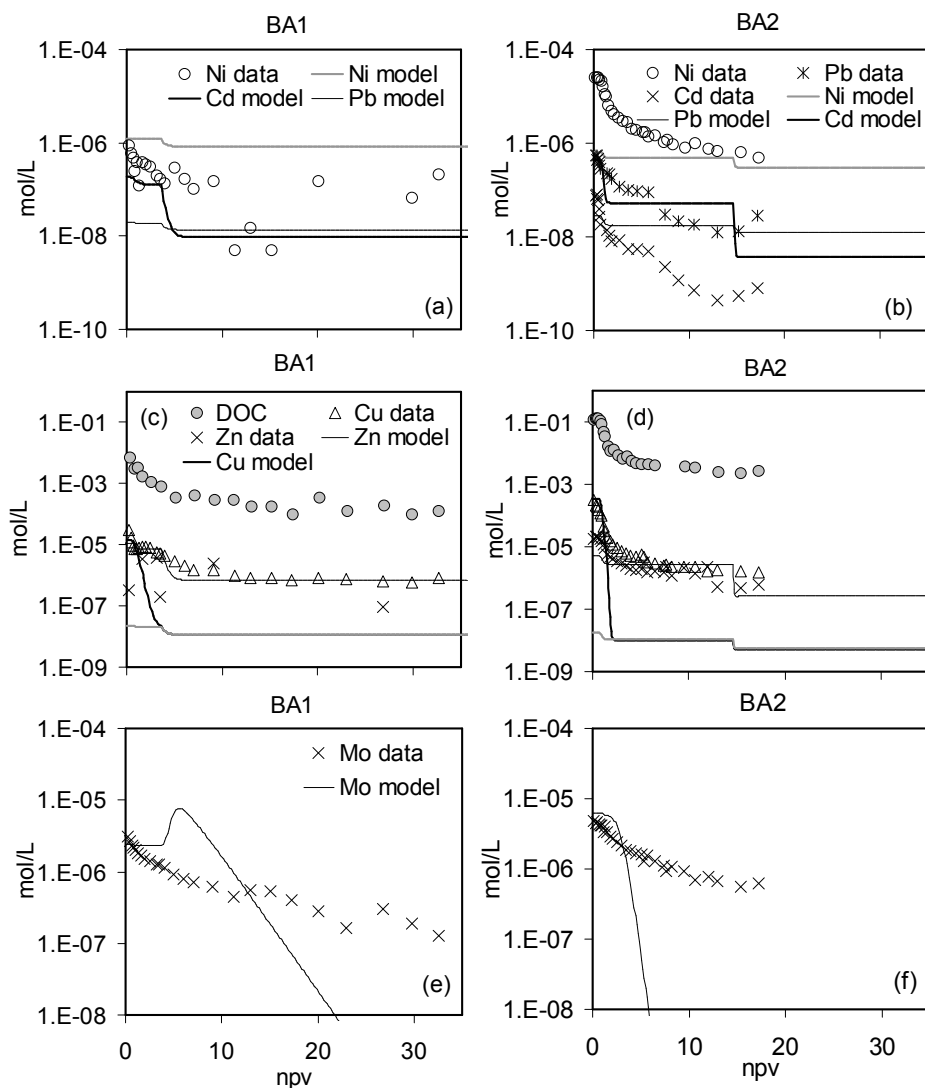
Figure 3. Results of the high-resolution column experiments on MSWI bottom ash samples BA1 and BA2. Ni, Pb and Cd (a and b); measured concentrations of DOC, Cu and Zn and modelling curves of Cu and Zn (c and d). Grey lines in 3c and 3d represent the model results when DOC/Cu complexation was not taken into account; measured concentrations and modelling curves of Mo (e and f). Concentrations of Cd and Pb in BA1 leachates were too low to be measureable with ICP-AES. Data are expressed as a function of number of pore volumes (npv).

from BA1 and BA2 are compared (Fig. 3c and 3d). Furthermore, changes in ionic strength may also affect metal sorption (*17*).

Heavy metal cation concentrations gradually decrease towards the end of the experiments. Because changes in the system only occur in the first few pore volumes and at the point where gypsum becomes exhausted, not many features can be observed that provide an accurate validation of the sorption-control of metal leaching in the transport model. Nevertheless, the modelling has shown that the leaching of heavy metals from MSWI bottom ash is strongly influenced by pH and competition for sorption sites on (hydr)oxide minerals in the ash matrix among the metals and between the metals and, in particular, the major elements Ca, SO_4 and PO_4.

Qualitatively, the leaching patterns of Zn, Cd, Pb and Ni are described reasonably well with respect to the elevated concentrations in the first pore volumes. Quantitatively, concentrations of Ni and Pb are strongly underestimated in BA2, Cd is overestimated by about a factor of five, but Zn is predicted rather accurately (Fig. 3a – 3d). However, towards the end of the experiments, concentrations of Zn, Cd, Pb and Ni are predicted within an accuracy of one order of magnitude. The initial concentrations of Cu in BA1 and BA2 are predicted rather well (Fig. 3c and 3d). However, after the first pore volumes, where in the model DOC is depleted from the column, Cu is strongly underestimated. In reality, DOC concentrations decrease only very gradually, which is likely the major reason for the underestimation. The model predictions make clear that knowledge and modelling of the processes controlling DOC concentrations would strongly improve the model predictions for Cu.

Modelled heavy metal cation concentrations remain virtually constant towards the end of the experiments, indicating that depletion does not occur. This absence of depletion is caused by the fact that 90-100% of the available metal concentrations is sorbed at pH values around 8 (Fig. 1).

In comparison with the heavy metal cations, the initial elevated concentrations of MoO_4 in the first pore volume are less pronounced, and concentrations decrease only very gradually. Although the initial concentrations in the first pore volumes were predicted rather accurately (Fig. 3e and 3f), the overall leaching pattern was not. As can be concluded from the batch pH stat data and modelling results (3.1), only a small part of the available MoO_4 is sorbed around pH 8 (Fig. 1). This results in a rapid depletion in the transport model, which is not observed in reality. An alternative

explanation would be that MoO_4 is solubility-controlled, but further research is necessary to confirm that.

In general, the modelled leaching curves of the major elements as well as the heavy metals show very abrupt changes in comparison with the data. This observation might be an indication for either physical nonequilibrium (e.g., diffusional mass transfer effects between "mobile" and "immobile" zones in the pore water) or chemical non-equilibrium (e.g., kinetics of dissolution or desorption). The "tailing" of presumed non-reactive components such as Na or Cl (not shown) may be an indication for physical non-equilibrium; the gradual concentration changes of major and minor elements and pH may point to both physical- and/or chemical non-equilibrium situations. In this respect, the observations made during tracer tests are evidently of importance for transport modelling, but further research using truly conservative tracers (e.g., tritiated water) is needed to investigate the role of mass transfer processes.

Given the possible absence of true local equilibrium, consideration of a kinetic term in the transport model may contribute to the identification of the underlying leaching processes and further improvement of model predictions.

Conclusions

Heavy metal leaching in batch experiments with a fresh and a weathered MSWI bottom ash sample can be described adequately with a surface complexation model that considers metal sorption to hydrous ferric oxide (HFO) and amorphous Al-(hydr)oxide minerals in the bottom ash matrix. It has been shown that this description can be adequately reproduced with a simplified modelling approach, which considers only the most important components and species.

Data from high-resolution column experiments were used to test transport model simulations, which were based on processes identified in the batch leaching experiments. Heavy metals concentrations were predicted with an accuracy of within approximately one order of magnitude. A better description of the pH and macro elements such as Ca, SO_4 and PO_4 would improve the description of heavy metal transport from MSWI bottom ash.

Model predictions make clear that knowledge and modelling of the processes controlling of DOC concentrations would strongly improve the model predictions for Cu.

The very abrupt changes that modelled leaching curves show in comparison with the measurements might indicate non-equilibrium processes. Given the possible absence of true local equilibrium, consideration of a kinetic term in the transport model may contribute to the identification of the underlying leaching processes and further improve model predictions of dynamic leaching of contaminants from MSWI bottom ash.

References

1.   Meima, J. A.; Comans, R. N. J. Geochemical modelling of weathering reactions in MSWI bottom ash. *Environ. Sci. Technol.* 1997, 31, 1269-1276.

2.   Meima, J. A.; Comans, R. N. J. Application of surface complexation/precipitation modeling to contaminant leaching from weathered municipal solid waste incinerator bottom ash. *Environ. Sci. Technol.* 1998, 32, 688-693.

3.   Meima, J. A.; Comans, R. N. J. The leaching of trace elements from municipal solid waste incinerator bottom ash at different stages of weathering. *Appl. Geochem.* 1999, 14, 159-171.

4.   Meima, J. A.; Van Zomeren, A.; Comans, R. N. J. Complexation of Cu with dissolved organic carbon in municipal solid waste incinerator bottom ash leachates. *Environ. Sci. Technol.* 1999, 33, 1424-1429.

5.   Zevenbergen, C.; Comans, R. N. J. *Geochemical factors controlling the mobilization of major elements during weathering of MSWI bottom ash.* In: *Environmental Aspects of Construction with Waste Materials*; Goumans, J. J. J. M.; Van der Sloot, H. A.; Aalbers, T.G. (eds.). Studies in Environmental Science 60, Elsevier Science B. V.: Amsterdam, The Netherlands, 1994, pp 179–194.

6.   Parkhurst, D. L.; Appelo, C. A. J. *User's guide to PHREEQC (version 2)- a computer program for speciation, batch-reaction, one-dimensional transport, and inverse geochemical calculations.* U. S. Geol. Surv., Water Resour. Inv. Report 99-4259, Denver CO, 1999.

7.   Allison, J. D.; Brown, D. S.; Novo-gradac, K. J. *MINTEQA2/PRODEFA2, a geochemical assessment model for environmental systems: version 3.11 databases and version 3.0 user's manual.* Environmental Research laboratory, U.S.-EPA: Athens, GA, 1991.

8. Morel, F. M. M.; Hering, J. G. *Principles and applications of aquatic chemistry.* New York: John Wiley & Sons, 1993.

9. Rai, D.; Zachara, R. M. *Chemical attenuation rates, coefficients, and constants in leachate migration, vol. 1: A critical review.* Report no. EPRI EA-5176, Electric Power Research Institute, 1984.

10. Martell, A. E.; Smith, R. M.; Motekaitis, R. J. (eds.). *Critically Selected Stability Constants of Metal Complexes*, version 3.0. National Institute of Standards and Technology (NIST), Gaithersburg, MD 20899-2310, 1997.

11. Essington, M. E. Formation of calcium and magnesium molybdate complexes in dilute aqueous solutions. *Soil Sci. Soc. Am. J.* 1992, 56, 1124-1127.

12. Stipp, S. L.; Parks, G. A.; Nordstrom, D. K.; Leckie, J. O. Solubility product and thermodynamic properties of synthetic otavite, $CdCO_3(s)$ and aqueous association constants for the Cd(II) – CO_2 – H_2O system. *Geochim. Cosmochim. Acta* 1993, 56, 2699-2713.

13. Perkins, R. B.; Palmer, C. D. Solubility of ettringite ($Ca_6(Al(OH)_6)_2(SO_4)_3.26H_2O$) at 5-75 ºC. *Geochim. Cosmochim. Acta* 1999, 63, 1969-1980.

14. Lindsay, W. L. *Chemical equilibria in soils.* John Wiley and Sons: New York, 1979.

15. Schindler, P.; Reinert, M.; Gamsjäger, H. Loslichkeitskonstanten und free bildungsenthalpien von $ZnCO_3$ and $Zn_5(OH)_6(CO_3)_2$ bei 25 °C. *Helvetica Chim. Acta* 1969, 52, 2327-2332.

16. Krupka, K. M.; Erikson, R. L.; Mattigod, S. V.; Schramke, J. A.; Cowan, C. E.; Eary, L. E.; Morrey, R. R.; Schmidt, R. L.; Zachara, J. M.; *Thermochemical data used by the FASTCHEM^{TM} Package.* Report no. EPRI EA-5872, Electric Power Research Institute, 1988.

17. Dzombak, D. A.; Morel, F. M. M. *Surface complexation modeling: Hydrous ferric Oxide.* John Wiley & Sons: New York, 1990.

18. Ferdelman, T. G. *The distribution of sulfur, iron, manganese, copper, and uranium in a salt marsh sediment core as determined by a sequential extraction method.* Masters Thesis, University of Delaware, 1988.

19. Kostka, J. G.; Luther III, G. W. Partitioning and speciation of solid phase iron in saltmarsh sediments. *Geochim. Cosmochim. Acta* 1994, 28, 1701-1710.

20. Blakemore, L. C.; Searle, P. L.; Daly, B. K. *Methods for chemical analysis of soils.* Science Report no. 80, NZ Soil Bureau: Lower Hutt, New Zealand, 1987.

21. Farley, K. J.; Dzombak, D. A.; Morel, F. M. M. A surface precipitation model for the sorption of cations on on metal oxides. *J. Colloid Interface. Sci.* 1985, 106, 226-242.

22. Dijkstra, J. J.; Comans, R. N. J. Manuscript in preparation.

23.   Schramke, J. A. Neutralization of alkaline coal fly ash leachates by $CO_2(g)$. *Appl. Geochem.* 1992, 7, 481-492.

24.   Kirby, C. S.; Rimstidt, J. D. Interaction of municipal solid waste ash with water. *Environ. Sci. Technol.* 1994, 28, 443-451.

25.   Van der Weijden, R. D. *Interactions between cadmium and calcite*. Ph. D. Thesis, Utrecht University, 1995.

Chapter 3

Leaching of heavy metals from contaminated soils: an experimental and modeling study

Abstract

In this paper, we characterize the leaching of heavy metals (Ni, Cu, Zn, Cd and Pb) from eight contaminated soils over a wide range of pH (pH 0.4 - 12) using an original approach based on batch pH-static leaching experiments in combination with selective chemical extractions and geochemical modeling. The leached concentrations of the heavy metals are generally much lower than the total concentrations and show a strong pH-dependency, resulting in "V-shaped" leaching curves with orders of magnitude changes in solution concentrations. The "multisurface" model used incorporates adsorption to dissolved and solid organic matter (NICA-Donnan), iron/aluminum (hydr)oxide (Generalized Two-Layer Model) and clay (Donnan model). These models were applied without modifications and only the standard set of binding constants and parameters was used (i.e. without any fitting). The model predictions of heavy metal leaching are generally adequate, and sometimes excellent. Results from speciation calculations are consistent with the well-recognized importance of organic matter as the dominant reactive solid phase in soils. The observed differences between soils with respect to element speciation in the solid phase correspond to the relative amounts of the reactive surfaces present in the soils. In the solution phase, complexes with dissolved organic matter (DOM) are predominant over most of the pH range. Free metal ions (Me^{2+}) are generally the dominant species below pH 4. The combination of the experimental and modeling approach as used in this study is shown to be promising, because it leads to a more fundamental understanding of the pH-dependent leaching processes in soils. The "multisurface" modeling approach, with the selected sorption models, is shown to be able to adequately predict the leaching of heavy metals from contaminated soils over a wide range of conditions, without any fitting of parameters.

Introduction

The potential risk of heavy metals in soils, with respect to their mobility and ecotoxicological significance, is determined by their solid-solution partitioning rather than the total heavy metal content (*1, 2*). The release of heavy metal cations to the water phase ("leaching"), and so the susceptibility for transport processes, depends on their solution speciation, and their affinity to bind to reactive surfaces in the soil matrix and pore water (such as particulate and dissolved organic matter, clays or metal (hydr)oxide-surfaces). Recently, a number of studies have demonstrated the successful application of mechanistic geochemical models in which the interactions with multiple reactive surfaces were taken into account to describe aqueous heavy metal concentrations in soils (*3-9*) and aquatic systems (*10*). Good agreement has been shown between modeled and measured metal species concentrations with the Donnan membrane technique (*3, 4, 7*), indicating that "multisurface" models may also provide valuable insights into the speciation of metals in the solution phase. However, the range of conditions of published leaching data is often limited to pH values imposed by the soil material itself, which are generally in the neutral to acidic region. Investigating the pH-dependence of heavy metal leaching from natural and waste materials is important for scenario-based risk assessment studies (*11*). Evaluation of the pH-dependence of leaching is an approach that has been recently introduced in waste management and research to assess the leaching of contaminated (waste) materials, both for research purposes (*12, 13*) as well as in the context of the development and harmonization of regulatory leaching tests (*11*).

In this paper, the leaching behavior of Ni, Cu, Zn, Cd and Pb from eight different contaminated soils is studied over a wide range of pH (pH 0.4 - 12) using an original experimental approach based on batch pH-static leaching experiments in combination with selective chemical extractions. In addition, we attempt to predict the measured solution concentrations of Ni, Cu, Zn, Cd and Pb as a function of pH, using the current knowledge of processes controlling leaching of heavy metals from soils in combination with a mechanistic "multisurface" modeling approach. Data from batch pH-static leaching experiments are used to obtain "geochemical fingerprints" of the soils under study. Selective chemical extractions are performed to provide input

parameters for the (sorption) models. A computer speciation model is then applied to identify for each element of interest the processes most likely to control leaching, such as mineral dissolution or sorption to (hydr)oxide surfaces, organic matter or clay minerals. With the independently determined set of parameters we attempt to predict the pH-dependent leaching of the elements of interest (i.e. without fitting any model parameters). Model results are used to provide insight into the speciation of heavy metals in the solid and the solution phase as a function of pH.

Experimental section

Soil samples

The soils with codes I to IV were sampled at different locations from road shoulders along 30-year old roads in the Veluwe area in The Netherlands. Soils V, VI and VII were collected from the sites of a (former) metallurgical company, a metal casting company and an electroplating company, respectively. Soil VIII was collected from a 3-year old urban runoff rainwater infiltration pond. General characteristics of the soil samples are summarized in Table 1.

Total element concentrations in the samples were determined on $\pm$ 500 mg sub samples (ground in an agate mortar) which were digested with concentrated HNO_3 and $HClO_4$ (in proportions of 20:1) in an autoclave at 190 °C for 10 h. The resulting solution was diluted and stabilized with HF. Residual material was digested similarly with $HNO_3/HF/HClO_4$ (in proportions of 10:10:1). Element concentrations in the resulting solutions were measured by ICP-AES.

Batch pH-static leaching experiments

The pH-stat leaching procedure used has been described in detail elsewhere (*13*). In short, the samples were subjected for 48 h (soils I – V and VIII) or 24 h (soils VI and VII) to batch leaching in acid-cleaned 300 mL PTFE vessels at various pH values between 2 and 12, using a computerized pH-stat system and a liquid to solid (L/S) ratio of 2 L/kg (soils I-IV, VI, VII) or 10 L/kg (soils V and VIII). Suspensions were kept in contact with the atmosphere. Solutions of 1 M HNO_3 and NaOH (analytical

grade) were used to adjust the pH of the suspensions. After the equilibration period, the suspensions were filtered through 0.2 μm membrane filters. The filters were pre-cleaned with Nanopure water, and the first approximately 2 mL of the filtrate was discarded. The clear filtrates were acidified with concentrated HNO_3 (suprapure) and analyzed by ICP-AES to obtain solution concentrations of a wide spectrum of elements. It was assumed that total S and P measured by ICP-AES equated to SO_4 and PO_4, respectively. A carbon analyzer (Shimadzu) was used to determine dissolved inorganic carbon (DIC) and dissolved organic carbon (DOC) in unacidified fractions. Chloride was determined by ion chromatography (IC).

Selective chemical extractions

The total amount of "reactive" organic carbon in the soil samples was estimated as the sum of the humic and fulvic fraction determined with a batch method derived from the currently recommended procedure of the International Humic Substances Society (IHSS) (*14*), explained in detail by van Zomeren and Comans (*15*). The amount of amorphous and crystalline iron (hydr)oxides in the soils was estimated by a dithionite extraction according to Lord (*16*) and Canfield (*17*), described in Kostka and Luther III (*18*) and will be referred to as Fe-DITH. The amount of amorphous Fe(hydr)oxides in the soils was estimated by an ascorbate extraction according to Ferdelman (*19*) described in Kostka and Luther III (*18*) and will be referred to as Fe-ASC. Amorphous Al-(hydr)oxides were estimated by an oxalate extraction according to Blakemore et al. (*20*) and will be referred to as Al-OX. The concentrations of the heavy metals that are "available" for sorption processes were estimated by extraction with 0.43 M HNO_3 similar to the procedure of Houba et al. (*21*), a procedure followed by several authors to determine heavy metal availability in soils (*5, 7, 22, 23*). The extraction was performed with a 0.43 M HNO_3 solution at an L/S ratio of 10 L/kg (dry weight) with an equilibration period of 24 h under continuous agitation. Filtration, further treatment and chemical analysis of the extractions were performed in the same way as for the pH-stat leachates. The extracted amounts were recalculated to the appropriate L/S ratio of our pH-stat experiments to enable their presentation in the concentration-pH diagrams (Figure 1).

Model description

Mineral saturation indices, solution speciation, and sorption processes were calculated with a speciation and transport model set up in the ORCHESTRA (*24*) modeling framework, in which we incorporated the different sub-models described below. Solution speciation was calculated using thermodynamic data from the MINTEQA2 (*25*) database, version 3.11, in combination with the Non-Ideal Competitive Adsorption (NICA)–Donnan model (*26-28*) (to include metal complexation with dissolved organic matter, see further below). For changes to the MINTEQA2 database for our work we refer to Dijkstra et al. (*29*). Component activities were calculated with the Davies equation and an oxidizing environment was assumed in all calculations (pH + pe = 15).

Binding to solid and dissolved organic matter

Specific and nonspecific sorption of protons and metal ions to organic matter was modeled with the NICA-Donnan model (*26-28*) using the set of "generic" binding parameters and constants of Milne et al. (*30, 31*). The amount of solid organic carbon in the model was calculated from the extracted total reactive organic carbon after correction for the concentration of DOC measured in each of the leachates of the pH-stat, assuming that 100% of the DOC in solution consists of reactive humic substances. Solid and dissolved organic matter (hereafter referred to as SOM and DOM) were represented in the model by humic acid (HA) by assuming that HA consists of 50% of carbon (*32*). The recommended "generic" parameters for binding to HA of Milne et al. (*31*) were included in the model for H, Ba, Sr, Ca, Mg, Mn, Fe(II), Fe(III), Al, Ni, Cu, Zn, Cd and Pb.

Binding to iron/aluminum (hydr)oxides

To take surface complexation to iron (hydr)oxide surfaces into account, we have used the Generalized Two-Layer Model of Dzombak and Morel (*33*) for specific binding of metal cations and (oxy)anions to "Hydrous Ferric Oxide" (HFO). For the determination of the required sorption parameters we followed the approach of Meima and Comans (*34*). The total amount of amorphous iron (hydr)oxides was

calculated from Fe-ASC and was represented by HFO in the model. In addition, amorphous aluminum (hydr)oxides were considered as potentially important sorbent minerals, for which HFO was taken as a surrogate sorbent in the model. The reason for this approach is the absence of a complete and systematic database for sorption reactions on amorphous aluminum (hydr)oxides. For a justification of this approach, based on similarities in the surface structure and reactivity of aluminum and iron (hydr)oxides, is referred to Meima and Comans (*34*). Following the approach of Meima and Comans (*34*), we have treated the extracted aluminum (hydr)oxides and HFO equally in the model assuming 1 mol Fe-ASC $\approx$ 1 mol Al-OX. The recommended specific surface area of 600 m²/g (*33*) for HFO was assumed, to calculate site densities for the amorphous iron and aluminum (hydr)oxides. The total amount of crystalline iron(hydr)oxides was calculated from the difference between Fe-DITH and Fe-ASC. HFO was also taken as a surrogate sorbent mineral for crystalline iron (hydr)oxide assuming an equal reactivity, however site densities were calculated using a specific surface area of 100 m²/g (*35*). The total amount of the iron and aluminum (hydr)oxide surfaces, used as input in the model, was corrected for mineral dissolution and adsorption to SOM and DOM as a function of pH by a separate calculation. For this calculation, goethite and amorphous $Al(OH)_3$ were assumed to control Fe and Al solubility, and their total amounts were set equal to Fe-DITH and Al-OX, respectively. The derived and estimated surface complexation constants of Dzombak and Morel (*33*) were included in the model for H, Ca, Ba, Sr, Mn, Mg, Ni, Cu, Zn, Cd, Pb, SiO_4, SO_4 and PO_4. The original surface complexation constant for the low-affinity site for Pb was considered by Dzombak and Morel (*33*) to be probably an underestimate. We used a higher log *K* value of 1.7 in the calculations to be consistent with the general trend of an approximately 3 log-unit difference between the sorption constants for the high and low affinity sites (*33*).

Binding to clay surfaces

Similar to Weng et al. (*4*), nonspecific sorption to permanently charged clay surfaces was simulated using a Donnan model assuming a charge density of 0.25 equiv/kg and a fixed Donnan volume of 1 L/kg, which may be considered as average values for illitic clay minerals (*36*). Specific adsorption of metal ions to variable charge

clay edges was not considered in our model. The amount of clay in the soils (grain size fraction <2 μm), needed as input in the model, was estimated by the pipet method (based on Stokes' settling) according to the Dutch standard NEN 5753 (*37*).

Model input

Model files to calculate saturation indices of potentially solubility controlling minerals included the measured total solution concentrations of Na, K, Ca, Mg, Mn, Al, Si, Fe, Ba, Sr, Zn, Cu, Cd, Ni, Pb, SO$_4$, PO$_4$, Cl, DIC (CO$_3$), and dissolved organic carbon (DOC). The pH was fixed to the measured value, and all solid precipitation was suppressed. Model input files to predict the leaching of the five heavy metals simultaneously, based on the adsorption processes described above, were composed of i) the concentrations of the different reactive surfaces in the solid and solution (i.e. SOM, DOM, iron and aluminum (hydr)oxide surfaces and clay); ii) the available concentrations of heavy metals (0.43 M HNO$_3$); iii) the pH, which was fixed at the measured value in the pH-stat; and iv) total solution concentrations of Na, K, Ca, Mg, Mn, Al, Si, Fe, Ba, Sr, SO$_4$, PO$_4$, Cl and CO$_3$, which were fixed at their measured values to fully account for the competitive adsorption between the heavy metals and major elements. The precipitation of minerals was suppressed during the calculation of the equilibrium speciation. Because preliminary calculations showed that the major competing ions Fe^{3+} and Al^{3+} in solution were close to equilibrium with their (hydr)oxides, the model was also run with the precipitation of these minerals allowed, using the extracted (rather than solution) concentrations of Fe and Al as input. The model predictions for the heavy metals were found to be virtually insensitive to this change in model setup.

Results and discussion

Selective chemical extractions

Results of the selective chemical extractions and other soil properties are given in Table 1. The results of the extraction of OM from the solid phase indicate that the total reactive organic matter content (FA+HA) amounts to about 46±14% of that of

the total organic matter determined by LOI (Table 1). This percentage is very similar to values estimated for sandy soils by Weng et al. (*4*) (between 16% and 46%) and for a variety of soils by Gustafson (*8*) (43±14)%.

Table 1. General characteristics and results of the selective chemical extractions of the soil samples used in this study.

Soil sample code	I	II	III	IV	V	VI	VII	VIII
Natural pH[a]	5.1	5.6	5.0	6.7	4.1	7.2	6.8	7.1
Loss On Ignition (LOI, %)[c]	3	4.2	2.6	3.9	nm[b]	3.8	4.5	3.1
Fraction < 2 µm (%)[d]	<1	4.8	3	<1	1.6	4.9	9.1	1.7
Fe-ASC (g Fe/kg)[e]	0.33	3.01	0.73	0.06	0.47	3.15	2.58	0.42
Fe-DITH (g Fe/kg)[e]	0.66	4.61	2.80	0.73	0.85	9.83	2.89	0.97
Al-OX (g Al/kg)[e]	1.06	1.30	0.90	0.06	2.94	0.42	1.19	0.99
Extractable HA (g C/kg d.m.)[f]	8.17	10.06	3.22	7.27	1.16	3.09	6.74	6.23
Extractable FA (g C/kg d.m.)[f]	1.92	1.68	1.62	1.04	0.48	1.69	2.48	2.14
Extractable OM (g C/kg d.m.)[f]	10.09	11.74	4.84	8.32	1.65	4.78	9.22	8.37
Reactive OM/ total OM (%)[g]	67	56	37	43	nm[b]	25	41	54

[a] Initial values measured in the pH-stat experiments (prior to addition of acid or base). Soil VI and VII: pH-H_2O measured according to the Dutch standard NEN 5750 (*42*). [b] n.m. = "not measured". [c] Loss On Ignition (LOI) determined as weight loss after 24 hours at 550 °C according to the Dutch standard NEN 5754 (*43*). [d] Determined by the pipette-method (based on Stokes' settling) according to the Dutch standard NEN 5753 (*37*). [e] Fe extracted by ascorbic acid or dithionite extraction (respectively, ASC and DITH,(*18*)), Al extracted by oxalate extraction (Al-OX, (*20*)), see text. [f] Estimated total content of reactive humic (HA) and fulvic (FA) acid in the samples determined by a method derived from Thurman and Malcolm (*14*), see text. [g] Apparent reactivity (%) of organic matter in the soil samples, expressed as g HA+FA extracted / g OM determined by Loss on Ignition (LOI), assuming that OM consists for 50% of elemental carbon. On average, the reactivity amounts to 46 ± 14 %.

pH stat leaching data and modeling results

Results of the pH-stat leaching procedure for Ni, Cu, Zn, Cd, and Pb are shown in Figure 1 together with total concentrations determined by acid digestion as well as concentrations determined by extraction with 0.43 M HNO_3. For reasons of clarity, only the results are shown here for soils I, IV, and VII, representing soils with a low, medium and high leachability of the studied metals, respectively. The results for the other soils are similar and are given in the Supporting Information.
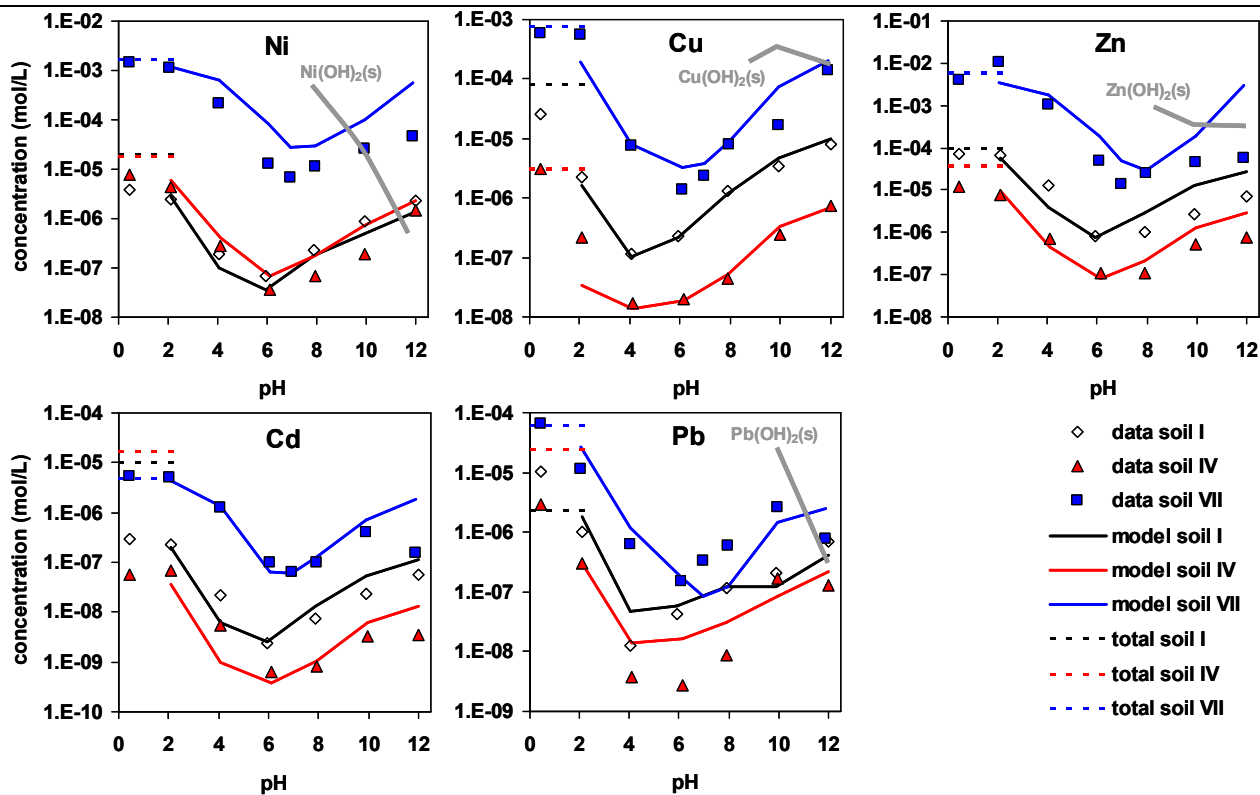
Figure 1. Leached concentrations and model predictions as a function of pH of Ni, Cu, Zn, Cd and Pb from the soil samples I, IV and VII. As an illustration, total contents (determined by acid digestion) are shown as horizontal dashed lines between pH 0-2. The concentrations "available" for adsorption, estimated by 0.43 M HNO_3 extraction (see text), are shown at pH 0.4. The solubility curves of potentially important metal hydroxides at high pH are illustrated for Ni, Cu, Zn and Pb (for reasons of clarity, only the solubility curves for soil IV are shown but curves obtained for soil I and VII are similar). The measurement of total content of Pb in soil I was below the detection limit. Results for the soils II, III, V, VI and VIII are provided in the supporting information.
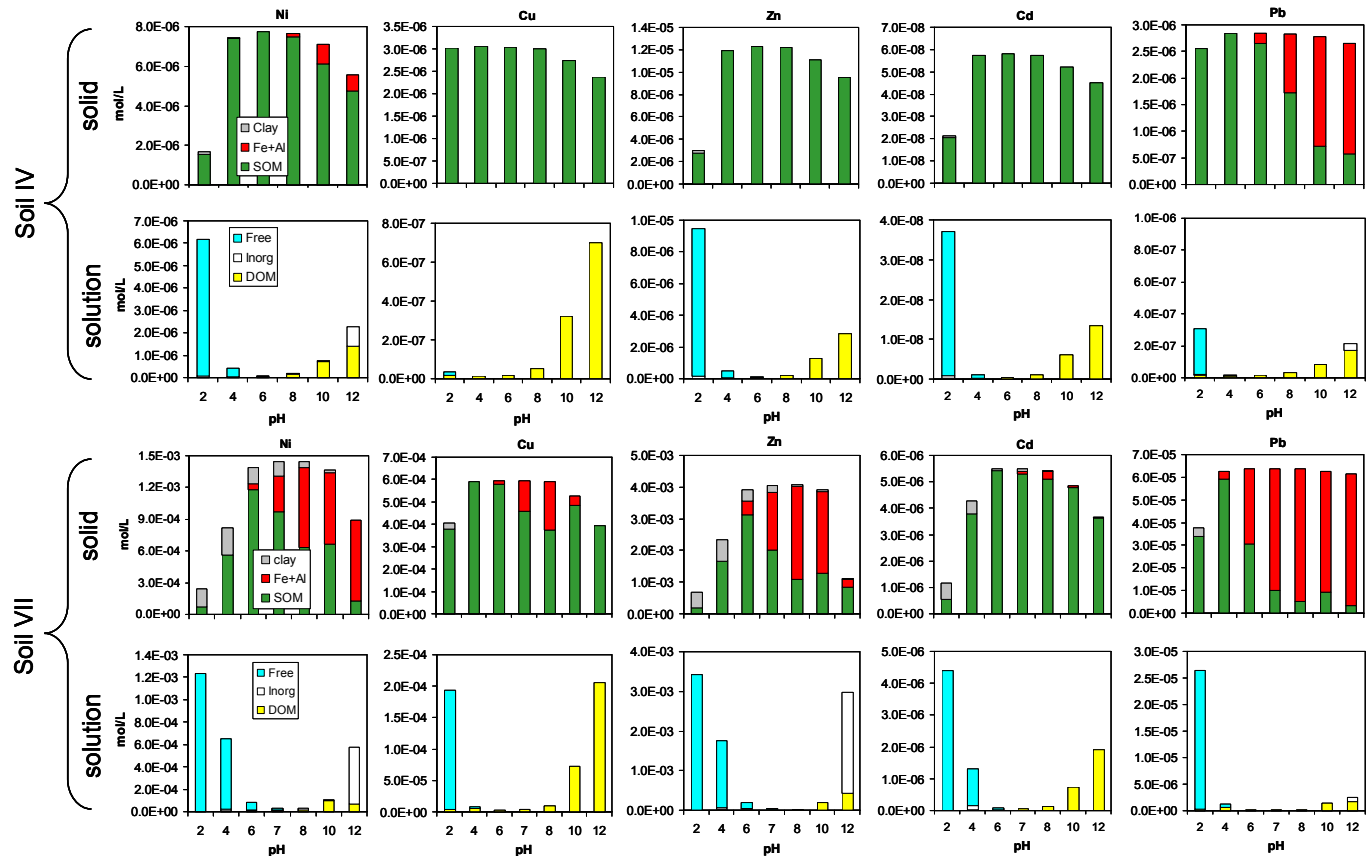
Figure 2. Calculation of the distribution of Ni, Cu, Zn, Cd and Pb among the different surfaces considered in the model. In the solid phase, "SOM" = solid organic matter;"Fe+Al" = the sum of amorphous Fe hydroxide, crystalline Fe(hydr)oxide and amorphous Al(hydr)oxide (proportions: 20, 37 and 43 % in soil IV and 51, 1 and 48 % in soil VII respectively); "Clay" = clay surfaces. In solution, "DOM" = dissolved organic matter; "Inorg" = inorganic complexes such as OH species; "Free" = free ions (Me^{2+}). Results for the soils II, III, V, VI and VIII are provided in the supporting information.

The leached concentrations of the heavy metals are generally much lower than the total concentrations and show a strong pH-dependence (Figure 1). Concentrations of heavy metals may drop over 2 orders of magnitude between pH 2 and neutral pH, and generally increase again from neutral pH toward strongly alkaline pH values resulting in "V-shaped" leaching curves. Common heavy metal minerals (hydroxides, carbonates, phosphates) were generally undersaturated by several orders of magnitude over almost the entire pH range, according to the calculated saturation indices. This indicates that sorption processes control leaching of heavy metals from these soils. The observed V-shaped leaching curves as a function of pH are well explained by the calculated speciation of the metals (Figure 2) which is discussed below. The model scenario used here incorporates sorption to solid and dissolved organic matter, iron and aluminum (hydr)oxide surfaces and clay, the major types of sorption processes in soils. Results of the modeling are presented as model "curves", which are actually separate model predictions for each data point (Figure 1).

The model predictions of heavy metal leaching are generally adequate and sometimes excellent, in particular for Ni, Cu, and Cd. Most of the leaching data can be described adequately over a wide range of pH and orders of magnitude changes in dissolved metal concentrations, without any fitting of parameters. In a number of cases, the model does not predict the leaching behavior adequately, in particular at (extremely) high pH values. For instance, in a number of cases concentrations of Cd, Pb and Zn show a sharp drop at pH 12 which is not predicted by the model (soils III, IV, and VII). The latter features may be caused by the precipitation of mineral phases, as illustrated in Figure 1 by solubility curves of a number of potentially important metal hydroxides. These curves were calculated considering all measured components and DHA and assuming the presence of an infinite amount of the metal hydroxide. For Cd, no mineral with a saturation index of close to zero in this pH range was found in our thermodynamic database. In general, systematic overprediction of solution concentrations toward higher pH values (such as observed in soil V) may be the result of an underestimate of the amounts of reactive surfaces in the soils. Furthermore, binding mechanisms that are not considered in the model at present may contribute to this effect. Dzombak and Morel (*33*) recommend considering surface precipitation in the model when [1] the dissolved sorbate concentration exceeds one-half the total amount of surface sites or [2] the sorbate concentration exceeds one

tenth of its solubility. Metal concentrations were in some cases close to compliance with these criteria. However, preliminary model runs using the surface precipitation reactions and constants of Zhu (*38*) for Ni, Cu, Zn, Cd and Pb sorption on HFO did not result in a consistent improvement of the model predictions when these criteria were met. Therefore, we have not further considered this process in our model in the present study.

Concentrations of Ni, Zn, and Cd seem to level off below pH 2 and show little or no increase between pH 2 and pH 0.4 (availability measurement with 0.43 M HNO_3). This suggests that at pH 2 desorption is virtually complete for these metals, and that a concentration measurement at this pH would provide an adequate estimate of the concentration available for adsorption processes. However, the observation that concentrations of Cu and Pb at pH 0.4 are generally much higher than those measured at pH 2 suggests that still a significant fraction of these elements is adsorbed at pH 2. This is supported by the model predictions (Figures 1 and 2). Furthermore, a large difference is observed in many cases between total content of heavy metals and the availability measured at pH 0.4, in particular for Cd in soils I – IV and VIII. It is noteworthy in this respect that nearly all Cd in these soils, contrary to the other metals, was liberated during the second digestion step (see experimental section) in which resistant Si matrixes are dissolved.

Speciation among the different reactive surfaces

With the model, we are able to investigate the relative importance of the different reactive surfaces in the soils as a function of pH. Even though the model descriptions are not in all cases adequate, particularly at strongly alkaline pH, this approach does provide a valuable indication of the relative importance of the different surfaces considered in the model. The calculated speciation in the solid and solution phase is given in Figure 2 for soils IV and VII (results for the other soils and elements are given in the Supporting Information). In general, organic matter is the predominant reactive surface in the solid phase, in particular for Cu, Ni, and Cd, over almost the entire pH range (Figure 2). These results are consistent with the well-recognized importance of organic matter in the complexation of heavy metals in soils (e.g., Buffle (*39*)) and correspond with the results of recent modeling studies (*3-8*). The

contribution of nonspecific adsorption to clay surfaces to overall adsorption is generally small, and only significant at low pH for Ni, Zn, and Cd in soils II, III, V-VII and Pb in soil VI. Adsorption to iron- and aluminum (hydr)oxides (referred to as "Fe+Al" in the figures) is the predominant binding mechanism for Zn in soils V and VI and Pb in soils II, III, and V-VIII at intermediate to high pH values. The observed differences between soils with respect to the element speciation in the solid phase correspond generally to the relative amounts of the reactive surfaces present in the soils. For instance, the ratio between extracted amount of "reactive" OM and the extracted amounts of iron and aluminum (hydr)oxides is relatively low in soil V and VI (derived from Table 1). Accordingly, iron and aluminum (hydr)oxides contribute significantly to the overall adsorption of all metals investigated around pH 8 in these soils (see speciation diagrams in the Supporting Information). The correlation between the total clay content and contribution of clay minerals to the overall adsorption in the low pH range is less pronounced. The observed differences between the investigated metals with respect to their distribution among the different reactive surfaces reflects their relative binding affinities for each of these surfaces (e.g., the extremely high affinity of Cu for adsorption to HA (*39*) relative to the other surfaces, and the high affinity of Pb for adsorption to both HFO (*33*) and HA (*39*)).

The speciation in the solution phase (Figure 2) is subdivided into "organic complexes", "inorganic complexes" and "free metal" (Me^{2+}). In general, the binding of metals to DOM constitutes by far the dominant solution complexation reaction at neutral to high pH values (in particular for Cu, Figure 2). The free Me^{2+} ions appear to be the predominant species below pH 4 for most metals. Of the inorganic species, OH complexes are significant at pH 12, CO_3-complexes at intermediate to alkaline pH values, and SO_4 and Cl complexes at low pH.

The calculated speciation explains the observed "V-shaped" leaching curves as function of pH. At low pH, heavy metal sorption to variably charged surfaces is generally weaker than at neutral pH values, due to competition for surface sites by protons and repulsive charge effects. At neutral to slightly alkaline pH, cation sorption generally increases due to deprotonation of the surface sites and the more favorable surface charge of (hydr)oxide minerals and organic matter, resulting in lower solution concentrations. At alkaline pH values, sorption to the solid surfaces is reduced due to inorganic and organic complexation of cations in solution. Toward higher pH values,

complexation with dissolved organic matter becomes more important because of the increased DOC concentrations in solution (see pH-dependent leaching curves of DOC in the Supporting Information).

The model predictions shown rely strongly on model parameters derived in the laboratory for well-characterized materials, while the conditions met in natural, heterogeneous soils may be very different from these model systems. Preliminary calculations showed a strong dependency of the model predictions on input parameters such as the available metal concentrations or the amount of SOM, indicating that measured input sorption parameters represent a source of uncertainty that warrants careful consideration. The assumption of taking HFO as "surrogate" for amorphous aluminum (hydr)oxides in the model may also introduce uncertainty. Further modelling challenges are to include a model for the pH dependent leaching of DOC (e.g., refs *40* and *41*), as well as to predict soil pH and buffering processes.

The combination of pH-static leaching tests, selective chemical extractions and a mechanistically based modeling approach as used in this study has been shown to be promising, because it leads to a more fundamental understanding of pH-dependent leaching processes in soils over a wide range of conditions. The "multisurface" modeling approach is able to capture the most essential features of the pH-dependency of leaching, and in most cases, adequately predicts the leaching of heavy metals from contaminated soils without any fitting of parameters. As such, this approach may contribute to further our understanding of the relationships between metal content, leaching and (bio)availability in contaminated soils.

Acknowledgments

Supporting information available

Figures containing measurements and model results for soils II, III, V, VI, and VIII. This material is available free of charge via the Internet at http://pubs.acs.org.

Literature cited

1. McBride, M. B.; Sauve, S.; Henderschot, W. Solubility control of Cu, Zn, Cd and Pb in contaminated soils. *Eur. J. Soil Sci.* 1997, 48, 337-346.

2. Sauve, S.; Henderschot, W.; Allen, H. E. Solid-solution partitioning of metals in contaminated soils: dependence on pH, total metal burden, and organic matter. *Environ. Sci. Technol.* 2000, 34, 1125-1131.

3. Weng, L.; Temminghoff, E. J. M.; Lofts, S.; Tipping, E.; van Riemsdijk, W. H. *Environ. Sci. Technol.* 2002, 36, 4804-4810.

4. Weng, L.; Temminghoff, E. J. M.; van Riemsdijk, W. H. Contribution of individual sorbents to the control of heavy metal activity in sandy soil. *Environ. Sci. Technol.* 2001, 35, 4436-4443.

5. Temminghoff, E. J. M.; van der Zee, S. E. A. T. M.; de Haan, F. A. M. Copper mobility in a copper contaminated sandy soil as affected by pH and dissolved organic matter. *Environ. Sci. Technol.* 1997, 31, 1109-1115.

6. Tipping, E.; Rieuwerts, J.; Pan, G.; Ashmore, M. G.; Lofts, S.; Hill, M. T. R.; Farago, M. E.; Thornton, I. The solid-solution partitioning of heavy metals (Cu, Zn, Cd, Pb) in upland soils of England and Wales. *Environ. Pollut.* 2003, 125, 213-225.

7. Cances, B.; Ponthieu, M.; Castrec-Rouelle, M.; Aubry, E.; Benedetti, M. F. Metal ions speciation in a soil and its solution:experimental data and model results. *Geoderma* 2003, 113, 341-355.

8. Gustafson, J. P.; Pechova, P.; Berggren, D. Modeling metal binding to soils: the role of natural organic matter. *Environ. Sci. Technol.* 2003, 37, 2767-2774.

9. Voegelin, A.; Vulava, V. M.; Kretzschmar, R. Reaction-based model describing competitive sorption and transport of Cd, Zn, and Ni in an acidic soil. *Environ. Sci. Technol.* 2001, 35, 1651-1657.

10. Lofts, S.; Tipping, E. An assemblage model for cation binding by natural particulate matter - Description of pH dependency, salt dependency, and cation-proton exchange. *Geochim. Cosmochim. Acta* 1998, 62, 2609-2625.

11. Kosson, D. S.; van der Sloot, H. A.; Sanchez, F.; Garrabrants, A. C. An integrated framework for evaluating leaching in waste management and utilization of secondary materials. *Env. Eng. Sci.* 2002, 19, 159-204.

12. Sloot van der, H. A.; Comans, R. N. J.; Hjelmar, O. Similarities in the leaching behaviour of trace contaminants from waste, stabilized waste, construction materials and soils. *Sci. Tot. Environ.* 1996, 178, 111-126.

13.   Meima, J. A.; Comans, R. N. J. Geochemical modelling of weathering reactions in MSWI bottom ash. *Environ. Sci. Technol.* 1997, 31, 1269-1276.

14.   Thurman, E. M.; Malcolm, R. L. Preparative isolation of aquatic humic substances. *Environ. Sci. Technol.* 1981, 15, 463-466.

15.   Van Zomeren, A.; Comans, R. N. J. Measurement of humic and fulvic acid concentrations and dissolution properties by a rapid batch procedure. *Environ. Sci. Technol*, submitted.

16.   Lord, C. J. *The chemistry and cycling of iron, manganese, and sulfur in salt marsh sediments.* Ph.D. Dissertation, University of Delaware, 1980.

17.   Canfield, D. E. *Sulfate reduction and diagenesis of iron in anoxic marine sediments.* Ph.D. Dissertation, Yale University, 1988.

18.   Kostka, J. E.; Luther III, G. W. Partitioning and speciation of solid phase iron in saltmarsh sediments. *Geochim. Cosmochim. Acta* 1994, 58, 1701-1710.

19.   Ferdelman, T. G. *The distribution of sulfur, iron, manganese, copper, and uranium in a saltmarsh sediment core as determined by a sequential extraction method.* MSc. thesis, University of Delaware, 1988.

20.   Blakemore, L. C.; Searle, P. L.; Daly, B. K. *Methods for chemical analysis of soils*; Science Report 80; NZ Soil Bureau: Lower Hutt, New Zealand, 1987.

21.   Houba, V. J. G.; van der Lee, J. J.; Novozamsky, I.; Wallinga, I. *Soil and Plant Analysis, A series of syllabi: Part 5. Soil Analysis Procedures.* Wageningen Agricultural University: Wageningen, The Netherlands, 1989.

22.   Gooddy, D. C.; Shand, P.; Kinniburgh, D. G.; van Riemsdijk, W. H. Field-based partition coefficients for trace elements in soil solutions. *Eur. J. Soil Sci.* 1995, 46, 285.

23.   Boekhold, A. E.; Temminghoff, E. J. M.; van der Zee, S. E. A. T. M. Influence of electrolyte composition and soil pH on Cd sorption by an acid sandy soil. *J. Soil Sci.* 1993, 44, 85-96.

24.   Meeussen, J. C. L. ORCHESTRA: An object-oriented framework for implementing chemical equilibrium models. *Environ. Sci. Technol.* 2003, 37, 1175-1182.

25.   Allison, J. D.; Brown, D. S.; Novo-gradac, K. J. MINTEQA2/PRODEFA2, Geochemical assessment model for environmental systems: version 3.11 databases and version 3.0 user's manual; Environmental Research Laboratory, US-EPA: Athens, GA, 1991.

26.   Benedetti, M. F.; Milne, C. J.; Kinniburgh, D. G.; van Riemsdijk, W. H.; Koopal, L. K. Metal ion binding to humic substances: application of the non-ideal competitive adsorption model. *Environ. Sci. Technol.* 1995, 29, 446-457.

27. Kinniburgh, D. G.; Milne, C. J.; Benedetti, M. F.; Pinheiro, J. P.; Filius, J.; Koopal, L. K.; van Riemsdijk, W. H. Metal ion binding by humic acid: application of the NICA-Donnan model. *Environ. Sci. Technol.* 1996, 30, 1687-1698.

28. Kinniburgh, D. G.; van Riemsdijk, W. H.; Koopal, L. K.; Borkovec, M.; Benedetti, M. F.; Avena, M. Ion binding to natural organic matter: competition, heterogeneity, stoichiometry and thermodynamic consistency. *J. Colloid Surf. A* 1999, 151, 147-166.

29. Dijkstra, J. J.; van der Sloot, H. A.; Comans, R. N. J. Process identification and model development of contaminant transport in MSWI bottom ash. *Waste Manage.* 2002, 22, 531-541.

30. Milne, C. J.; Kinniburgh, D. G.; Tipping, E. Generic NICA-Donnan model parameters for proton binding by humic substances. *Environ. Sci. Technol.* 2001, 35, 2049-2059.

31. Milne, C. J.; Kinniburgh, D. G.; van Riemsdijk, W. H.; Tipping, E. Generic NICA-Donnan model parameters for metal-ion binding by humic substances. *Environ. Sci. Technol.* 2003, 37, 958-971.

32. De Wit, J. C. M. *Proton and metal ion binding by humic substances;* Ph.D. Dissertation, Wageningen University, 1992.

33. Dzombak, D. A.; Morel, F. M. M. *Surface complexation modeling: hydrous ferric oxide*; John Wiley & Sons: New York, 1990.

34. Meima, J. A.; Comans, R. N. J. Application of surface complexation/precipitation modelling to contaminant leaching from weathered municipal solid waste incinerator bottom ash. *Environ. Sci. Technol.* 1998, 32, 688-693.

35. Hiemstra, T.; de Wit, J. C. M.; van Riemsdijk, W. H. Multisite proton adsorption modeling at the solid/solution interface of (hydr)oxides: a new approach, II. application to varous important (hydr)oxides. *J. Colloid Interface Sci.* 1989, 133, 105-117.

36. McBride, M. B. *Environmental Chemistry of Soils*; Oxford University Press: New York, 1994.

37. *Soil; Determination of clay content and particle size distribution of soil samples by sieve and pipet (NEN 5753:1994);* NEN (Netherlands Standardisation Institute): The Netherlands, 1994.

38. Zhu, C. Estimation of surface precipitation contants for sorption of divalent metals onto hydrous ferric oxide and calcite. *Chem. Geol.* 2002, 188 , 23-32.

39. Buffle, J. *Complexation reactions in aquatic systems*; Ellis Horwood Ltd.: Chichester, U.K., 1988.

40. Filius, J. D.; Meeussen, J. C. L.; Lumsdon, D. G.; Hiemstra, T.; van Riemsdijk, W. H. Modelling the adsorption of fulvic acid by goethite. *Geochim. Cosmochim. Acta* 2003, 67, 1463-1474.

41. Lumsdon, D. G. Partitioning of organic carbon, aluminium and cadmium between solid and solution in soils: application of a mineral-humic particle additivity model. *Eur. J. Soil Sci.* 2004, 55, 271-285.

42. *Soil; Determination of pH in soil samples* (NEN 5750:1989), NEN (Netherlands Standardisation Institute): The Netherlands, 1989.

43. *Soil; Determination of organic matter content in soil as loss-on-ignition* (NEN 5754:1992). NEN (Netherlands Standardisation Institute), The Netherlands, 1992.

Supporting Information

Chapter 3

Contents (Figures S1-S6):

- Experimental and modeling results for the soils II, III, V, VI and VIII
- pH-concentration diagrams for dissolved organic carbon (DOC) in pH-stat leachates
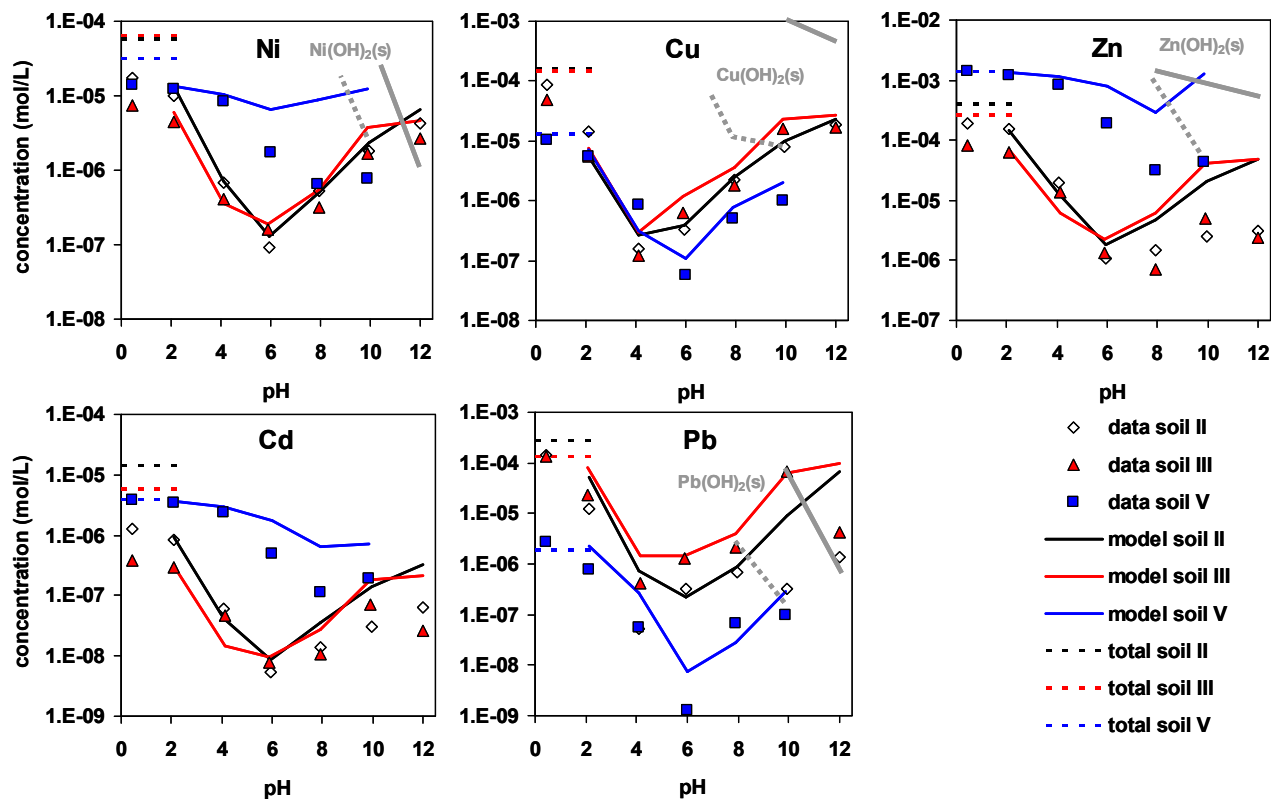
Figure S1. Leached concentrations and model predictions as a function of pH of Ni, Cu, Zn, Cd and Pb from the soil samples II, III and V. As an illustration, total contents (determined by acid digestion) are shown as horizontal dashed lines between pH 0-2. The concentrations "available" for adsorption, estimated by 0.43 M HNO$_3$ extraction (see text), are shown at pH 0.4. The solubility curves of potentially important metal hydroxides at high pH are illustrated for Ni, Cu, Zn and Pb (for reasons of clarity, curves for soil III are shown as solid lines, for soil V as dashed lines. The curves obtained for soil II were similar to soil III). The measurement of total content of Pb in soil V was below the detection limit.
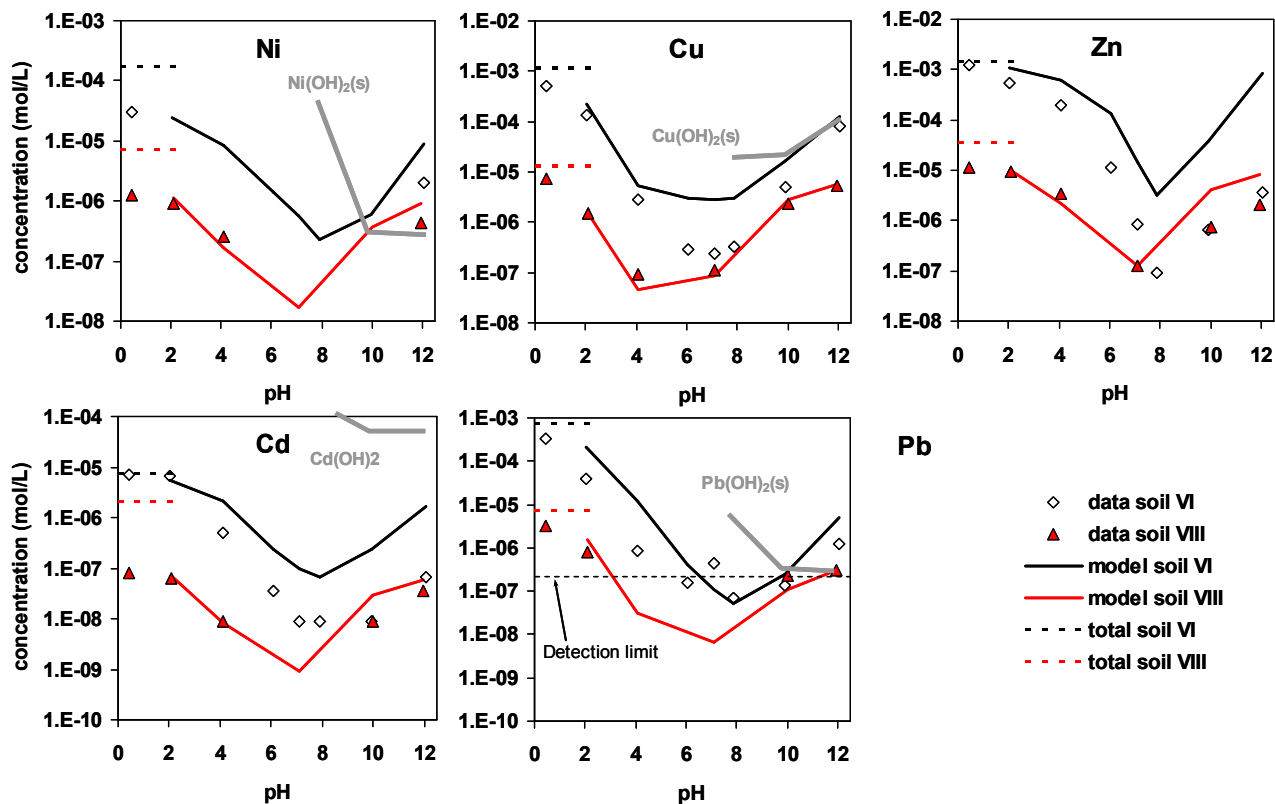
Figure S2. Leached concentrations and model predictions as a function of pH of Ni, Cu, Zn, Cd and Pb from the soil samples VI and VIII. As an illustration, total contents (determined by acid digestion) are shown as horizontal dashed lines between pH 0-2. The concentrations "available" for adsorption, estimated by 0.43 M HNO_3 extraction (see text), are shown at pH 0.4. The solubility curves of potentially important metal hydroxides at high pH are illustrated for Ni, Cu, Zn and Pb (for reasons of clarity, only curves for soil VI are shown, curves obtained for soil VIII were similar). In soil VI, Ni was not measured between pH 2 and 10.

Figure S3. Calculation of the distribution of Ni, Cu, Zn, Cd and Pb among the different surfaces considered in the model. In the solid phase, "SOM" = solid organic matter; "Fe+Al" = the sum of amorphous Fe hydroxide, crystalline Fe(hydr)oxide and amorphous Al(hydr)oxide (proportions: 13, 2 and 85 % in soil I and 50, 4 and 45 % in soil II respectively); "Clay" = clay surfaces. In solution, "DOM" = dissolved organic matter; "Inorg" = inorganic complexes such as OH species; "Free" = free ions (Me^{2+}).
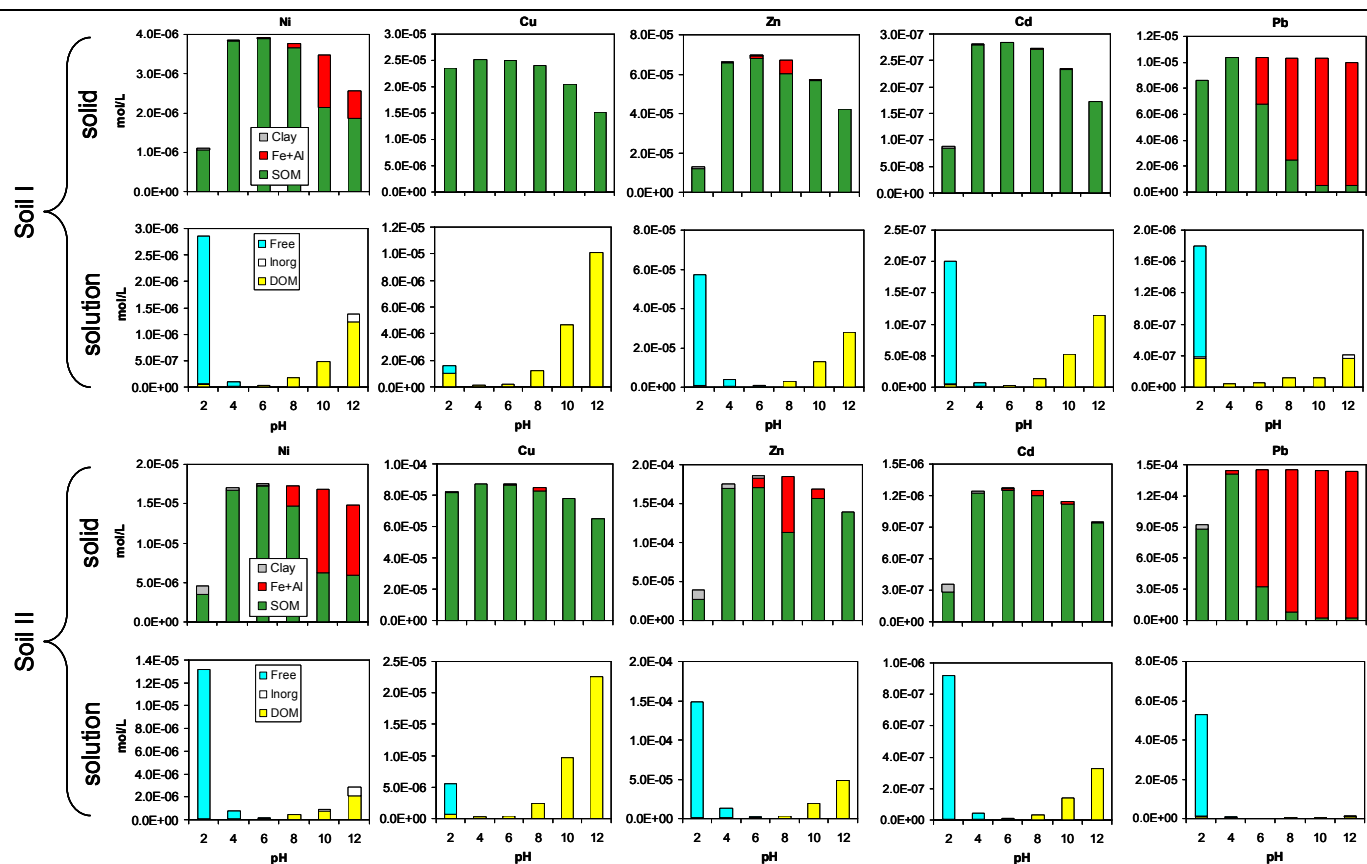
Figure S4. Calculation of the distribution of Ni, Cu, Zn, Cd and Pb among the different surfaces considered in the model. In the solid phase, "SOM" = solid organic matter; "Fe+Al" = the sum of amorphous Fe hydroxide, crystalline Fe(hydr)oxide and amorphous Al(hydr)oxide (proportions: 25, 12 and 64 % in soil III and 7, 1 and 92 % in soil V respectively); "Clay" = clay surfaces. In solution, "DOM" = dissolved organic matter; "Inorg" = inorganic complexes such as OH species; "Free" = free ions (Me^{2+}).
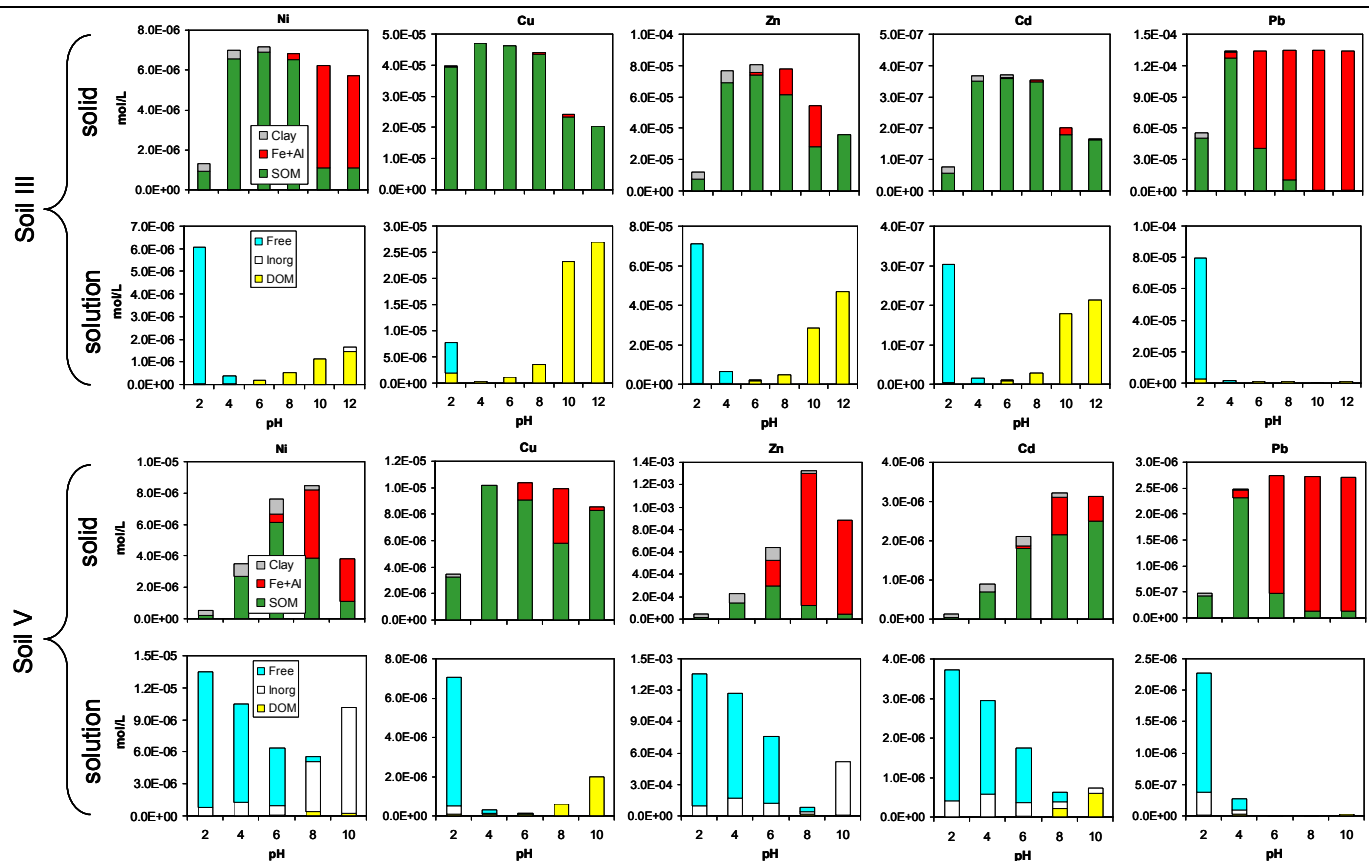
Figure S5. Calculation of the distribution of Ni, Cu, Zn, Cd and Pb among the different surfaces considered in the model. In the solid phase, "SOM" = solid organic matter; "Fe+Al" = the sum of amorphous Fe hydroxide, crystalline Fe(hydr)oxide and amorphous Al(hydr)oxide (proportions: 61, 22 and 17 % in soil VI and 16, 4 and 80 % in soil VIII respectively); "Clay" = clay surfaces. In solution, "DOM" = dissolved organic matter; "'Inorg" = inorganic complexes such as OH species; "Free" = free ions (Me^{2+}).

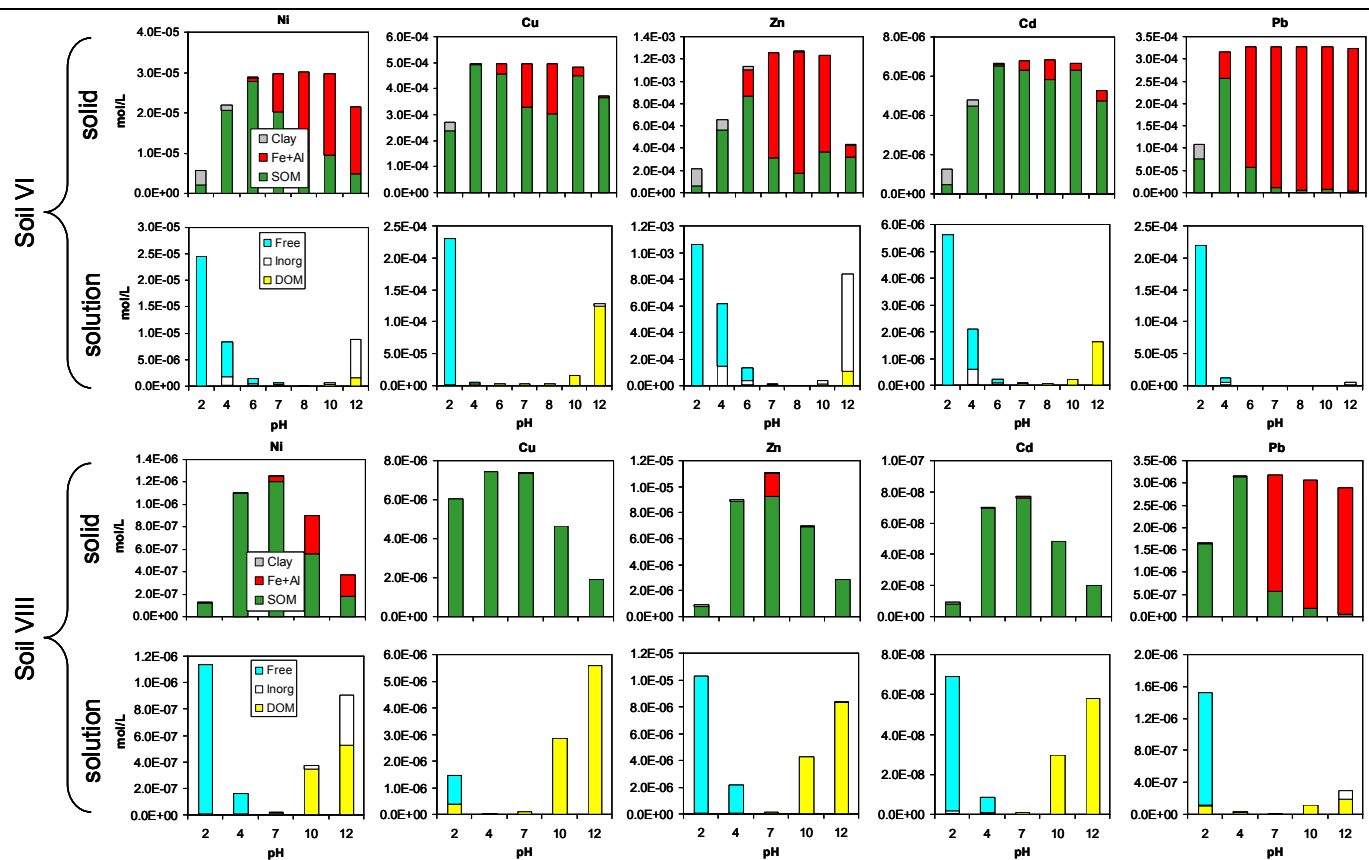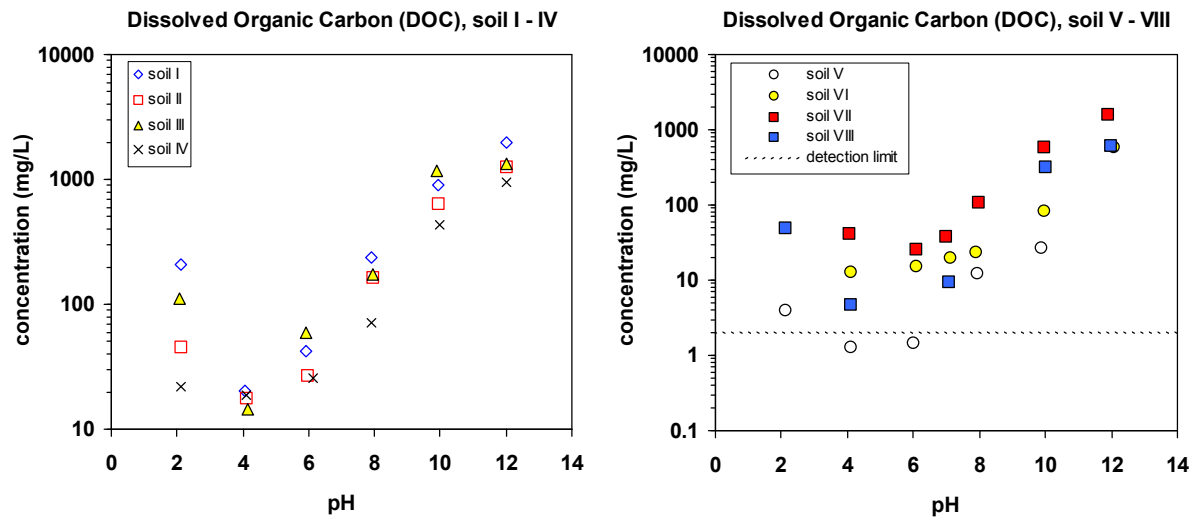Figure S6: Measured solution concentrations of dissolved organic carbon (DOC) in mg/L as a function of pH in each of the pH-stat leachates.

Chapter 4

The leaching of major and trace elements
from MSWI bottom ash
as a function of pH and time

Abstract

In this paper, the leaching behaviour of major components (Al, Ca, SO_4, Mg, Si, Fe, Na and DOC) and trace elements (Ni, Zn, Cd, Cu, Pb, Mo and Sb) from MSWI bottom ash is studied as a function of time over a wide range of pH, under pH-controlled conditions. Equilibrium geochemical modelling using the modelling framework ORCHESTRA is used to enable a process-based interpretation of the results and to investigate whether "equilibrium" is attained during the time scale of the experiments. Depending on the element and setpoint-pH value, net concentration increases or decreases of up to one order of magnitude were observed. Different concentration–time trends (increase or decrease) are observed in different pH ranges. The direction of the concentration–time trends depends on: (1) the shape of the "equilibrium" solubility curve, and (2) the position of the setpoint-pH in the leaching test relative to the natural pH of the sample. Although the majority of the elements do not reach steady state, leached concentrations over a wide pH range have been shown to closely approach "equilibrium" model curves within an equilibration time of 168 h. The different effects that leaching kinetics may have on the pH dependent leaching patterns have been identified for a wide range of elements, and can generally be explained in a mechanistic way. The results are in support of the currently prescribed equilibration time of 48 h in the European standard for the pH-static leaching test (TS14997). Finally, this study demonstrates that pH-static leaching experiments such as described in the European standards (TS14497 and TS14429), in combination with selective chemical extractions and a mechanistically based modelling approach, constitute a powerful set of tools for the characterization of leaching processes in waste materials over a wide range of conditions.

Introduction

The risks associated with the presence of potentially hazardous constituents in waste materials, with respect to their mobility and ecotoxicological significance, are determined by their leaching potential rather than their total content (*1, 2*). The evaluation of the pH dependency of leaching is an important tool in the assessment of the expected long-term leaching behaviour of materials in utilization/disposal scenarios (*1*). Standardized protocols for pH-dependence leaching tests for waste materials have been developed in the European standardization organization CEN (TS14997 and TS14429 (*3, 4*)). In addition, the measurement of the pH dependency of leaching provides an adequate basis for the investigation of the underlying leaching mechanisms using mechanistic geochemical modelling (e.g., *5-8*).

Municipal solid waste incineration (MSWI) bottom ash is a commonly used reference material for leaching studies, for it is the most significant residual waste stream from MSW incineration and is re-used in many countries (*7*). In addition, the material is known for its complex physicochemical characteristics and metastable mineralogical composition (*9, 10*). The pH-dependent leaching of major elements from MSWI bottom ash has been shown to be often controlled by the dissolution of common minerals (*6*), whereas in weathered bottom ash, heavy metals are presumably controlled by sorption to neoformed Fe- and Al (hydr)oxides (*7, 8, 11*).

However, literature focusing on the time dependency of leaching of constituents from MSWI residues is relatively scarce (*12-17*). This lack of information is remarkable, considering that leaching tests are generally believed to resemble long-term leaching processes in the field, for which usually "local equilibrium" is assumed. Kirby and Rimstidt (*16*) distinguished four different concentration–time patterns that elements may show upon contact of MSWI bottom ash with water, i.e., (1) rapid dissolution of a phase until exhaustion; (2) dissolution until equilibrium is obtained; (3) dissolution of a phase that does not reach equilibrium over the course of the experiment and (4) rapid dissolution of a phase until exhaustion (pattern 1) followed by a slower dissolution of a less soluble phase. A fifth pattern, not considered by Kirby and Rimstidt (*16*), is a concentration decrease. It should be noted that concentration–time patterns that elements display may be the result of

dissolution/precipitation of minerals (congruent or incongruent), as well as sorption/desorption processes.

In the studies cited above, the elements in soluble salts (e.g., Na, K, Cl) generally show pattern 1, whereas solubility controlled elements (e.g., Fe, Al, Ca, S, Mg) and heavy metals (Pb, Zn, Cu) show patterns anywhere between 2 and 4. A decrease over time (pattern 5) was found in several cases, e.g., for Si (*15*), for Pb and Cd (*16*) and, Pb and Cr (*17*).

Most of the above cited studies are performed at the "natural" pH of the bottom ash samples, which for fresh samples is usually alkaline (pH 10–12) and for weathered samples around pH 8 (*6*). As the pH is generally allowed to vary over time in leaching studies, a mechanistic interpretation of the leaching kinetics is complicated as the leaching of most environmentally relevant elements is strongly dependent on pH (e.g., *1,9*). Therefore, when the purpose is to study the underlying geochemical leaching processes and their kinetics, a test method with controlled pH is preferred over a test method with no or initial acid/base addition. In the latter case, the pH may not be assumed truly constant due to potentially slow buffering processes. However, largely similar results are found with both methods as long as the leached amounts are plotted as a function of (end-) pH (*18*).

In this paper, the leaching behaviour of major components (Al, Ca, SO_4, Mg, Si, Fe, Na and DOC) and trace elements (Ni, Zn, Cd, Cu, Pb, Mo and Sb) from MSWI bottom ash is studied as a function of time over a wide range of pH under pH-controlled conditions. The objective of this paper is to provide a mechanistic insight into the time dependency of the leaching of major and trace elements over a wide pH range, with the focus on the underlying geochemical processes. The time dependency of leaching is evaluated between 3 and 168 h, which is in the range of typical equilibration times for laboratory leaching experiments.

The purpose was not to compare observed dissolution rates in the experiments with known dissolution rates of pure phases (e.g., *19-21*). Such a comparison requires knowledge on typically unknown parameters such as the quantities, crystallinity and specific surface area of these minerals in the bottom ash matrix. In addition, dissolution rates may be obscured by the precipitation of secondary phases, and the rates at which elements are released from the bottom ash matrix may also be influenced by physical processes such as intraparticle diffusion (*17*).

In this study, equilibrium geochemical modelling using the ORCHESTRA modelling framework (*22*), is used to evaluate to what extent "equilibrium" is attained with respect to mineral dissolution/precipitation and adsorption processes, for a wide range of major and trace elements. It should be noted that true thermodynamic equilibrium might not be attained in the experiments, as slow mineral transformations (e.g., Ostwald step rule; (*23*)) may take place over longer time scales.

The predictive modelling approach as deployed in this study has been applied previously to MSWI bottom ash (*6, 8, 11*) and is based on mineral dissolution/precipitation reactions, adsorption processes to reactive surfaces present in the MSWI bottom ash matrix and complexation reactions in the leachates. The modelling approach is expanded with a mechanistic description of metal complexation with dissolved organic C (DOC), in accordance with recent developments on the characterization and quantification of solid and dissolved organic matter in MSWI bottom ash leachates (*24, 25*). Finally, possible implications that the results have on test settings are discussed.

Materials and methods

MSWI Bottom ash samples

A freshly quenched MSWI bottom ash sample was collected from the same Dutch MSWI plant from which samples were collected for the authors' earlier studies (*6, 11*). The sample has a natural pH of about 10.6 in a suspension of L/S 10 (L/kg), which is typical for freshly quenched MSWI bottom ash (*6*).

pH-static leaching experiments

The dataset was collected at the authors' institute in 1998 and was later used as a contribution to discussions on test settings for the pH-dependent leaching tests developed in CEN/TC292 (TS14429 and TS14997, refs *3* and *4*). Below a detailed description of the followed pH-static leaching protocol will be provided (e.g., as used by Meima and Comans (*6*)) as it may differ from the present version of TS14997. An air-dried MSWI bottom ash sample was crushed to <2 mm (using a jaw crusher) and divided in 5 test portions, which were each subjected to batch leaching in acid-cleaned

300 mL PTFE vessels at a liquid to solid (L/S) ratio of 10 L/kg (25 g dry bottom ash and 250 mL nanopure demineralized water) and a total equilibration time of 168 h. Each suspension was brought to a specific pH value (pH 4, 6, 8, 10 or 12), which was kept constant for the total duration of the experiment using a computerized pH-stat system. Solutions of 1 N HNO_3 and NaOH (analytical grade) were used to maintain the pH of the suspensions, which were continuously stirred and kept at a constant temperature of 20 °C using thermostatic jackets. The vessels are equipped with a small opening serving as outlet for gases that may form upon reaction of bottom ash with water, but the exchange with the atmosphere is kept minimal to prevent uptake of $CO_2(g)$. Dosage of acid and base started about 10 min after the start of the experiment, when a relatively stable initial pH value was measured ("natural" pH of the sample, ~10.6). At different equilibration times (3, 6, 24, 48 and 168 h), the suspensions were allowed to settle for 15 min and small aliquots of 5 mL of the upper liquid were taken and immediately filtered through 0.2 μm membrane filters. The filters were precleaned with nanopure demineralized water, and the first approximately 2 mL of the filtrate was discarded. The clear filtrates were acidified with concentrated HNO_3 (suprapure) and analyzed by ICP-AES to obtain solution concentrations of Na, K, Ca, Mg, Mn, Al, Si, Fe, Ba, Sr, Zn, Cu, Mo, Cd, Ni, Sb, Pb, S and P. It was assumed that total S and P as measured by ICP-AES represented SO_4 and PO_4, respectively. A Shimadzu carbon analyzer was used to determine CO_3 and DOC in unacidified subsamples. Concentrations of NO_3 were derived from acid dosage in the pH-stat procedure. Chloride concentrations were not measured but were assumed to roughly balance the measured Na concentrations, as observed in similar MSWI bottom ash leachates (*6*). The calculated charge balance of the leachates ranged from -6% (pH 4) to +16% (pH 6), which is typical for many waste leachates (unpublished results).

Estimates of the amount of reactive surfaces

Independent estimates of the amount of reactive surfaces present in the bottom ash matrix, needed for sorption modelling, were made by selective chemical extractions. The amount of amorphous and crystalline Fe (hydr)oxides in the bottom ash matrix was estimated by a dithionite extraction described in Kostka and Luther (*26*), and will be referred to as Fe–DITH. The portion of amorphous Fe (hydr)oxides

was estimated by an ascorbate extraction according to Ferdelman (*27*) described in Kostka and Luther (*26*), and will be referred to as Fe–ASC. The amount of amorphous Al (hydr)oxides was estimated by an oxalate extraction according to Blakemore et al. (*28*) and will be referred to as Al–OX. Assumptions on the concentrations of "reactive" organic C in the solid and solution phase were derived from van Zomeren and Comans (*24*) (see "model description"). The results of the selective chemical extractions are summarized in Table 1.

Table 1. Results of the selective chemical extractions to estimate sorption parameters and assumed reactivity of solid and dissolved organic carbon.

	DHA[a] % DOC	DFA[a] % DOC	THA[b] g C /kg	TFA[b] g C/kg	Fe-ASC[c] g Fe/kg	Fe-DITH[c] g Fe/kg	Al-OX[c] g Al/kg
Value	0.2	19.7	0.086	0.228	1.92	12.66	4.71

[a] Reactivity of dissolved organic carbon (DOC) as measured at pH 10.39 in a similar MSWI bottom ash sample by van Zomeren and Comans (*24*), expressed in percentage of total DOC in solution. DHA = dissolved humic acid; DFA = dissolved fulvic acid.
[b] Total amounts of humic acid (THA) and fulvic acid (TFA), measured by van Zomeren and Comans (*24*) in a similar MSWI bottom ash sample.
[c] Results of the selected chemical extractions, Fe extracted by ascorbic acid or dithionite (respectively, Fe-ASC and Fe-DITH, (*26*)), Al extracted by oxalate extraction (Al-OX, (*28*)).

Geochemical modelling

Mineral saturation indices, solution speciation, and sorption processes were calculated with the ORCHESTRA (*22*) modelling framework, in which the different sub-models described below were implemented. Solution speciation was calculated using thermodynamic data from the MINTEQA2 (*29*) database, version 3.11, in combination with the Non-Ideal Competitive Adsorption (NICA)-Donnan model (*30-32*) to include metal complexation with dissolved organic matter, see further below. For general changes to the MINTEQA2 database for the present work Dijkstra et al. (*8*) is referred to. Species activities were calculated with the Davies equation as ionic strengths in the leachates were up to 0.2 M, at which Debye–Hückel is not applicable (*33*). An oxidizing environment was assumed in all calculations (pH + pe = 15) in accordance with measured redox potentials in similar MSWI bottom ash samples (*6*).

Binding to solid and dissolved organic matter

Specific and non-specific sorption of protons and metal ions to organic matter was modelled with the NICA-Donnan model (*32*) using the set of "generic" binding parameters and constants of Milne et al. (*34, 35*) for FA and HA. The amounts of "reactive" organic C in the solid and the solution phase were assumed to be identical to the values measured in a sample from the same incinerator by van Zomeren and Comans (*24*), therein referred to as "QUE1". In the study of van Zomeren and Comans (*24*), the amount of humic and fulvic acid (referred to as HA and FA, respectively), was determined by the procedure of Thurman and Malcolm (*36*) currently recommended by the International Humic Substances Society (IHHS). In the solution phase, 19.7% FA and 0.2% HA (relative to total DOC) as measured by van Zomeren and Comans (*24*) at the natural pH of the QUE1 sample (10.39) was assumed for all the leachates. In the solid phase, the total amounts of HA (0.086 g C/kg) and FA (0.228 g C/ kg) as measured in the QUE1 sample were assumed (after correction for the amounts of HA and FA in solution). It was assumed that 50% of FA and HA consists of C (*37*). The recommended "generic" parameters for binding to HA and FA of Milne et al. (*34, 35*) were included in the model for H, Ba, Sr, Ca, Mg, Mn, Fe(II), Fe(III), Al, Ni, Cu, Zn, Cd and Pb.

Binding to Fe/Al (hydr)oxides

To take surface complexation and surface precipitation to Fe (hydr)oxide surfaces into account, the Generalized Two Layer Model (GTLM) of Dzombak and Morel (*38*) was used. For the determination of the required adsorption parameters, the approach of Meima and Comans (*11*) was followed. The total amount of amorphous Fe (hydr)oxides was calculated from Fe–ASC and represented by hydrous ferric oxide ("HFO") in the model. Similar to Meima and Comans (*11*), amorphous Al-(hydr)oxides were considered as potentially important sorbent minerals, for which HFO was taken as a surrogate sorbent in the model. The reason for this approach is the absence of a complete and systematic database for sorption reactions on Al (hydr)oxides. For a justification of this approach, based on similarities in the surface structure and reactivity of Al and Fe (hydr)oxides, the reader is referred to Meima and Comans (*11*). Following the approach of Meima and Comans (*11*) the extracted Al

(hydr)oxides and HFO were treated equally in the model assuming 1 mol of Al–OX = 1 mol of Fe–ASC. The by Dzombak and Morel (*38*) recommended specific surface area of 600 m²/g was used to calculate site densities for the amorphous Fe and Al (hydr)oxides. HFO was also used as a surrogate sorbent mineral for crystalline Fe (hydr)oxide surfaces, however, site densities were calculated using a specific surface area of 100 m²/g (*39*). The total amount of crystalline Fe (hydr)oxides was calculated from the difference between Fe–DITH and Fe–ASC. The estimated total amounts of Fe- and Al (hydr)-oxides that serve as input in the adsorption models were corrected for the dissolution of these phases, by simply subtracting the measured solution concentrations of Fe and Al at each pH value, for each time step.

The surface complexation constants of Dzombak and Morel (*38*) were included in the model for H, Ca, Ba, Sr, Mn, Mg, Ni, Cu, Zn, Cd, Pb, Sb, Mo, H_4SiO_4, SO_4 and PO_4. The original surface complexation constant for the low-affinity site for Pb was considered by Dzombak and Morel (*38*) to be an underestimate. A higher log *K* value of 1.7 was used in the calculations to be consistent with the general trend of an approximately 3 log-unit difference between the sorption constants for the high and low-affinity sites (*38*).

The surface precipitation model (SPM) is an integral part of the GTLM (*38*). Dzombak and Morel (*38*) recommend consideration of surface precipitation when [1] the dissolved sorbate concentration exceeds half the total amount of surface sites or [2] when the sorbate concentration exceeds one tenth of its solubility. Based on the above estimates of the amount of surface sites, none of the heavy metals comply with these criteria in the leachates. However, similar to the results of Meima and Comans (*11*) and Dijkstra et al. (*8*), an adequate description for Zn using the GTLM could only be found by assuming surface precipitation for Zn.

The "available" concentrations of sorbates were estimated from the leached concentrations at pH values unfavourable for adsorption, for the situation after 168 h. The lowest pH in the dataset was 4, at which the measured concentrations of cations (Ni, Cu, Zn, Cd and Pb) were used as input availability in the model. For Cu and Pb this choice deviates from the authors' earlier studies (*8, 11*). The consequences of this choice are further discussed below. The availability of Mo and Sb (assumed to be present in anionic form) was estimated at pH 12, assuming complete desorption at this pH value for these elements (*11, 40*). The sum of the molar concentrations of Ni,

Cu, Zn, Cd, Pb, Sb and Mo at pH 4 is approximately 20% of the total amount of surface sites on the extracted Fe- and Al (hydr)oxides.

Model input files

Model files to calculate saturation indices of potential solubility controlling minerals included the measured total solution concentrations of a wide range of elements, as well as FA and HA derived from dissolved organic C (DOC, see above). The pH was fixed to the measured value and all solid precipitation was suppressed. The choice of potentially solubility controlling solids used for the calculations was based on the approach of Meima and Comans (*6, 7*), i.e., potential solubility controlling minerals were selected based on (i) likeliness of their presence or formation in MSWI bottom ash under the experimental conditions (for literature on this subject refer to e.g., refs *41-43* and references in therein), (ii) calculated log saturation indices relatively close to zero (-1 < log SI < 1), and/or (iii) model-predicted curve shapes following the measured data in the concentration vs. pH graphs. Model files to calculate the leachate composition in equilibrium with a selected mineral, were based on the "infinite solid approach" outlined in detail by Meima and Comans (*6*). Model files to predict the leaching of Ni, Cu Zn, Cd, Pb, Sb and Mo simultaneously, based on the adsorption processes described above, were composed of [1] the concentrations of the different reactive surfaces in the solid and solution (i.e., solid and dissolved organic matter, Fe and Al (hydr)oxide surfaces); [2] the available concentrations of heavy metals and Sb and Mo (see above); [3] the pH, which was fixed at the measured value in the pH-stat and [4] total solution concentrations of Na, K, Ca, Mg, Mn, Al, Si, Fe, Ba, Sr, SO_4, PO_4, Cl and CO_3, which were fixed at their measured values to fully account for the competitive adsorption between the heavy metals and major elements. The precipitation of minerals was suppressed during the calculation of the sorption equilibrium.

Results and discussion

Buffering reactions

The setpoint-pH values in the pH-stat system are generally reached within 15–30 min from the start of the acid/base dosage. The acid/base consumption (expressed in acid neutralizing capacity (ANC), eq. H^+/kg) as a function of time is shown in Fig. 1.
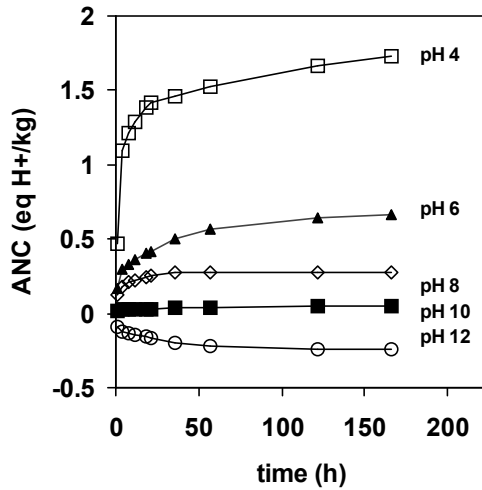

Figure 1. Acid – base consumption as a function of time for the different setpoint- pH values in the pH-static experiments, expressed as Acid Neutralising Capacity (ANC, eq. H^+/kg).

The buffering reaction upon acid or base addition is initially fast, but levels off gradually (Fig. 1). At pH 6 and 4, a plateau is not reached, indicating that the material is still reacting. The gradual acid consumption observed at the lower pH values is likely to be caused by the slow dissolution of alkaline components from the bottom ash matrix. The amount of acid consumed between 3 and 168 h at pH 4 amounts to 0.67 eq. H^+/kg. This amount corresponds well to the equivalent concentration increase of the major ions Fe, Al, Mg and Ca of 0.63 eq./kg at this pH value, which may be caused by the solubility of minerals and/or desorption from reactive surfaces. Modelling the complex neutralization behaviour of MSWI bottom ash as a function of pH was not the primary focus of this study. Johnson et al. (*44*) and Yan et al. (*45*)

have made detailed studies on this topic and conclude that primarily Ca, Mg and Si bearing phases are responsible for the buffering reactions in MSWI bottom ash.

Time-dependent leaching behaviour

The time-dependent leaching behaviour generally varied per element and setpoint-pH. Five different time-dependent concentration patterns have been observed in the experiments, of which typical examples are shown in Fig. 2.
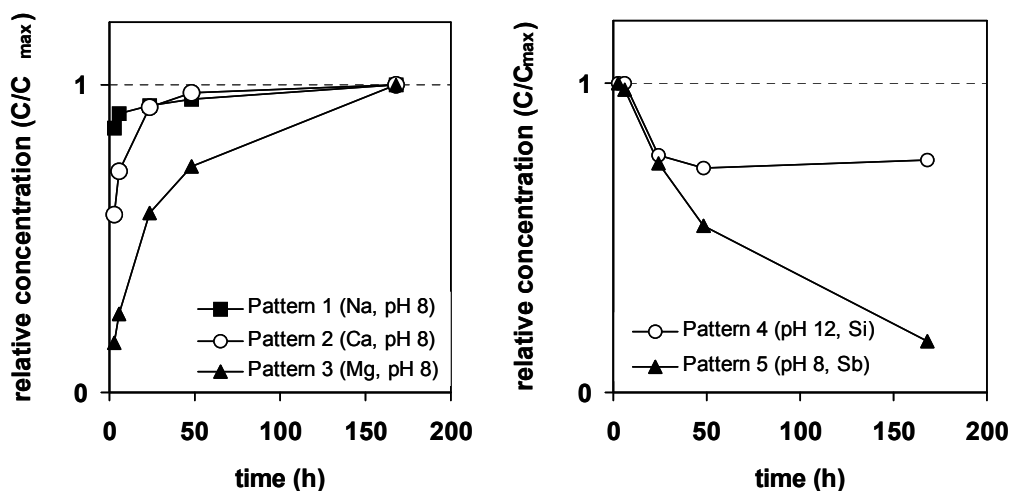

Figure 2. Typical examples of observed concentration changes over time in the pH-static experiments, expressed as relative concentration (C = concentration at the different equilibration times, C_{max} = maximum concentration).

Three different types of a concentration increase with time were observed in the experiments (Fig. 2, left); pattern (1) a rapid concentration increase followed by a slow release during the course of the experiment; (2) a slow concentration increase until a steady state is attained; (3) a slow concentration increase, but steady state is not attained over the course of the experiment. An example of the dissolution of a phase until complete exhaustion (i.e., no further concentration increase) as observed by Kirby and Rimstidt (*16*) could not be identified in the experiments. Two different types of a concentration decrease over time were observed (Fig. 2, right) referred to as pattern (4) and (5). Pattern (4) represents the concentration decrease until steady state

is attained; pattern (5) is representative for a concentration decrease that does not result in steady state. Mixed patterns (e.g., an increase followed by a decrease or vice versa) were observed in a number of cases. For clarity, this pattern was not categorized in Fig. 2, but will be discussed in individual cases. Similar to Kirby and Rimstidt (*16*), in the next section the time dependency of leaching that a particular element displays, will be discussed on the basis of the five patterns shown in Fig. 2.

The leaching of an element may display different time trends in different pH ranges, as will be illustrated for each of the investigated elements in the next section. Fig. 3 is a schematic diagram showing the theoretical solubility curve of a cationic metal (the same principles also apply to anions) and the reactions that are expected to occur in a pH-dependence test.
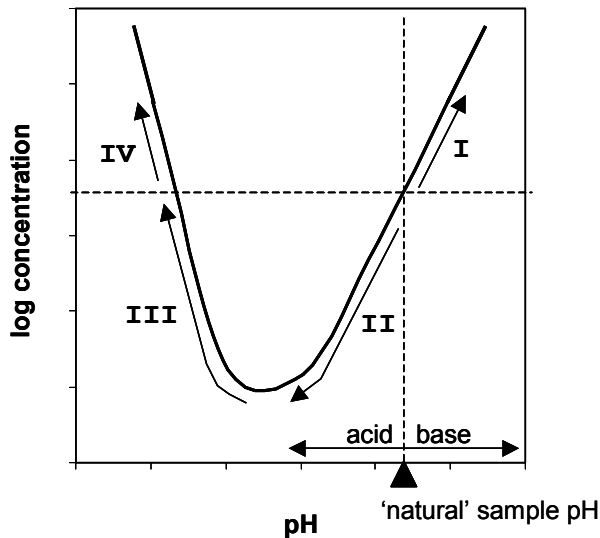
Figure 3. Schematic diagram showing the theoretical solubility curve of a cationic metal and the reactions that are expected to occur in a pH-dependence test in different pH regions. See text for explanation.

The theoretical solubility curve of this metal (Fig. 3) may be the result of different processes, such as the solubility of mineral phases and/or sorption processes for metals that are controlled by reactive surfaces. When a sample is brought in contact with water, it will impose its "natural" pH to the surrounding solution (around 10–11

for fresh MSWI bottom ash, indicated by a black triangle at the X-axis, Fig. 3) and metal concentrations will tend towards the theoretical solubility at the "natural" pH value (indicated in Fig. 3 by the junction of the vertical dashed line and the solubility curve). Upon acid or base addition, the metal concentrations will either increase or decrease, depending on the shape of the solubility curve. In this example, acid addition will result in a concentration decrease due to precipitation and/or sorption until the minimum of the curve is reached (Region II in Fig. 3); further acid addition will result in (re)dissolution/desorption (Regions III and IV). In Region III a net concentration decrease may be observed, while Region IV is characterized by a net concentration increase, relative to the metal concentration at the natural pH. Base addition will result in a net concentration increase due to mineral dissolution or desorption processes (Region I).

Depending on the element, the minimum of the solubility curve can also be positioned at a higher pH than the "natural" pH. It may be expected that the concentration time trends that occur as a result of acid or base addition are more pronounced at pH values away from the "natural" pH, i.e., where the system is forced to non-equilibrium conditions. Observed time trends are indicated by arrows in the pH–concentration diagrams of Figs. 4 and 5.

pH-dependent leaching behaviour

Measured concentrations of the major elements Al, Ca, SO_4, Mg, Si, Fe, Na and DOC are presented in Fig. 4. These elements are chosen as they constitute the bulk (by weight) of MSWI bottom ash (*9*). The leaching of the trace elements Ni, Zn, Cd, Cu, Pb, Mo and Sb are presented in Fig. 5. For clarity, model predictions are only shown for the situation after 168 h. The leaching behaviour and model predictions are treated for the major and trace elements separately below.

Major elements

Aluminium

The pH dependent leaching of Al is adequately described over a large pH range by the solubility behaviour of Al (hydr)oxide forms such as gibbsite (Fig. 4), in agreement with Meima and Comans (*6*). Around the natural pH (10.6), measured Al

concentrations show little time dependency, indicating that steady state is rapidly attained. Meima and Comans (*6*) suggested three minerals act simultaneously as pH- and solubility-controlling phases for Al, Ca and SO_4; gibbsite ($Al(OH)_3(s)$), gypsum ($CaSO_4.2H_2O$) and ettringite ($Ca_6Al_2(SO_4)_3(OH)_{12}.26H_2O(s)$). Aluminium is indeed well described by both gibbsite and ettringite at this pH value (Fig. 4). Below the natural pH, precipitation of presumably Al (hydr)oxides from solution occurs (pH 8 and 6, see also Fig. 3) and is apparently rapid as absolute changes of Al concentrations are small. At pH 4, Al is (re)dissolving, and a concentration increase is observed largely following pattern no. 3 in Fig. 2. At this pH value the solution concentrations of Al approach the theoretical solubility curve of gibbsite after 168 h (Fig. 4), but as a steady stateis not reached, Al might be controlled by more amorphous Al (hydr)oxide forms (amorphous $Al(OH)_3$, see Fig. 4) suggesting that Al concentrations may continue to rise significantly after 168 h. At pH 12, a strong time-dependent increase of Al concentrations is observed between 3 and 168 h. Also at pH 12, the increase follows pattern no. 3 of Fig. 2. Aluminium concentrations apparently exceed the solubility of gibbsite, suggesting more soluble Al minerals are controlling solubility (Fig. 4). Concentrations also exceed the solubility of ettringite, although this phase is expected to precipitate at this pH value (see discussion for Ca and SO_4 below). Zevenbergen and Comans (*15*) and Meima and Comans (*6*) suggested that slowly dissolving aluminosilicate minerals may control Al leaching at these pH values.

Calcium

The solubility of Ca between pH 4 and 8 is well described by the dissolution of gypsum (Fig. 4). The time-dependent increase generally follows pattern no. 3 in Fig. 2; pattern no. 2 (steady state is obtained) is only observed at pH 8. Between pH 8 and 12, Ca concentrations are qualitatively well described by calcite, although calcite is slightly oversaturated after 168 h (log SI ~+0.7). Meima and Comans (*6*) suggested that ettringite might be a possible solubility-controlling phase around the natural pH of freshly quenchedMSWI bottom ash. The model curves of ettringite indeed follow the trend of the measured Ca closely between pH 10 and 12 (Fig. 4). In addition, the log SI of ettringite at pH 10 gradually approaches values around zero over time (log SI = -2.05 after 3 h to +0.76 after 168 h), although steady state Ca concentrations are not
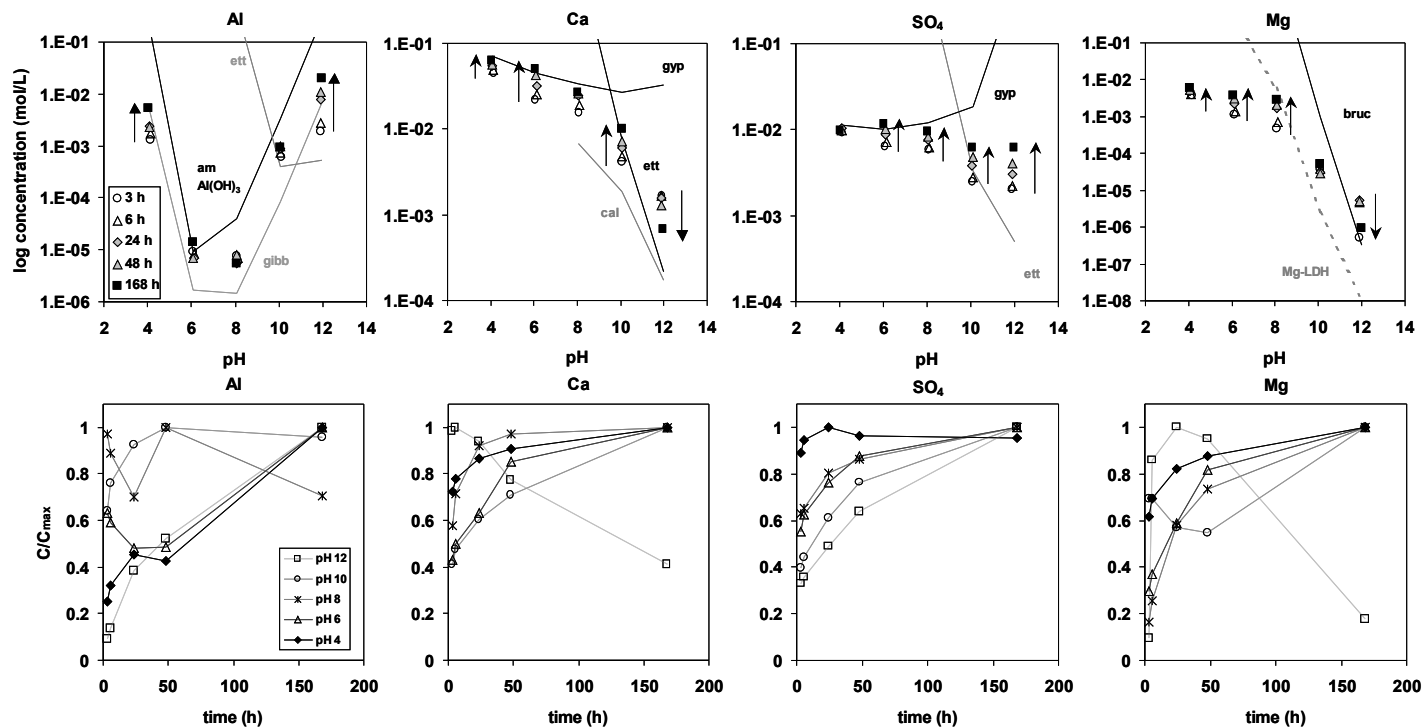
Figure 4. Measured concentrations of major elements as a function of pH (upper figures) and different equilibration times (lower figures, expressed as relative concentration, C = concentration at different equilibration times, C_{max} = maximum concentration). In the concentration-pH diagrams, clear time trends are indicated with arrows. For clarity, equilibrium model curves are only shown for the situation after 168 hours. Abbreviations: gibb = gibbsite; ett = ettringite; cal = calcite; gyp = gypsum; bruc = brucite, LDH = Layered Double Hydroxide.

Figure 4 (*continued*). Abbreviations: wai = wairakite; Fe(1) = ferrihydrite calculated in the absence of fulvic and humic acid (purely inorganic), Fe(2) = ferrihydrite calculated using generic constants for binding of Fe(III) to fulvic and humic acid; Fe(3) = ferrihydrite calculated with modified binding parameters for binding of Fe(III) to fulvic and humic acid, see text. For Na, only data is shown at which no NaOH was added.

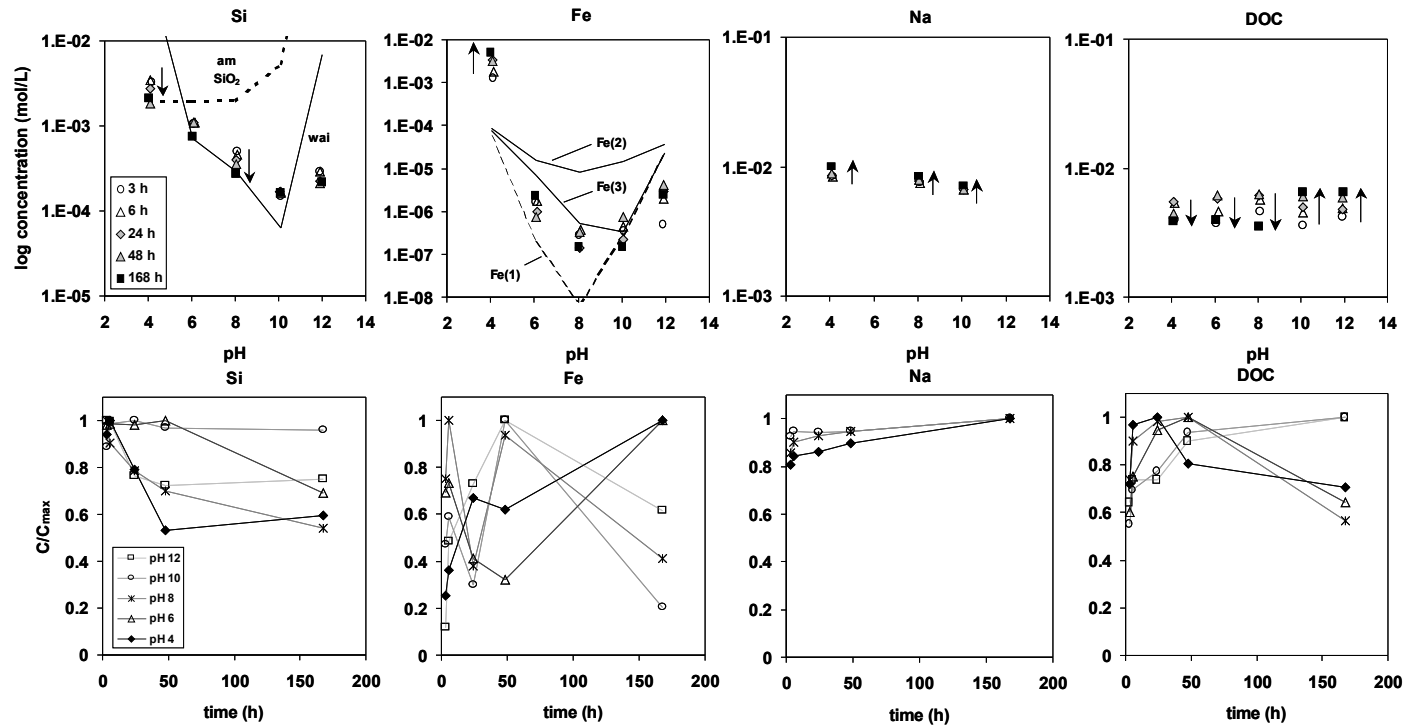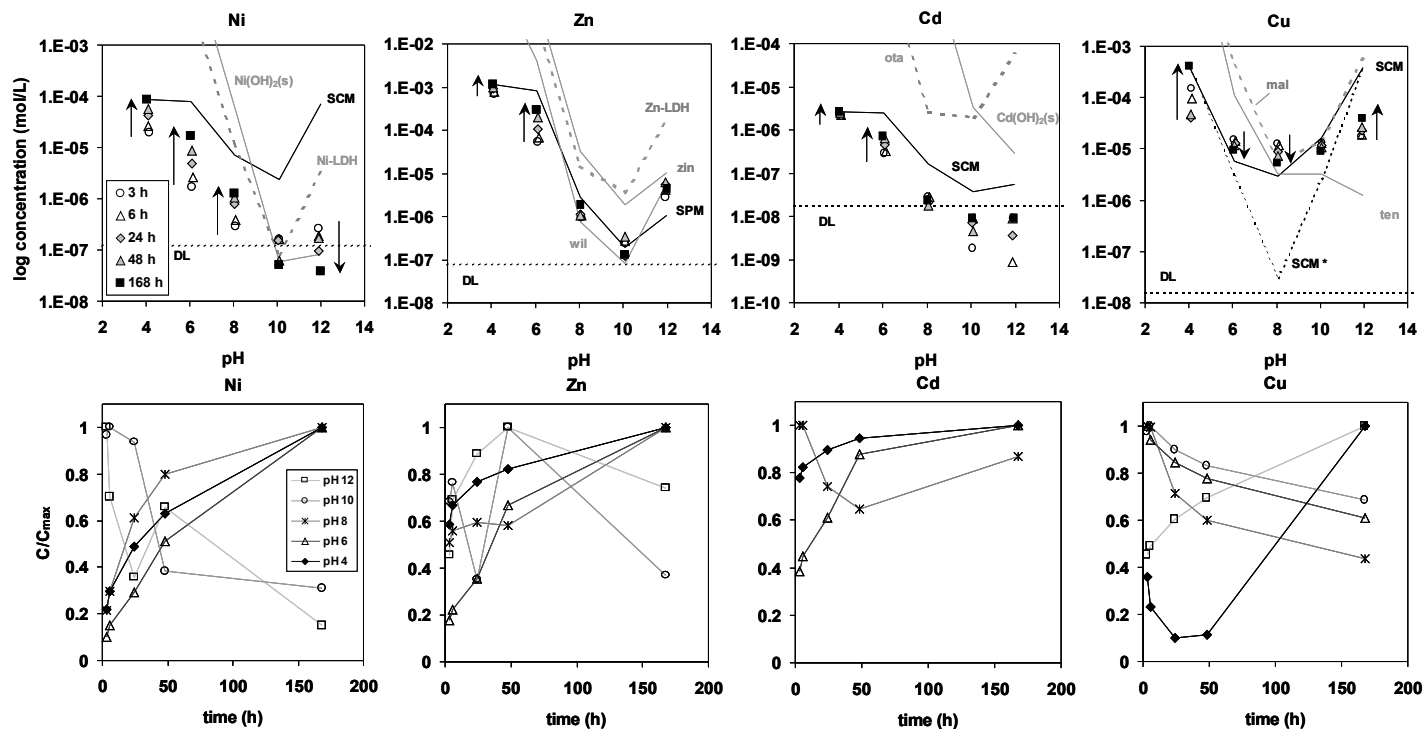Figure 5. Measured concentrations of trace elements (Ni, Cu, Zn, Cd, Pb, Mo and Sb) as a function of pH (upper figures) and different equilibration times (lower figures, expressed as relative concentration, C = concentration at different equilibration times, C_{max} = maximum concentration). In the concentration-pH diagrams, clear time trends are indicated with arrows. For clarity, equilibrium model curves are only shown for the situation after 168 hours. DL = detection limit. For Cd and Pb, time trends are only shown where concentrations exceed the detection limit. Abbreviations: SCM = model prediction based on surface complexation with iron- and aluminium (hydr)oxides; SPM = model prediction based on surface precipitation on iron- and aluminium (hydr)oxides. For Cu and Pb, SCM* refers to the model prediction calculated in the absence of the reactive components in DOC, i.e. humic and fulvic acid (see text); LDH = Layered Double Hydroxide, zin = zincite, wil = willemite, ota = otavite, mal = malachite, ten = tenorite.
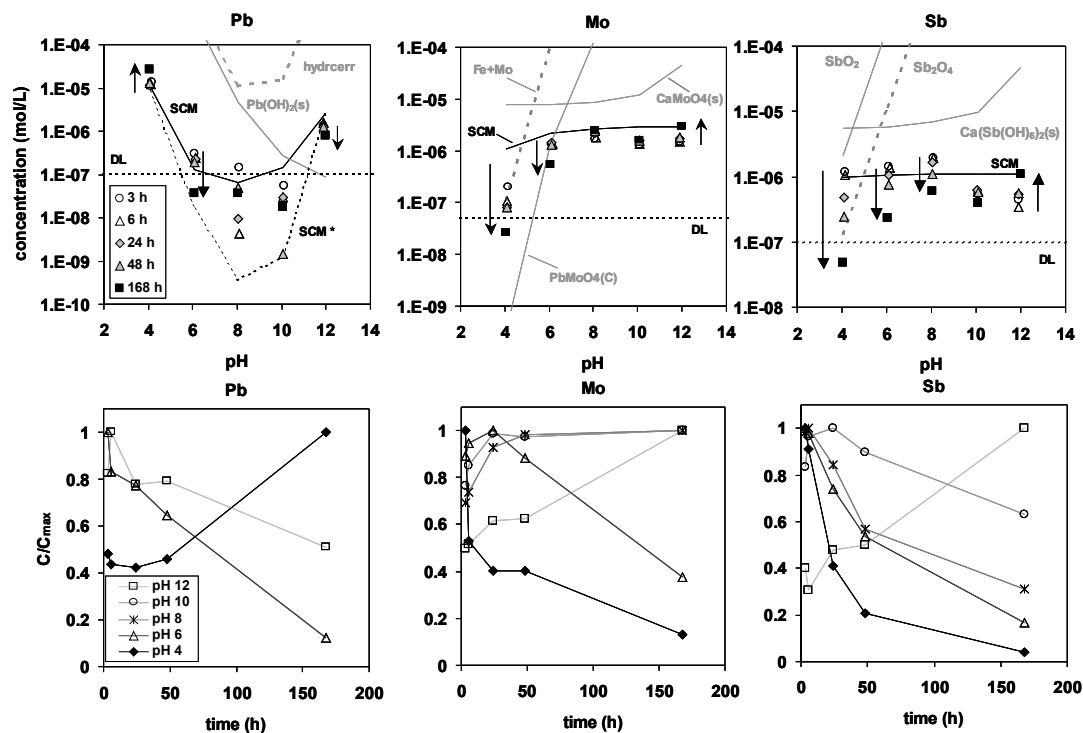
Figure 5 (*continued*). Abbreviations: SCM = model prediction based on surface complexation with iron- and aluminium (hydr)oxides, 'SCM*' refers to the model prediction for Pb calculated in the absence of the reactive components in DOC, i.e. humic and fulvic acid (see text); hydrcerr = hydrocerrusite, Fe+Mo = $Fe_2(MoO_4)_3$ calculated in the presence of ferrihydrite. For Sb, solubility curves are shown for $Ca(Sb(OH)_6)_2(s)$ (*56*) SbO_2 and Sb_2O_4. The latter mineral is calculated at a lower redox potential (pH+pe = 10) than used elsewhere in this study (pH+pe = 15), see text.

reached after 168 h. At pH 12, the saturation index of ettringite follows a parabolic behaviour over time (log SI = +2.97 after 3 h; +4.20 after 24 h +3.18 after 168 h). This suggests a kinetic constraint on the precipitation of ettringite. Also calcite is expected to precipitate as it is oversaturated (log SI = +0.6 after 168 h), and compared to ettringite, thermodynamically the more stable Ca phase at pH > 10 (Fig. 4). As the pH-static test is in principle open to the atmosphere, the uptake of CO_2 may ultimately cause all ettringite to dissolve, with calcite as one of the reaction products.

Sulphate

Concentrations of SO_4 in the leachates show virtually pH independent leaching behaviour and are limited by the solubility of gypsum in the pH range between pH 4 and 8 (Fig. 4). The time-dependent concentration changes of SO_4 show similarities with those of Ca, i.e., generally show pattern 3 in Fig. 2. Only at pH 4, concentrations rapidly approach the solubility curve of gypsum. This behaviour is also expected for the SO_4 concentrations between pH 4 and 8, however, steady state is not reached over the course of the experiment. Gypsum becomes increasingly undersaturated towards higher pH values, and at pH 10 ettringite is a plausible controlling phase (see Fig. 4 and the discussion for Al and Ca). At pH 12, the solubility curve of ettringite strongly underestimates the measured concentrations (Fig. 4). No other potentially solubility controlling minerals could be identified at this pH value.

Magnesium

The leaching of Mg above pH 8 is adequately described by either the solubility of brucite ($Mg(OH)_2(s)$) or the more stable Mg layered double hydroxide (LDH) phase ($Mg_2Al(OH)_6(CO_3)_{0.5}.H_2O$, using the solubility constant of Johnson and Glasser (*46*)). Brucite has been suggested earlier to control the leaching of Mg from both fresh and weathered MSWI bottom ash at alkaline pH (e.g., *6*), while Mg–Al–LDH has been reported to form in weathered MSWI bottom ash (ref *46* and references therein). A strong time dependency was observed between pH 4 and 8, which shows pattern no. 3 in Fig. 2. Between pH 4 and 8, concentrations measured after an equilibration time of 168 h show little pH dependency and approach rather similar concentrations (Fig. 4), which supports the hypothesis of Meima and Comans (*6*) that there are no solubility controlling minerals at this pH value, and that the "available" Mg is largely

leached from the bottom ash. A noticeable pH-dependency is observed in the release rates between pH 4 and 8 (Fig. 4). This pattern is consistent with the kinetics of brucite dissolution, which is a function of pH (e.g., ref *47*). A relatively small time dependency is observed at pH 10, indicating that steady state concentrations are apparently rapidly attained around the natural pH of the bottom ash (pH 10.6). At pH 12, the concentration change is parabolic, i.e., a strong increase from 3 to 24 h, followed by an almost equally strong decrease up to 168 h, while steady state is not reached. Apparently, the net dissolution of Mg during the initial stages of the experiment is counterbalanced by the precipitation of brucite during the course of the experiment.

Silicon

Concentrations of silicon tend to approach the solubility of the zeolite mineral wairakite ($CaAl_2Si_4O_{12}.2H_2O$) over a large pH range (pH 6–10). Good model descriptions based on wairakite were obtained by Meima and Comans (*6*). However, in their study, a potential solubility-controlling phase was not found for the low leaching of Si at strongly alkaline pH. It should be noted that wairakite is a high-temperature mineral that may not be stable under the experimental conditions. The agreement between the model curve and the data may point to the presence of other zeolites in MSWI bottom ash, such as gismondine and laumontite that have been identified in (weathered) MSWI bottom ash (*43*). The leaching of Si between pH 4 and 8 shows a slightly decreasing trend over time; pattern no. 5 in Fig. 2 was observed at pH 8. At pH 4 concentrations tend to decrease towards the theoretical solubility curve of amorphous SiO_2 over time, which is the more insoluble Si-containing phase at this pH value (Fig. 4). At pH 12, again a decreasing trend was observed that apparently reached a steady state (pattern no. 4 in Fig. 2). Zevenbergen and Comans (*15*) earlier observed a slow decrease in concentrations of Si over time. This decrease was attributed to the transformation of glassy materials into more insoluble phases such as aluminosilicates, which was supported by observations made by Analytical Electron Microscopy (AEM) (*15*). Kirby and Rimstidt (*16*) also suggested precipitation of a secondary silica phase in bottom ash leachates.

Iron

The leaching pattern of Fe is characteristic for the solubility of Fe (hydr)oxides such as ferrihydrite (Fig. 4). Iron (III) forms strong complexes with HA and FA (*35*). This property may be illustrated by a model curve calculated with ferrihydrite in the absence of HA and FA (i.e., purely inorganic), which results in a strong underestimate of the measured Fe concentrations in the neutral pH range (Fe(1) in Fig. 4). Model calculations based on ferrihydrite in the presence of HA and FA (using the NICA-Donnan approach, see modelling section) result in a strong overestimate of the measured Fe concentrations (Fe(2) in Fig. 4). However, the estimated parameters of Milne et al. (*35*) for Fe(III) sorption to the phenolic groups of both HA and FA is based on a limited dataset for Fe(III) sorption to HA (*48*). Re-evaluating this dataset, the authors obtained a better description of the data when the Fe(III) binding to the phenolic sites of HA was neglected. Although the binding of Fe(III) to HA and FA clearly needs further investigation, the authors have chosen to neglect the adsorption of Fe(III) to the phenolic groups of FA and HA. With these modified parameters, an adequate description of the Fe-solubility based on ferrihydrite was found (Fe(3) in Fig. 4).

Sodium

The release of Na (Fig. 4) is only shown for the pH values at which no NaOH has been added (i.e., pH 4, 8 and 10). Sodium exhibits leaching behaviour almost independent of pH, suggesting the rapid dissolution of soluble salts such as halite (NaCl) ((*6*) and references therein). The time-dependent increase of Na follows pattern no. 1 in Fig. 2, i.e., a rapid concentration increase followed by a much slower release. The slow release process of Na has been suggested to be the result of kinetically controlled dissolution of less soluble phases (*16*).

Dissolved organic carbon (DOC)

The leaching pattern of DOC is rather independent of pH (Fig. 4). Initially, DOC concentrations increase as a function of time. Between pH 4 and 8, the initial increase of DOC is followed by a sharp decrease (Fig. 5). Possibly microbial degradation of degradable organic substances, or binding of reactive fractions of DOC (e.g., HA and FA) to the solid phase may contribute to this effect. Recently, DOC from a sample of

the same incinerator has been shown to consist of about 0.2% of HA, 20% of FA and about 80% of hydrophilic acids (*25*). The pH dependent leaching of these specific fractions have not been modelled so far, but progress in that field has been made by Lumsdon (*49*) and Filius et al. (*50*).

Trace elements

Despite the fact that this bottom ash is relatively fresh and unweathered, an attempt is made to explain the pH dependent leaching of these elements by surface complexation to (neoformed) Fe and Al (hydr)oxides present in the bottom ash matrix, using the same approach as the authors' previous studies (*8, 11*).

Nickel

The leaching of Ni between pH 4 and 8 shows a strong increase over time and follows pattern no. 3 in Fig. 2. In this pH range the leaching of Ni after 168 h is reasonably well predicted by the model, which suggests that the concentration increase is caused by slow desorption (Fig. 5). At pH 10 and 12, Ni data is partially below the detection limit but is adequately explained by the precipitation of $Ni(OH)_2(s)$. Both at pH 10 and 12, the time dependency of Ni leaching is best represented by pattern 4 in Fig. 2 and the final concentrations correspond well with the theoretical solubility line of $Ni(OH)_2(s)$ (Fig. 5). Nickel solubility has also been calculated using the solubility constants derived for the pure Ni–LDH phase synthesized by Johnson and Glasser (*46*). The solubility curve of this phase (Fig. 5) is quite similar to that of $Ni(OH)_2$ at pH 10 and lower, but is unable to explain the Ni concentrations found at pH 12.

Zinc

The leaching of Zn as a function of pH is well described by the surface precipitation model (Fig. 5), in agreement with the studies of Meima and Comans (*11*) and Dijkstra et al. (*8*). However, an equally adequate description of Zn concentrations is provided by the solubility curve of willemite (Zn_2SiO_4) (Fig. 5). Although Meima and Comans (*11*) were unable to precipitate willemite in the laboratory from oversaturated solutions, willemite has recently been identified by X-ray adsorption spectroscopy (XAS) in (untreated) MSWI fly ash (*51*). Zincite (ZnO) is too soluble to

explain Zn leaching at high pH (Fig. 5). Zinc solubility has also been calculated using the solubility constants derived for the pure Zn–LDH phase synthesized by Johnson and Glasser (*46*). Also this phase is too soluble to explain Zn leaching towards high pH values (Fig. 5). More research is needed to confirm whether Zn minerals or adsorption processes are responsible for Zn leaching from MSWI residues. The leaching of Zn shows a strong time dependency between pH 4 and 8 that is best represented by pattern 3 of Fig. 2. At pH 8–12, absolute time trends are small, suggesting that steady state is approached.

Cadmium

In spite of the fact that the experimental data of Cd leaching above pH 10 is below the detection limit of the ICP-AES, the leaching of Cd is described adequately by the surface complexation model over a large pH range (Fig. 5), in line with Meima and Comans (*11*) and Dijkstra et al. (*8*). Otavite ($CdCO_3$) is too soluble to explain the observed Cd concentrations (Fig. 5). A consistent increase in concentrations with time is only observed at pH 4 and pH 6, while no steady state is reached (pattern 3 in Fig. 2).

Copper

The leaching of Cu is described adequately by surface complexation to Fe- and Al (hydr)oxides (Fig. 5). The carbonate mineral malachite ($Cu_2(OH)_2CO_3$) provides an equally adequate description of Cu leaching above pH 8, but fails to explain Cu leaching at lower pH values (Fig. 5). Model predictions for both Cu and Pb (see below) are strongly determined by the complexation of these metals with dissolved humic and fulvic acids (HA and FA, respectively), the major reactive components of dissolved organic C (DOC) in MSWI bottom ash leachates (*24, 25*). The importance of Cu complexation with DOC is illustrated by the model curve predicted in the absence of FA and HA, which results in a strong underestimate of the leaching of Cu (Fig. 5). Only at pH 12, is the leaching of Cu overestimated. The time trend of the concentrations at pH 12 is consistently upwards (Fig. 5) following pattern no. 3 in Fig. 2. A slight but continuous decrease in Cu concentrations was observed at pH 6, 8 and 10 following pattern no. 4 in Fig. 2. The solubility of tenorite (CuO) in the presence of DOC is unable to explain the leaching of Cu over a large pH range (Fig. 5).

The high degree of complexation of Cu and Pb with DOC is caused by the higher affinity of these metals for specific binding to humic substances, relative to Ni, Zn and Cd (*35, 52*). These differences in affinity become particularly apparent in systems with a high competition among the adsorbing metals for the available organic sorption sites. Competition for these sites is of importance in environments with concentrations of dissolved humic substances that are low relative to the availability of strongly binding heavy metals (e.g., Cu and Pb) and major elements (e.g., Fe and Ca). These conditions are typically met in MSWI bottom ash.

Lead

The model curves for Pb based on surface complexation seem to follow the measured data adequately, although between pH 6 and 10, measured concentrations of Pb are well below the detection limit. Hydrocerrusite ($Pb_3(CO_3)_2(OH)_2$) was found to be too soluble to explain the observed Pb concentrations (Fig. 5) as was also the case for cerrusite ($PbCO_3$, not shown). Similar to Cu, complexation of Pb with DOC is important, as is illustrated by the model curve calculated in the absence of FA and HA. This model scenario results in much lower predicted concentrations (Fig. 5).

Molybdenum

The leaching of Mo shows a pH dependency characteristic for the adsorption of anions (MoO_4^{2-}), i.e., an increased adsorption towards lower pH values (*38*). However, the model curve based on surface complexation cannot fully explain this decrease at low pH (Fig. 5). At pH 6 and lower, concentrations of Mo seem to decrease towards the equilibrium solubility curves of $Fe_2(MoO_4)_3$, suggested by Meima and Comans (*7*), or $PbMoO_4(s)$ (wulfenite). The measured concentrations as a function of time do not seem to reach steady state both at pH 6 and pH 4 (i.e., pattern 5 in Fig. 2). This leaching pattern may be interpreted as a kinetically hindered precipitation of $Fe_2(MoO_4)_3$ or wulfenite, the latter being the more insoluble mineral. At pH 8 and 10, concentrations of Mo increase and have reached a steady state after 48 h (i.e., pattern 2 in Fig. 2), except for pH 12, where concentrations seem to increase further after 48 h. Between pH 8 and 12, model calculations indicate that adsorption of MoO_4^{2-} is virtually absent. Model predictions based on the solubility of powellite ($CaMoO_4$), suggested by Meima and Comans (*7*) and Johnson et al. (*53*), using the solubility

constant of Essington (*54*), overestimate the steady state concentrations at pH 8 and 10. Alternatively, Mo concentrations in the high pH region are limited by the availability of Mo in the bottom ash matrix.

Antimony

The leaching pattern of Sb largely follows that of Mo, i.e., that of a "typical" anion with a low pH dependency at high pH (pH 10–12) and a concentration decrease at lower pH. In particular at low pH, concentrations decrease strongly over time (Fig. 5). At the assumed redox potential (pH + pe = 15), the dominant Sb species in solution calculated using the MINTEQA2 database is SbO_3^- , which is an Sb(V) species also written as $Sb(OH)_6^-$ (e.g., (*55*)) or $SbO(OH)_4^-$ (*38*). Similar to Meima and Comans (*40*), the authors have attempted to explain the leaching pattern of Sb by adsorption to Fe- and Al (hydr)oxides using the adsorption constants for Sb(V) to HFO of Dzombak and Morel (*38*). The following Sb-species have been implemented into the MINTEQA2 (version 3.11) database: $\log K\ HSbO_3^0 = +2.72$, $\log K_{int}\ (\equiv FeSbO_3^0) = +8.4$, $\log K_{int}\ (\equiv FeOHSbO_3^-) = +1.3$ (data taken from Dzombak and Morel (*38*) and written in terms of SbO_3^-). The adsorption of Sb to Fe- and Al (hydr)oxides calculated this way is far too weak to explain the sharp concentration decrease at low pH (Fig. 5). However, adsorption as the process controlling Sb leaching cannot be ruled out, as the adsorption parameters for Sb to HFO have been estimated by a linear free energy relationship (LFER) (*38*) and are inherently uncertain. An alternative explanation is the precipitation of Sb-minerals in this pH region. As an example the calculated solubility curves for SbO_2 (calculated to be the most insoluble Sb mineral of the MINTEQA2 database at the chosen redox conditions, i.e., pH + pe = 15) and Sb_2O_4 (the most insoluble mineral in the work of Krupka and Serne (*55*) and calculated for a lower redox potential of pH + pe = 10; at higher redox potentials the mineral is too soluble) are shown. These minerals become very insoluble towards low pH values, but the likeliness of their presence and/or formation under the experimental conditions is uncertain. At high pH, Sb solubility may be controlled by Ca antimonate ($Ca(SbO_3)_2$, $K = [Ca^{2+}][SbO_3^-] = 10^{-12.55}$, data taken from Johnson et al. (*56*) and written in terms of SbO_3^-), although the solubility curve consistently overestimates Sb leaching (Fig. 5). It is emphasized that the solubility curves for Sb shown in Fig. 5 should be interpreted with care, as the thermodynamic data for the solid and aqueous speciation

of Sb is limited (*55*). More research is needed to investigate Sb speciation in general, and the solubility controlling mechanisms that control the leaching of Sb from MSWI bottom ash in particular.

Synthesis and conclusions

Processes controlling the leaching of major and trace elements

The experimental results show that time-dependent concentration changes of up to one order of magnitude occur during leaching in a pH-static test. However, the concentration–time trends generally proceed towards "equilibrium" with respect to mineral dissolution and precipitation and adsorption processes over a large pH range, as demonstrated by equilibrium geochemical modelling. Although the model predictions presented in this work do not represent "true" thermodynamic equilibrium of the system as a whole, the results contribute to gaining an improved understanding of the main leaching mechanisms that occur at relatively short equilibration times typical for leaching tests.

The model predictions for the major and trace elements, obtained without fitting any parameter, are generally adequate and sometimes excellent. This result is promising, given the fact that the model predictions, in particular those based on adsorption processes (trace elements), rely strongly on model parameters derived in the laboratory for well-characterized materials (usually a single trace element and a single sorbent), and the conditions met in natural and waste environments might well be different from these. The model predictions suggest that the formation of metal–DOC complexes strongly enhance the leaching potential of particularly Cu and Pb in MSWI bottom ash leachates. Therefore, challenges for future research include the characterization of dissolved organic C (DOC) in the leachates over a wide pH range, as well as the development and application of a model to predict DOC concentrations (e.g., refs *49* and *50*).

Preliminary calculations showed a strong dependency of the model results on input parameters such as the available heavy metal concentrations (see also below), the amount of Fe- and Al (hydr)oxides and the amount of reactive organic C (in particular, type and amount as a function of pH). This finding indicates that the

measured input parameters used for adsorption modelling represent a source of uncertainty that warrants careful consideration. Taking HFO as "surrogate" for amorphous Al (hydr)oxides in the model may also introduce uncertainty.

Implications for the development and interpretation of standardized leaching tests

The development of leaching tests protocols generally aims for an optimal balance between the attainment of steady state conditions and operational issues such as the time needed to complete the test. Apparent steady state conditions in leaching test results performed at relatively short time scales may differ from those in a field situation, as waste materials such as MSWI bottom ash are complex mixtures of stable and unstable minerals and are continuously subject to dynamic changes such as weathering, including slow mineralogical alterations, biodegradation of organic matter and microbial processes (e.g., refs *6* and *57* and references therein). Therefore, it is highly unlikely that true thermodynamic equilibrium conditions for all elements will be established in short-time leaching tests performed on such complex and heterogeneous waste materials. Aiming for conditions as close as possible to "equilibrium" in a leaching test would require additional measures, such as a truly closed system and much longer equilibration times, but these measures would be impractical and may still lead to different results than under field conditions at any moment. As such, it is necessary to make a carefully motivated, but practical choice on equilibration times needed in standardized test protocols.

Although the vast majority of major and trace elements discussed in this study do not reach steady state, leached concentrations over a wide pH range have been shown to closely approach "equilibrium" model curves within relatively short equilibration times. This is an important result of this work, given the orders of magnitude concentration changes as a function of pH. In addition, the different effects that leaching kinetics may have on the pH dependent leaching patterns have been identified for a wide range of elements, and can generally be explained in a mechanistic way. It is likely that the observed kinetic effects and the underlying geochemical mechanisms play a role in many leaching/extraction tests, with or without controlled pH.

Although an equilibration time of 168 h gives results that are closer to modelled equilibrium conditions, Figs. 4 and 5 indicate that an equilibration time of 48 h as selected in the European standard TS14997 (*3*) would be a suitable operational choice as concentrations are not very different from those measured after 168 h. The present European standard TS14997 (*3*) prescribes a grain size fraction of <1 mm (sieved, oversized material broken to pass a 1 mm sieve), which is smaller than that used in this study (<2 mm). A smaller particle size is expected to lead more rapidly to steady state leaching conditions, as the transport path in the particles is smaller and more surface area is exposed. These considerations endorse the currently prescribed equilibration time of 48 h in the European standard TS14997 (*3*).

In earlier papers (*8, 11*) the authors have used pH 2 to estimate the "available" concentrations of Cu and Pb, because calculations showed that desorption of these elements may not be complete at pH 4 (*11*). In this study, pH 4 has been used as data at lower pH values were not available. However, no significant adsorption of Ni, Zn, Cd and Cu at pH 4 is calculated at pH 4, as can be seen from the model predictions in Fig. 5 that closely match the input "available" concentrations of these metals. Only for Pb, model predictions underestimate the measured concentrations by about a factor of 2 (Fig. 5), indicating that about half of the input "available" concentration of Pb is still adsorbed at pH 4. Using a lower pH to estimate the "available" heavy metal concentrations, e.g., pH 2, is therefore recommended. However, MSWI bottom ash is not necessarily representative for other materials. For instance, in organic rich materials such as soils, it has been shown that a measurement as low as pH 0.5 is needed to provide an adequate estimate of heavy metal "availability" (*58*). In summary, further research is needed to better define the conditions at which the "availability" of contaminants can be estimated.

The results of this study demonstrate that pHstatic leaching experiments such as described in the European standards TS14497 and TS14429 (*3, 4*), in combination with selective chemical extractions and a mechanistically based modelling approach, constitute a powerful set of tools for the characterization of leaching processes in waste materials over a wide range of conditions.

Acknowledgements

This work was partially funded by basic funding from the Dutch Ministry of Housing, Spatial Planning and the Environment for the Environmental Research Program of ECN. We thank Petra Geelhoed-Bonouvrie for her careful experimental work. Dr. Hans Meeussen is thanked for the stimulating discussions and for critically reading earlier versions of the manuscript. We also acknowledge the thorough and constructive reviews by Dr. Annette Johnson and Dr. Patrice Piantone, which have improved the manuscript substantially.

References

1. Van der Sloot, H. A.; Heasman, L.; Quevauviller, P. *Harmonisation of leaching / extraction tests*. Elsevier Science B.V.: Amsterdam, The Netherlands, 1997.
2. Kosson, D. S.; van der Sloot, H. A.; Sanchez, F.; Garrabrants, A. C. An integrated framework for evaluating leaching in waste management and utilization of secondary materials. *Environ. Eng. Sci.* 2002, 19, 159-204.
3. CEN/TC292. *Characterization of waste - Leaching behaviour tests - Influence of pH on leaching with continuous pH-control*. TS14997, 2005.
4. CEN/TC292. *Characterization of waste - Leaching behaviour tests - Influence of pH on leaching with initial acid/base addition*. TS14429, 2005.
5. Eighmy, T. T.; Eusden, J.D.; Krzanowski, J. E.; Domingo, D. S.; Stämpfli, D.; Martin, J. R.; Erickson, P. M. Comprehensive approach toward understanding element speciation and leaching behavior in municipal solid waste incineration electrostatic precipitator ash. *Environ. Sci. Technol.* 1995, 29, 629-646.
6. Meima, J. A.; Comans, R. N. J. Geochemical modelling of weathering reactions in MSWI bottom ash. *Environ. Sci. Technol.* 1997, 31, 1269-1276.
7. Meima, J. A.; Comans, R. N. J. The leaching of trace elements from municipal solid waste incinerator bottom ash at different stages of weathering. *Appl. Geochem.* 1999, 14, 159-171.
8. Dijkstra, J. J.; Van der Sloot, H. A.; Comans, R. N. J. Process identification and model development of contaminant transport in MSWI bottom ash. *Waste Manage.* 2002, 22, 531-541.
9. Chandler, A. J.; Eighmy, T. T.; Hartlen, J.; Hjelmar, O.; Kosson, D. S.; Sawell, S. E.; Van der Sloot, H. A.; Vehlow, J. *Municipal solid waste incinerator residues*. Elsevier Science B. V.: Amsterdam, The Netherlands, 1997.

10. Zevenbergen, C.; Vander Wood, T.; Bradley, J. P.; Van der Broeck, P. F. C. W.; Orbons, A. J.; van Reeuwijk, L. P. Morphological and chemical properties of MSWI bottom ash with respect to the glassy constituents. *Hazard. Waste Hazard. Mater.* 1994, 11, 371–383.

11. Meima, J. A.; Comans, R. N. J. Application of surface complexation/precipitation modelling to contaminant leaching from weathered municipal solid waste incinerator bottom ash. *Environ. Sci. Technol.* 1998, 32, 688-693.

12. Talbot, R. W.; Anderson, M. A.; Andren, A. W. Qualitative model of heterogeneous equilibria in fly ash pond. *Environ. Sci. Technol.* 1978, 12, 1056-1062.

13. Belevi, H.; Stämpfli, D.; Baccini, P. Chemical behaviour of municipal solid waste incinerator bottom ash in monofills. *Waste Manage. & Res.* 1992, 10, 153-167.

14. Comans, R. N. J.; Van der Sloot, H. A.; Bonouvrie, P.A. *Speciatie van contaminanten tijdens uitloging van AVI-bodemas.* ECN Report no. ECN-C--93-090 (Dutch Language), 1993.

15. Zevenbergen, C.; Comans, R. N. J. *Geochemical factors controlling the mobilization of major elements during weathering of MSWI bottom ash.* In *Environmental Aspects of Construction with Waste Materials*; Goumans, J. J. J. M.; Van der Sloot, H. A.; Aalbers, T.G. (eds.). Studies in Environmental Science 60, Elsevier Science B. V.: Amsterdam, The Netherlands, 1994, pp 179–194.

16. Kirby, C. S.; Rimstidt, J.D. Interaction of municipal solid waste ash with water. *Environ. Sci. Technol.* 1994, 28, 443-451.

17. Fällman, A. Performance and design of the availability test for measurement of potentially leachable amounts from waste materials. *Environ. Sci. Technol.* 1997, 31, 735-744.

18. Van der Sloot, H. A; Hoede, D. *Comparison of pH static leach test data with ANC test data;* ECN Report no. ECN-R--97-002, 1997.

19. Furrer, G.; Stumm, W. The coordination chemistry of weathering: I. dissolution kinetics of d-Al_2O_3 amd BeO. *Geochim. Cosmochim. Acta* 1986, 50, 1847-1860.

20. Bloom, P. R.; Erich, M. S. Effect of solution composition on the rate and mechanism of gibbsite dissolution in acid solutions. *Soil Sci. Soc. Am. J.* 1987, 51, 1131-1136.

21. Ludwig, C.; Casey, W. H. On the mechanisms of dissolution of bunsenite[NiO(s)] and other simple oxide minerals. *J. Colloid Interface Sci.* 1996, 178, 176-185.

22. Meeussen, J. C. L. ORCHESTRA: An object-oriented framework for implementing chemical equilibrium models. *Environ. Sci. Technol.* 2003, 37, 1175-1182.

23.   Steefel, C. I.; Van Capellen, P. A new kinetic approach to modeling water-rock interaction: The role of nucleation, precursors, and Ostwald ripening. *Geochim. Cosmochim. Acta* 1990, 54, 2657-2677.

24.   Van Zomeren, A.; Comans, R. N. J. *Speciation and characterization of organic carbon in Municipal Solid Waste Incinerator (MSWI) bottom ash.* WASCON 2003 Conference proceedings; Ortiz de Urbina, G.; Goumans, J. J. J. M. (eds), San Sebastian, Spain, 2003; pp 657-666.

25.   Van Zomeren, A.; Comans, R. N. J. Contribution of natural organic matter to copper leaching from municipal solid waste incinerator bottom ash. *Environ. Sci. Technol.* 2004, 38, 3927-3932.

26.   Kostka, J. E.; Luther III, G. W. Partitioning and speciation of solid-phase iron in saltmarsh sediments. *Geochim. Cosmochim. Acta* 1994, 58, 1701-1710.

27.   Ferdelman, T.G. *The distribution of sulfur, iron, manganese, copper, and uranium in a saltmarsh sediment core as determined by a sequential extraction method;* Ph.D. Thesis, University of Delaware, 1988.

28.   Blakemore, L. C.; Searle, P. L.; Daly, B. K. *Methods for chemical analysis of soils.* Science report 80; NZ Soil Bureau: Lower Hutt, New Zealand, 1987.

29.   Allison, J. D.; Brown, D. S.; Novo-gradac, K. J. *MINTEQA2/PRODEFA2, Geochemical assessment model for environmental systems: version 3.11 databases and version 3.0 user's manual*; Environmental Research Laboratory, U.S.-EPA: Athens, GA, 1991.

30.   Benedetti, M. F.; Milne, C. J.; Kinniburgh, D. G.; Van Riemsdijk, W. H.; Koopal, L. K. Metal ion binding to humic substances: application of the non-ideal competitive adsorption model. *Environ. Sci. Technol.* 1995, 29, 446–457.

31.   Kinniburgh, D. G.; Milne, C. J.; Benedetti, M. F.; Pinheiro, J. P.; Filius, J. D.; Koopal, L. K.; Van Riemsdijk, W. H. Metal ion binding by humic acid: application of the NICA-Donnan model. Environ. Sci. Technol. 1996, 30, 1687-1698

32.   Kinniburgh, D. G.; Van Riemsdijk, W. H.; Koopal, L. K.; Borkovec, M.; Benedetti, M. F.; Avena, M. J. Ion binding to natural organic matter: competition, heterogeneity, stoichiometry and thermodynamic consistency. *Colloids Surf A* 1999, 151, 147-166.

33.   Stumm, W.; Morgan, J. J.; Aquatic Chemistry, *An Introduction Emphasizing Chemical Equilibria in Natural Waters*, 2nd ed. John Wiley & Sons: New York, 1981.

34.   Milne, C. J.; Kinniburgh, D. G.; Tipping, E. Generic NICA-Donnan model parameters for proton binding by humic substances. *Environ. Sci. Technol.* 2001, 35, 2049-2059.

35. Milne, C. J.; Kinniburgh, D. G.; Van Riemsdijk, W. H.; Tipping, E. Generic NICA-Donnan model parameters for metal-ion binding by humic substances. *Environ. Sci. Technol.* 2003, 37, 958-971.

36. Thurman, E. M.; Malcolm, R. L. Preparative isolation of aquatic humic substances. *Environ. Sci. Technol.* 1981, 15, 463-466.

37. De Wit, J. C. M. *Proton and metal ion binding by humic substances;* Ph.D. Thesis, Wageningen University, Department Soil Quality, 1992.

38. Dzombak, D. A.; Morel, F. M. M. *Surface complexation modeling: hydrous ferric oxide*; John Wiley & Sons: New York, 1990.

39. Hiemstra, T.; De Wit, J. C. M.; Van Riemsdijk, W. H. Multisite proton adsorption modeling at the solid/solution interface of (hydr)oxides: a new approach, II. application to varous important (hydr)oxides. *J. Colloid Interface Sci.* 1989, 133, 105-117.

40. Meima, J. A.; Comans, R. N. J. Reducing Sb-leaching from municipal solid waste incinerator bottom ash by addition of sorbent minerals. *J. Geochem. Expl.* 1998, 62, 299-304.

41. Meima, J. A. *Geochemical Modelling and Identification of Leaching Processes in MSWI Bottom Ash.* Ph.D. Thesis, Utrecht University, 1997.

42. Dykstra Eusden Jr, J.; Eighmy, T. T.; Hockert, K.; Holland, E.; Marsella, K. Petrogenesis of municipal solid waste combustion bottom ash. *Appl. Geochem.* 1999, 14, 1073-1091.

43. Piantone, P.; Bodenan, F.; Chatelet-Snidaro, L. Mineralogical study of secondary mineral phases from weathered MSWI bottom ash: implications for the modelling and trapping of heavy metals. *Appl. Geochem.* 2004, 19, 1891-1904.

44. Johnson, C. A.; Brandenberger, S.; Baccini, P. Acid neutralizing capacity of municipal waste incinerator bottom ash. *Environ. Sci. Technol.* 1995, 29, 142-147.

45. Yan, J.; Baverman, C.; Moreno, L.; Neretnieks, I. Evaluation of the time-dependent neutralising behaviours of MSWI bottom ash and steel slag. *Sci. Tot. Environ.* 1998, 216, 41-54.

46. Johnson, C. A.; Glasser, F. P. Hydrotalcite-like minerals $(M_2Al(OH)_6(CO_3)_{0.5}.XH_2O$, where M = Mg, Zn, Co, Ni) in the environment: synthesis, characterization and thermodynamic stability. *Clays & Clay Min.* 2003, 51, 1-8.

47. Pokrovsky, O. S.; Schott, J. Experimental study of brucite dissolution and precipitation in aqueous solutions: surface speciation and chemical affinity control. *Geochim. Cosmochim. Acta* 2004, 68, 31-45.

48. Liu, X.; Millero, F. J. The solubility of iron hydroxide in sodium chloride solutions. *Geochim. Cosmochim. Acta* 1999, 63, 3487-3497.

49.   Lumsdon, D. G. Partitioning of organic carbon, aluminium and cadmium between solid and solution in soils: application of a mineral-humic particle additivity model. *Eur. J. Soil Sci.* 2004, 55, 271-285.

50.   Filius, J. D.; Meeussen, J. C. L.; Lumsdon, D. G.; Hiemstra, T.; Van Riemsdijk, W. H. Modeling the adsorption of fulvic acid by goethite. *Geochim. Cosmochim. Acta* 2003, 67, 1463-1474.

51.   Struis, R. P. W.; Ludwig, C.; Lutz, H.; Scheidegger, A. M. Speciation of zinc in municipal solid waste incineration fly ash after heat treatment: an X-ray absorption spectroscopy study. *Environ. Sci. Technol.* 2004, 38, 3760-3767.

52.   Buffle, J. *Complexation reactions in aquatic systems.* Ellis Horwood Ltd.: Chichester, UK, 1988.

53.   Johnson, C. A.; Kersten, M.; Ziegler, F.; Moor, H. C. Leaching behaviour and solubility-controlling solid phases of heavy metals in municipal solid waste incinerator ash. *Waste Manage.* 1996, 16, 129-134.

54.   Essington, M. E. Formation of calcium and magnesium molybdate complexes in dilute aqueous solutions. *Soil Sc. Soc. Am. J.* 1992, 56, 1124-1127.

55.   Krupka, K. M.; Serne, R. J. *Geochemical factors affecting the behavior of antimony, cobalt, europium, technetium, and uranium in vadose sediments.* Pacific Northwest National Laboratory operated by Battelle for the United States Department of Energy, report number PNNL-14126, 2002.

56.   Johnson, C. A.; Moench, H.; Wersin, P.; Kugler, P.; Wenger, C. Solubility of antimony and other elements in samples taken from shooting ranges. *J. Env. Qual.* 2005, 34, 248-254.

57.   Zevenbergen, C. *Natural weathering of MSWI bottom ash.* Ph.D. Thesis, Wageningen University, The Netherlands, 1994.

58.   Dijkstra, J. J.; Meeussen, J. C. L.; Comans, R. N. J. Leaching of heavy metals from contaminated soils: an experimental and modeling study. *Environ. Sci. Technol.* 2004, 38, 4390-4395.

Chapter 5

Effect of accelerated aging of MSWI bottom ash on the leaching mechanisms of copper and molybdenum

Abstract

The effect of accelerated aging of MSWI bottom ash on the leaching of Cu and Mo was studied using a "multisurface" modeling approach, based on surface complexation to iron/aluminum (hydr)oxides, mineral dissolution/precipitation, and metal complexation by humic substances. A novel experimental method allowed us to identify that the solid/liquid partitioning of fulvic acids (FA) quantitatively explains the observed beneficial effect of accelerated aging on the leaching of Cu. Our results suggest that iron/aluminum (hydr)oxides are the major reactive surfaces that retain fulvic acid in the bottom ash matrix, of which the aluminum (hydr)oxides were found to increase after aging. A new modeling approach, based on the surface complexation of FA on iron/aluminum (hydr)oxides is developed to describe the pH-dependent leaching of FA from MSWI bottom ash. Accelerated aging results in enhanced adsorption of FA to (neoformed) iron/aluminum (hydr)oxides, leading to a significant decrease in the leaching of FA and associated Cu. Accelerated aging was also found to reduce the leaching of Mo, which is also attributed to enhanced adsorption to (neoformed) iron/aluminum (hydr)oxides. These findings provide important new insights that may help to improve accelerated aging technology.

Introduction

Municipal Solid Waste Incinerator (MSWI) bottom ash, the major waste stream originating from the incineration of municipal solid waste, is considerably enriched in potentially toxic trace elements compared to its parent material (*1*). The material, when either re-used or disposed, can be qualified as a potential risk to the environment, depending on the availability of the contaminants for leaching. MSWI bottom ash is re-used as a construction material in many countries, but its application is often restricted by regulatory limits based on its leaching potential. In the Netherlands, the leaching of particularly Cu and Mo are critical with respect to environmental regulations (e.g., Dutch Building Materials decree (*2*))

MSWI bottom ash, being a high temperature product, is thermodynamically unstable under atmospheric conditions and is therefore subject to similar weathering processes as observed in natural equivalents such as volcanic ashes (e.g., ref *3*). The uptake of atmospheric CO_2 is the primary weathering reaction of MSWI bottom ash and generally leads to a decreased leachability of a number of critical metal contaminants (e.g, refs *4-6*). Accelerating the natural weathering process of MSWI bottom ash by optimizing parameters such as CO_2 pressure and humidity have been demonstrated to be a potentially promising technology, both with respect to improved leaching properties as well as to reduce CO_2 emissions from industrial sources (e.g., refs *6, 7*, and references therein). Therefore, an improved understanding of the processes and parameters that control the leaching of contaminants before and after accelerated aging may contribute to further development of this technology.

Recently, natural humic substances (humic (HA) and fulvic acid (FA)) have been identified in MSWI bottom ash and their leaching has been shown to constitute the key process responsible for the facilitated leaching of copper and possibly other metals (*8*). At present, no knowledge exists on the processes controlling the leaching of humic substances from MSWI bottom ash, and their relation with contaminant leaching.

The objective of this paper is to provide a mechanistic insight in the effects of accelerated aging on the leaching of Cu and Mo as typical and important metal and oxyanionic contaminants in MSWI bottom ash. We focus particularly on the

potentially important factors that influence the leaching of these contaminants, particularly pH-control, the contents of reactive surfaces in the bottom ash matrix and the quantities and composition of dissolved organic carbon (DOC).

Given the key role of DOC in facilitating the leaching of Cu and possibly other metals, DOC is characterized in terms of humic, fulvic and hydrophylic acids over a wide pH-range, in order to identify the processes controlling the solid/liquid partitioning of these reactive organic ligands. With an independently determined set of analytical parameters, we attempt to predict the leaching of Cu and Mo over a wide pH-range, both before and after accelerated aging, using a "multisurface" modeling approach (i.e. adsorption processes to (hydr)oxide surfaces and humic substances). Model results are used to gain further insight in the major chemical factors that control the leaching of contaminants such as Cu and Mo in MSWI bottom ash treated by accelerated aging. A novel approach is developed to model the pH-dependent leaching of fulvic acid from MSWI bottom ash, being the major process controlling the leaching of Cu and possibly other metals.

Experimental section

MSWI Bottom ash samples

A batch of about 900 tons (by weight) of freshly quenched MSWI bottom ash was treated by accelerated aging early 2004. Before the treatment, the ashes were sieved to a particle size of < 4 cm, and metal parts were removed. The treatment was carried out in a large indoor facility using air enriched with carbon dioxide ($p\mathrm{CO_2}$ = 0.1 bar). Before the start of the treatment and after 24 hours of treatment, samples were taken at different depths within the bottom ash heap (in the surface, in the middle and at the bottom) and mixed. Until further treatment, the samples were stored for about 2 weeks at 4 °C. Prior to the leaching and extraction experiments, the samples were dried at 40 °C and sieved to pass a < 4 mm stainless steel sieve, yielding about 43% of the initial dry sample weight for both the fresh and the aged material. Sieving was preferred over size-reduction to prevent breaking-up of (weathered) grains and the creation of fresh surfaces.

Batch pH-static leaching experiments

Leaching experiments were carried out on individual subsamples that were each equilibrated for 48 h, as prescribed by the European standard for the pH-static test TS14497 (*9*), at a specific pH value between pH 2 and 12 (including the native pH of the bottom ash samples that was not adjusted). 25 g of dry bottom ash was suspended in 250 g Nanopure demineralized water (a liquid to solid (L/S) ratio of 10 L/kg) in acid-cleaned 300 mL PTFE vessels, under continuous stirring at 20 °C. The pH of the different suspensions was controlled using solutions of 1 M HNO_3 and NaOH (analytical grade) and a computerized pH-stat system. The suspensions were in contact with the atmosphere. After the equilibration period, the suspensions were filtered through 0.2 μm membrane filters. The clear filtrates were acidified with concentrated HNO_3 (suprapure) and analyzed by ICP-AES to obtain solution concentrations of Al, As, Ba, Ca, Cd, Co, Cr, Cu, Fe, K, Mg, Mn, Mo, Na, Ni, P, Pb, S, Sb, Se, Si, Sn, Sr, V, and Zn. It was assumed that total S and P as measured by ICP-AES equated to SO_4 and PO_4, respectively. A carbon analyzer (Shimadzu) was used to determine dissolved inorganic and organic carbon in non-acidified fractions. Chloride was determined by ion chromatography (IC).

It has recently been shown that pH-concentration patterns, particularly of dissolved organic carbon (DOC), may be influenced by leaching kinetics (*10*). Therefore, we have included independent experiments at selected pH values with a longer equilibration time of 168 h.

Selective chemical extractions

Independent estimates of the amount of reactive surfaces present in the bottom ash matrix, which are required for sorption modeling, were made by selective chemical extractions. The solid and dissolved organic carbon in the samples was characterized quantitatively in terms of three fractions, i.e. HA, FA and hydrophilic acids (denoted by HY) by a batch procedure (*11*) derived from the method currently recommended by the International Humic Substances Society (IHHS) (*12, 13*). The amount of amorphous and crystalline iron (hydr)oxides in the bottom ash matrix was estimated by a dithionite extraction described in Kostka and Luther III (*14*), and will be referred to as Fe-DITH. The portion of amorphous iron (hydr)oxides was estimated by an

ascorbate extraction (*14*), and will be referred to as Fe-ASC. The amount of amorphous aluminum (hydr)oxides was estimated by an oxalate extraction according to Blakemore (*15*) and will be referred to as Al-OX.

Geochemical modeling

The analytical leaching data are compared to geochemical modeling predictions based on the solubility of minerals, sorption to (hydr)oxide minerals and FA/HA in the solid and solution phase. A similar modeling approach was followed by Dijkstra et al. (*10*) to which the reader is referred for further detail. In short, mineral saturation indices (SI), solution speciation, solubility of minerals and sorption processes were calculated with the ORCHESTRA (*16*) modeling framework, in which we incorporated the different sub-models described below. Inorganic speciation and mineral solubility was calculated using thermodynamic data from MINTEQA2 (version 3.11) (*17*), with modifications listed in Dijkstra et al. (*18*). Specific and non-specific sorption of protons and ions to HA and FA was modeled with the NICA-Donnan model (*19*) using the set of "generic" binding parameters of Milne et al. (*20*). It was assumed that 50% of FA and HA consists of carbon (*21*).

Dissolved element concentrations corresponding with solubility control by an infinite amount of a selected mineral was calculated according to the "infinite solid approach" as outlined by Meima and Comans (*22*). We used the Generalized Two Layer Model (GTLM) of Dzombak and Morel (*23*) for modeling surface complexation of ions to Hydrous Ferric Oxide (HFO). In accordance with Meima and Comans (*24*), amorphous aluminum (hydr)oxides present in the bottom ash matrix were considered as potentially important sorbent minerals, for which HFO was taken as a surrogate sorbent in the model. The reason for this approach is the absence of a complete and systematic database for sorption reactions on aluminum (hydr)oxides. For detail and justification of this approach the reader is referred to Meima and Comans (*24*). HFO was also used as a surrogate sorbent mineral for crystalline iron (hydr)oxide surfaces, however, site densities were calculated using a lower specific surface area of 100 m²/g (*25*). Low pH (pH 2) extracts were used to estimate concentrations of Cu available for adsorption, and alkaline pH (pH 12) extracts to estimate concentrations of Mo that are available for adsorption, respectively, assuming

complete desorption at these pH values (*24*). Component activities were calculated with the Davies equation and a moderately oxidizing environment was assumed (pH + pe = 15), in accordance with measured redox potentials in similar MSWI bottom ash samples (*22*). The sorption equilibrium was calculated simultaneously for Cu and Mo, in the presence of solution concentrations of a broad range of elements (Na, K, Ca, Mg, Mn, Al, Si, Fe, Ba, Sr, SO_4, PO_4, Cl, CO_3, Ni, Zn, Cd and Pb), which were fixed in the model at their measured values at each pH value to fully account for competitive adsorption on iron- and aluminum (hydr)oxide surfaces, HA and FA.

Results and discussion

Results of the pH-static leaching experiments, selective chemical extractions and geochemical modeling are discussed in detail below. We focus on potentially important factors that influence the leaching of Cu and Mo, particularly pH-control, the contents of reactive surfaces in the bottom ash matrix and the quantities and composition of dissolved organic carbon (DOC).

pH-dependent leaching data

Measured concentrations of Cu, Mo and DOC in leachates as a function of pH are shown in Figure 1, along with predicted concentrations based on geochemical modeling. Additional graphs are presented in the Supporting Information for the important major elements Ca, Al and SO_4 (Figure S1). In comparing the pH-dependent leaching data with modeling results, it should be noted that in cases where the "infinite solids approach" (*22*) has been used, leaching may be overpredicted at pH values where mineral solubility is high relative to the maximum leachable amount of elements (i.e. the "availability", as estimated by the amounts leached at pH 2 and 12 for cations and anions, respectively).

For an adequate assessment of the result of the treatment with respect to the leaching under field conditions, leached concentrations should be compared particularly at the native pH values of the fresh and aged sample (pH 11.1 and 8.6, respectively). When judged in this way, the aging process leads to a reduction of the Cu leaching by a factor of 3 and of Mo by about a factor of 1.5 (see also Supporting Information for a linear plot of measured concentrations in this particular pH range).
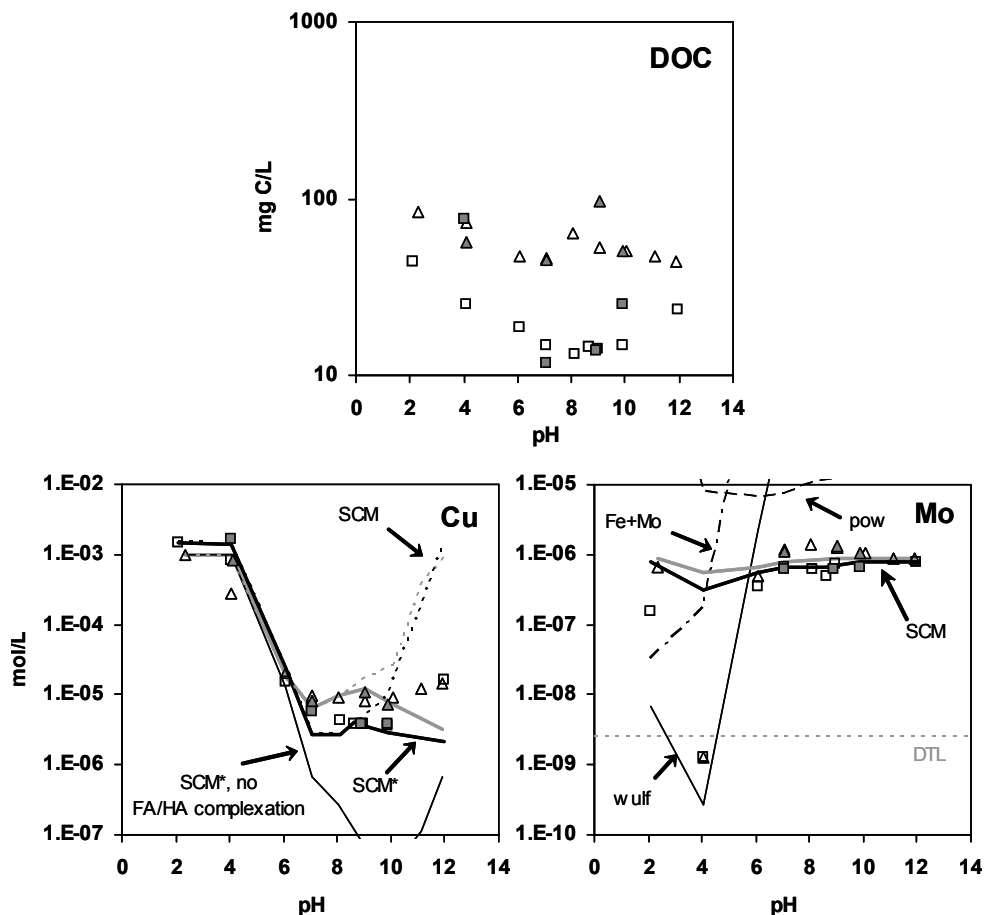
Figure 1. Leached concentrations of Cu, Mo and dissolved organic carbon (DOC) as a function of pH, for the fresh and aged sample (fresh = triangles, aged = squares; closed symbols are independent experiments obtained after a longer equilibration time of 168 h) shown together with model predictions. Grey model curves refer to model predictions of the fresh sample, black to the samples treated by accelerated aging. Abbreviations of model predictions are "SCM" = surface complexation to Fe/Al (hydr)oxides, "SCM*" = surface complexation to Fe/Al (hydr)oxides with $Cu(OH)_2(s)$ allowed to precipitate. In the panel for Cu, also a model scenario is shown for SCM* without FA/HA complexation in solution (for clarity only shown for the aged sample). Panel for Mo: "pow" = powellite, "Fe+Mo" = ferrihydrite + $Fe_2MoO_4(s)$, "wulf" = wulfenite (model curves for these minerals are only shown for the aged sample); DTL = Detection Limit.

Native pH and major element leaching

The "native" pH of the fresh sample is about 11.1 and has decreased to 8.6 in the aged sample (Table 1). The native pH of the fresh sample is consistent with the coexistence of ettringite $(Ca_6Al_2(SO_4)_3(OH)_{12}:26H_2O)$, $Al(OH)_3$ and gypsum $(CaSO_4:2H_2O)$, which results in a pH of 10-11, depending on the degree of undersaturation of gypsum (*22*). The native pH of the aged sample (8.6) is typical for weathered MSWI bottom ash (*22, 26*). The observed changes in the pH-dependent leaching patterns of important major elements (Ca, SO_4) after the accelerated aging of the bottom ash (see Supporting Information) are consistent with the processes identified previously for naturally aged bottom ash (*22*).

Table 1. Native pH and results of the selective chemical extractions of the MSWI bottom ash samples used in this study [a]

	Fresh	*Aged*
Native pH [b]	11.1	8.6
Fe-ASC (g Fe/kg dry ash) [c]	1.6 ± 0.1	1.6 ± 0.1
Fe-DITH (g Fe/kg dry ash) [c]	8.7 ± 0.5	9.4 ± 0.4
Al-OX (g Al/kg dry ash) [c]	4.8 ± 0.2	6.2 ± 0.2

[a] Values represent the mean ± standard deviation of experiments carried out in triplicate (*n*=3).
[b] Measured pH in L/S=10 (L/kg) bottom ash suspensions after a 48–hour equilibration period in the pH stat vessels without acid/base dosage.
[c] Fe extracted by ascorbic acid or dithionite extraction (denoted with Fe-ASC and Fe-DITH, respectively), Al extracted by oxalate extraction (denoted with Al-OX), see text.

Reactive surfaces present in the bottom ash matrix

Table 1 shows the estimated contents of iron/aluminum (hydr)oxides before and after the treatment, which are needed as input in the adsorption models to predict the leaching of Cu and Mo. A clear increase in Fe-ASC and Fe-DITH was not observed (Table 1). However, Al-OX has increased considerably by about 1.4 g Al/kg (Table 1), equivalent to 4 g $Al(OH)_3$/kg. This value is consistent with the amount estimated from the observed release of SO_4 after aging. Assuming that this release results from the dissolution of ettringite, the simultaneous release of Al would result in the formation of 3.6 g $Al(OH)_3$/kg (see Supporting Information for further detail).

Leaching and characterization of Dissolved Organic Carbon (DOC)

DOC concentrations show a slight pH-dependency and have consistently decreased after the treatment (Figure 1). Figure 2 shows the measured composition of DOC with respect to the quantities of humic substances (FA and HA) and hydrophilic acids (HY) as a function of pH. Figure 2 also includes the total extractable amounts of these substances from the samples. Results are shown for equilibration times of 48 hours and 168 hours. Generally, the major fraction of DOC is composed of HY, with a FA contribution of between 10 and 40%. Virtually no dissolved HA was detected in both samples (Figure 2). Below we focus on the leaching behavior of FA, which is thought to play a key role in the facilitated leaching of Cu from MSWI bottom ash leachates (*8*).

The primary effect of the accelerated aging treatment on DOC is a strong decrease of FA concentrations over almost the entire pH range. Degradation of FA is unlikely to be the process responsible for the observed differences, as [1] the total extracted amounts of FA hardly changed after treatment (Figure 2); [2] humic substances have been shown to be only slowly degradable with ^{14}C-ages of up to several thousands of years (*27*). Therefore, the decrease of FA concentrations after accelerated aging is more likely explained by stronger adsorption to the bottom ash matrix, presumably to reactive surfaces formed during the aging process such as iron/aluminum (hydr)oxide surfaces (Table 1).

Leached FA concentrations show a pH-dependency consistent with adsorption of anionic species to (hydr)oxide surfaces, i.e. strong adsorption (low solution concentrations) at low pH and a decreasing adsorption (i.e. increasing solution concentrations) towards higher pH values (*28, 29*). At pH 2, solution concentrations of FA increase again, consistent with protonation of the carboxylic groups of FA in this pH range, as well as the enhanced dissolution of iron/aluminum (hydr)oxide surfaces at low pH. At pH 2 and pH > 8 in the fresh sample, leached FA concentrations are similar to the measured total FA content, suggesting virtually complete FA desorption at these pH values. Leached FA concentrations in the aged sample are less than 50% of the total content, indicating that most of the FA content remains adsorbed to the solid phase over the full pH range. The stronger adsorption of FA in the aged sample is consistent with the larger aluminum (hydr)oxide content
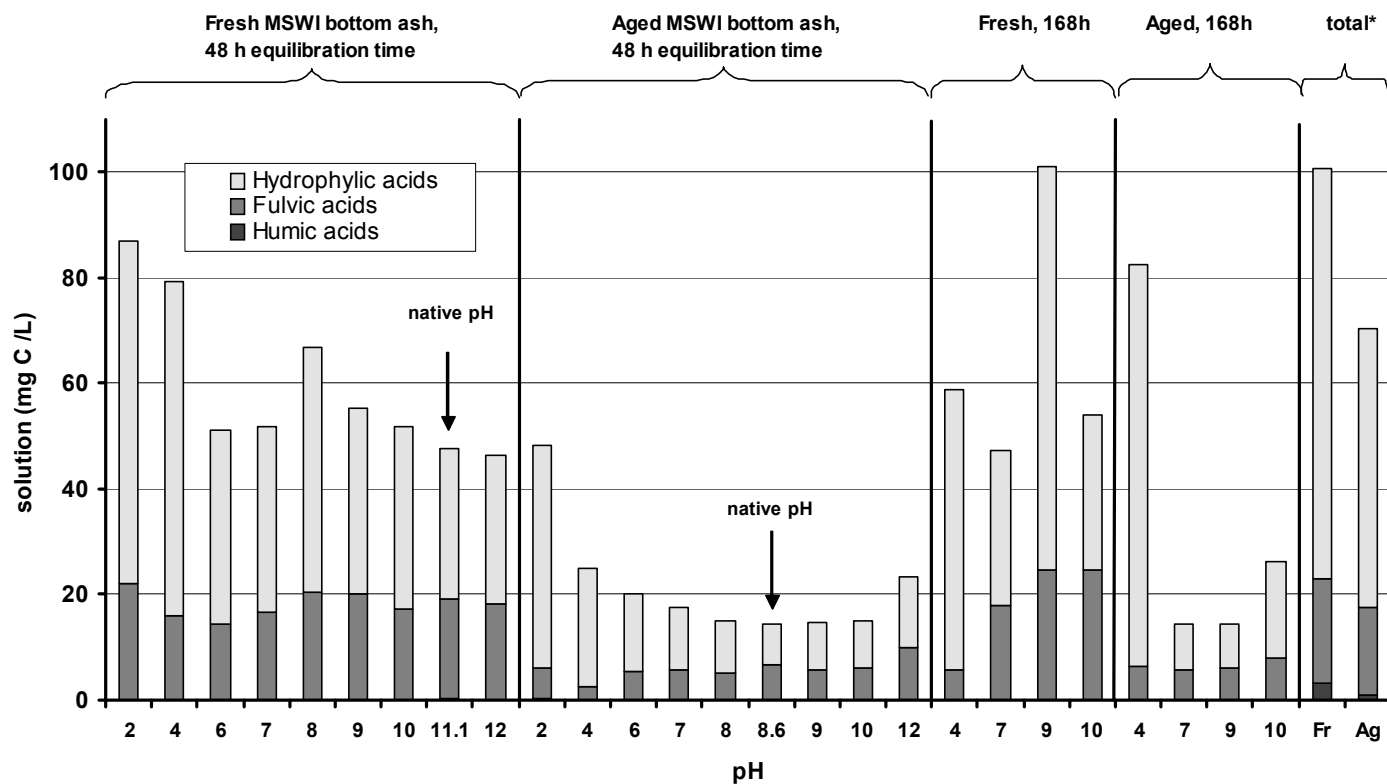
Figure 2. Results of the characterization of organic carbon present in the fresh and aged MSWI bottom ash samples with respect to hydrophilic acids, fulvic acids and humic acids. Results are shown for the standard equilibration time of 48 h and for 168 h (the latter at selected pH values). Arrows indicate the "native" pH of the samples. Total concentrations measured in the samples are shown for comparison (Fr = fresh, Ag = aged) and are expressed in the same units as the dissolved concentrations (mg C/L).

of this sample, as reflected by Al-OX in Table 1. An increase of the amount of reactive surface area would result in an increased adsorption of FA towards higher pH values. This feature has been observed for FA sorption on goethite (*29*), and is also clearly visible in the pH dependency of FA concentrations before and after aging (Figure 2). In our data, these features are more strongly pronounced in the data collected after an equilibration time of 168 hours (Figure 2), indicating a potential role of kinetics in the process that controls the leaching of FA.

Adsorption of fulvic acid on iron- and aluminium (hydr)oxides

Given the key role of FA in controlling the leaching of Cu and possibly other metals, it is important to further identify the processes that control the pH-dependent leaching of FA from fresh and aged MSWI bottom ash. Therefore, we have developed a modeling approach based on the surface complexation of FA on iron- and aluminium (hydr)oxides. This approach is derived from that of Filius et al. (*28*) for FA adsorption on goethite (α-FeOOH). The first step in our approach was to describe the pH dependent charging behavior of FA in solution by eight discrete protonation reactions, following Filius et al. (*28*). Like these authors, we also assume a molar weight of 1000 g FA/mol (1 mg FA/L ~ 10^{-6} mol/L).

Next, we have derived surface complexation parameters for FA adsorption to iron- and aluminum (hydr)oxides in the untreated MSWI bottom ash sample by defining surface complexation reactions, largely following the approach of Dzombak and Morel (*23*) for anionic species. The following surface complexation reactions were considered:

$$\equiv FeOH + 0.25\ FA^{-8} = \equiv FeOHFA_{0.25}^{-2} \tag{1}$$

$$\equiv FeOH + 0.25\ FA^{-8} + H^+ = \equiv FeFA_{0.25}^{-1} + H_2O \tag{2}$$

$$\equiv FeOH + 0.25\ FA^{-8} + 2H^+ = \equiv FeFA_{0.25}H^0 + H_2O \tag{3}$$
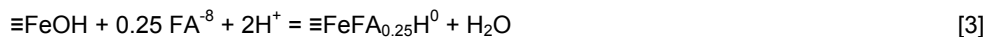
In reactions 1-3, $\equiv FeOH$ are the sites on the (hydr)oxide surface and $\equiv FeOHFA_{0.25}^{-2}$, $\equiv FeFA_{0.25}^{-1}$ and $\equiv FeFA_{0.25}H^0$ are the adsorbed species, which differ in their degree of protonation. Note that each of the adsorbed species describes the adsorption of ¼ FA

molecule, i.e. one adsorbed FA molecule occupies 4 ≡FeOH sites, in line with the approach of Filius et al. (*28*). As the fully deprotonated FA species has a charge of –8 eq/kg (the sum of carboxylic and phenolic groups of FA, see Filius et al., (*28*)), we model, for reasons of simplicity, the adsorption of ¼ FA molecule to each ≡FeOH site as a divalent anion ($0.25*-8 = -2$ eq/kg).
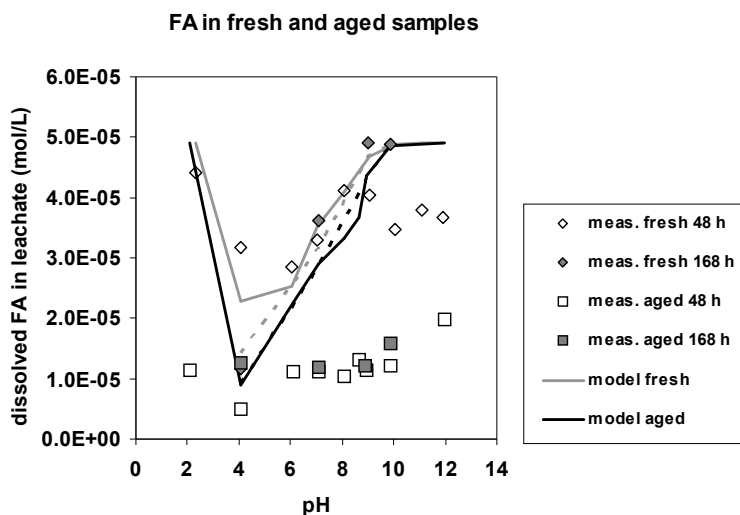
FA in fresh and aged samples

Figure 3. Measured FA concentrations in the bottom ash leachates and model curves based on surface complexation of FA to (hydr)oxide surface (see text for details). The dashed lines are obtained with the same parameters but are calculated for the leachates equilibrated for 168 h.

Reactions 2 and 3 were found to be sufficient to describe the leaching of FA in the fresh bottom ash sample over the full pH range (Figure 3). The amount of FA extracted at pH 12 after 168 h was taken as the total sorbate concentration, while the same sorbent concentration was used as described for the geochemical modeling approach in the Methods section. The log K values were fitted manually until an adequate description of the FA leaching in the fresh sample was obtained. The only fitting parameters are the log K values of reactions 2 and 3, which were found to be +10.48 and +17, respectively. Note that our log K values for FA adsorption to the iron- and aluminium (hydr)oxide surface are conditional, as they include the effects of leached cations on the speciation and binding properties of FA. These effects are

negligible in the system of Filius et al. (*28*) that only contained FA, goethite and an inert electrolyte.

Figure 3 shows that pH dependent leaching of FA from the fresh bottom ash is adequately described. We note that the difference in the predicted pH dependent FA leaching after 48 and 168 h is caused by the lower competition by phosphate and sulfate at the longer reaction time. Although the leaching behavior of FA can be described by surface complexation, the model does not predict the observed strong decrease of FA concentrations after aging, in particular at higher pH values. Possibly, the properties of the (neoformed) reactive surfaces in the aged bottom ash differ from those in the fresh material (e.g., a higher reactivity than currently assumed in the model) and/or the representation of FA speciation in our model is too simple (e.g., interactions with cations other than H^+). Important new insights in the binding of humic substances to (hydr)oxide minerals have been made by Filius et al. (*30*) and recently by Weng et al. (*31*), which may contribute to further identification of the mechanisms controlling the solid/solution partitioning of FA in materials such as MSWI bottom ash.

Copper

Leached concentrations of Cu follow a strong pH-dependency in the acidic-neutral pH range and a weaker pH-dependency towards higher pH values. Compared to the fresh sample, a consistently lower Cu leaching is observed in the aged sample between pH 6 and 10 (Figure 1), indicating that the effect of aging is not exclusively the result of the pH decrease from pH 11.1 to 8.6.

Model predictions based on surface complexation on iron/aluminum (hydr)oxides and complexation with the measured concentrations of FA in solution, denoted with SCM in Figure 1, are generally adequate up to pH 9 for both the fresh and the aged sample. However, strong overestimates of leached concentrations are found at pH 12. Although kinetic experiments with MSWI bottom ash have shown that Cu concentrations at pH 12 slowly increase beyond 48 hours (*10*), we consider this time effect to be too small to explain the large discrepancy between the model and the data at pH 12. In this high pH region (hydr)oxide minerals such as $Cu(OH)_2(s)$ and tenorite (CuO), which have been found in MSWI bottom ash (e.g., ref *4* and references

therein), become oversaturated and are expected to precipitate. Therefore, an alternative surface complexation scenario is shown in which $Cu(OH)_2(s)$ is allowed to precipitate as soon as it becomes oversaturated (denoted with SCM* in Figure 1). This model scenario provides an excellent description of Cu leaching up to pH 10, but still underestimates Cu leaching somewhat at higher pH values (Figure 1). Model scenarios based solely on the solubility of a number of common Cu carbonates and (hydr)oxide phases, calculated by the "infinite solid approach" (*22*), provide less adequate predictions as these generally fail to explain Cu leaching both at low and/or high pH (see model predictions for tenorite, $Cu(OH)_2(s)$, malachite ($Cu_2(OH)_2CO_3$) and azurite ($Cu_3(OH)_2(CO_3)_2$ in the Supporting Information).
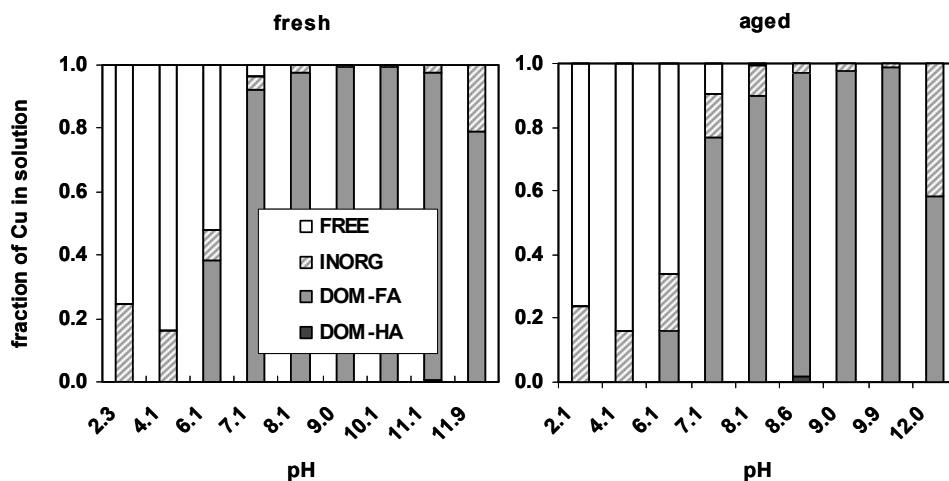
Figure 4. Calculation of the solution speciation of Cu among the different surfaces considered in the model shown for the fresh and aged sample. "DOM-FA" = bound to Fulvic Acids, "DOM-HA" = bound to Humic Acids, "Inorg" = inorganic complexes such as Cl and OH species; Free = free ions (Cu^{2+}). This figure complements predicted Cu concentrations based on the model scenario referred to as SCM* in Figure 1, see text.

With the model we are able to investigate the relative importance of the different solution species of Cu as a function of pH, as is shown in Figure 4 for the SCM* model scenario. The solution speciation is subdivided into "complexed with FA", "complexed with HA", "inorganic complexes" and "free metal" (Me^{2+}). At values of pH 6 and lower, Cu is mainly present in its free ionic form (Cu^{2+}). Above pH 7, the

binding of Cu to FA is by far the dominant solution complexation reaction in both the fresh and the aged sample. The strong predominance of organically bound Cu species at the natural pH of the samples is in agreement with earlier studies based on measurements and modeling (*8, 32*), but the strong complexation extends to both lower and higher pH values as well. When interactions with dissolved FA are neglected in the geochemical modeling calculations (shown for the SCM* model scenario in Figure 1), Cu leaching is underestimated by up to several orders of magnitude in the relevant pH range. These calculations clearly show that the leaching of Cu from MSWI bottom ash is primarily controlled by the availability and reactivity of humic substances present in the MSWI bottom ash matrix. As a consequence, the positive effect of accelerated aging on the leaching of Cu is primarily caused by the changed leaching behavior of FA, which is in turn most likely caused by an enhanced adsorption to (neoformed) iron/aluminum (hydr)oxides.

Molybdenum

The leaching of Mo between pH 6 and 10 has decreased significantly after ageing (Figure 1). Processes controlling the leaching of Mo from MSWI bottom ash have been discussed in previous publications (*4, 10, 33*), from which we show a number of potentially solubility controlling minerals in Figure 1, i.e. $Fe_2(MoO_4)_3$, wulfenite ($PbMoO_4$), and powellite ($CaMoO_4$). Figure 1 also shows predictions based on the surface complexation of for MoO_4^{-2} on iron/aluminum (hydr)oxides. Wulfenite can explain the measured concentrations below pH 6, but the leaching in the more relevant pH range between pH 8 and 11 can only be explained on the basis of the weak surface complexation of molybdate (MoO_4^{-2}) on iron/aluminum (hydr)oxides.

The measured beneficial effect of aging on the Mo concentrations between pH 8 and 11 is also predicted by the adsorption of molybdate (MoO_4^{-2}) to the increased amounts of iron/aluminum (hydr)oxides, albeit to a much lesser extent (Figure 1). It should be noted that the adsorption parameters for MoO_4^{-2} to HFO have been estimated by a Linear Free Energy Relationship (LFER)(*23*) and are, therefore, uncertain. However, in line with our findings regarding the adsorption of FA to the solid phase, the difference between the modeled and measured effect of aging is possibly related to different properties of the (neoformed) reactive surfaces in the

aged bottom ash. Although the current model cannot fully account for the reduced leaching of Mo after accelerated aging, we conclude that this positive effect is the result of a stronger Mo adsorption to (neoformed) iron/aluminum (hydr)oxides. These findings are consistent with earlier observations based on the carbonation of MSWI bottom ash leachates (*34*).

This study lends mechanistic support for the sustainability of the observed beneficial effect of accelerated aging on the leaching of Cu and Mo from MSWI bottom ash. This work provides important new insights that may help to improve accelerated aging technology, particularly the notion that the facilitated leaching of Cu and possibly other metals is predominantly controlled by the adsorption properties of fulvic acid in MSWI bottom ash. Our results suggest that iron/aluminum (hydr)oxides are the major reactive surfaces that retain fulvic acid in this matrix, of which the aluminum (hydr)oxides have been shown to increase after aging. The observed amount of neoformed Al(hydr)oxides is probably close to the maximum that can be reached by accelerated aging, given that the dissolution of ettringite, which is believed to be the major Al source in fresh bottom ash, is complete at the final pH of 8.6. Therefore, the effect of this treatment may be optimized by the addition of reactive minerals such as iron/aluminum (hydr)oxides, that can further enhance the adsorption of humic substances, associated trace contaminants and oxyanions such as MoO_4^{-2}.

Acknowledgements

Supporting information available

Major element leaching before/after accelerated ageing; linear concentration-pH plots for Cu, Mo and SO_4, model predictions for common Cu-carbonates and hydroxides. This material is available free of charge via the Internet at http://pubs.acs.org.

Literature cited

1. Chandler, A. J.; Eighmy, T. T.; Hartlen, J.; Hjelmar, O.; Kosson, D. S.; Sawell, S. E.; Van der Sloot, H. A.; Vehlow, J. *Municipal solid waste incinerator residues*; Elsevier Science B. V.: Amsterdam, The Netherlands, 1997.

2. Dutch Building Materials Decree (Bouwstoffenbesluit bodemen oppervlaktewaterenbescherming). Staatsblad van het Koninkrijk der Nederlanden 567, 1995.

3. Zevenbergen, C.; Vander Wood, T.; Bradley, J. P.; Van der Broeck, P. F. C. W.; Orbons, A. J.; Van Reeuwijk, L. P. Morphological and chemical properties of MSWI bottom ash with respect to the glassy constituents. *Hazard. Waste Hazard. Mater.* 1994, 11, 371-383.

4. Meima, J. A.; Comans, R. N. J. The leaching of trace elements from municipal solid waste incinerator bottom ash at different stages of weathering. *Appl. Geochem.* 1999, 14, 159-171.

5. Chimenos, J. M.; Fernandez, A. I.; Nadal, R.; Espiell, F. Shortterm natural weathering of MSWI bottom ash. *J. Hazard. Mater.* 2000, 79, 287-299.

6. Van Gerven, T.; Van Keer, E.; Arickx, S.; Jaspers, M.; Wauters, G.; Vandecasteele, C. Carbonation of MSWI-bottom ash to decrease heavy metal leaching, in view of recycling. *Waste Manage.* 2005, 25, 291-300.

7. Rendek, E.; Ducom, G.; Germain, P. Carbon dioxide sequestration in municipal solid waste incinerator (MSWI) bottom ash. *J. Hazard. Mater.* 2006, 128, 73-79.

8. Van Zomeren, A.; Comans, R. N. J. Contribution of natural organic matter to copper leaching from municipal solid waste incinerator bottom ash. *Environ. Sci. Technol.* 2004, 38, 3927-3932.

9. CEN/TC292. Characterization of waste - leaching behaviour tests - influence of pH on leaching with continuous pH-control. TS14997 (under development, http://www.cenorm.be/cenorm/index.htm), 2006.

10. Dijkstra, J. J.; Van der Sloot, H. A.; Comans, R. N. J. The leaching of major and trace elements from MSWI bottom ash as a function of pH and time. *Appl. Geochem.* 2006, 21, 335- 351.

11. Van Zomeren, A.; Comans, R. N. J. Measurement of humic and fulvic acid concentrations and dissolution properties by a rapid batch procedure. *Environ. Sci. Technol.* submitted.

12. Swift, R. S. *Organic matter characterization*; In *Methods of soil analysis. Part 3. Chemical methods*; Sparks, D. L., Ed.; Soil Science Society of America: Madison, WI, 1996; pp 1011-1069.

13. Thurman, E. M.; Malcolm, R. L. Preparative isolation of aquatic humic substances. *Environ. Sci. Technol.* 1981, 15, 463-466.

14. Kostka, J. E.; Luther III, G. W. Partitioning and speciation of solid-phase iron in saltmarsh sediments. *Geochim. Cosmochim. Acta* 1994, 58, 1701-1710.

15. Blakemore, L. C.; Searle, P. L.; Daly, B. K. *Methods for chemical analysis of soils*; sci. rep. 80; NZ Soil Bureau: Lower Hutt, New Zealand, 1987.

16. Meeussen, J. C. L. ORCHESTRA: An object-oriented framework for implementing chemical equilibrium models. *Environ. Sci. Technol.* 2003, 37, 1175-1182.

17. Allison, J. D.; Brown, D. S.; Novo-gradac, K. J. *MINTEQA2/PRODEFA2, Geochemical assessment model for environmental systems: version 3.11 databases and version 3.0 user's manual*; Environmental Research Laboratory, U.S.-EPA: Athens, GA, 1991.

18. Dijkstra, J. J.; Van der Sloot, H. A.; Comans, R. N. J. Process identification and model development of contaminant transport in MSWI bottom ash, *Waste Manage.* 2002, 22, 531-541.

19. Kinniburgh, D. G.; Van Riemsdijk, W. H.; Koopal, L. K.; Borkovec, M.; Benedetti, M. F.; Avena, M. J. Ion binding to natural organic matter: competition, heterogeneity, stoichiometry and thermodynamic consistency. *Colloids Surf A* 1999, 151, 147-166.

20. Milne, C. J.; Kinniburgh, D. G.; Van Riemsdijk, W. H.; Tipping, E. Generic NICA-Donnan model parameters for metal-ion binding by humic substances. *Environ. Sci. Technol.* 2003, 37, 958-971.

21. De Wit, J. C. M. *Proton and metal ion binding by humic substances.* Ph.D. Thesis, Wageningen University, Department Soil Quality, 1992.

22. Meima, J. A.; Comans, R. N. J. Geochemical modelling of weathering reactions in MSWIbottom ash. *Environ. Sci. Technol.* 1997, 31, 1269-1276.

23. Dzombak, D. A.; Morel, F. M. M. *Surface complexation modeling: hydrous ferric oxide*; John Wiley & Sons: New York, 1990.

24. Meima, J. A.; Comans, R. N. J. Application of surface complexation/precipitation modeling to contaminant leaching from weathered municipal solid waste incinerator bottom ash. *Environ. Sci. Technol.* 1998, 32, 688-693.

25. Hiemstra, T.; De Wit, J. C. M.; Van Riemsdijk, W. H. Multisite proton adsorption modeling at the solid/solution interface of (hydr)oxides: a new approach, II. application to varous important (hydr)oxides. *J. Colloid Interface Sci.* 1989, 133, 105-117.

26.   Johnson, C. A.; Brandenberger, S.; Baccini, P. Acid neutralizing capacity of municipal waste incinerator bottom ash. *Environ. Sci. Technol.* 1995, 142-147.

27.   Pettersson, C.; Ephraim, J.; Allard, B. On the composition and properties of humic substances isolated from deep groundwater and surface waters. *Org. Geochem.* 1994, 21, 443-451.

28.   Filius, J. D.; Lumsdon, D. G.; Meeussen, J. C. L.; Hiemstra, T.; Van Riemsdijk, W. H. Adsorption of fulvic acid on goethite. *Geochim. Cosmochim. Acta* 2000, 64, 51-60.

29.   Strathmann, T. J.; Myneni, S. C. B. Effect of soil fulvic acid on nickel(II) sorption and bonding at the aqueous-boehmite (ç-AlOOH) interface. *Environ. Sci. Technol.* 2005, 39, 4027-4034.

30.   Filius, J. D.; Meeussen, J. C. L.; Lumsdon, D. G.; Hiemstra, T.; Van Riemsdijk, W. H. Modeling the adsorption of fulvic acid by goethite. *Geochim. Cosmochim. Acta* 2003, 67, 1463-1474.

31.   Weng, L.; Van Riemsdijk, W. H.; Hiemstra, T. Adsorption free energy of variable-charge nanoparticles to a charged surface in relation to the change of the average chemical state of the particles. *Langmuir* 2006, 22, 389-397.

32.   Meima, J. A.; Van Zomeren, A.; Comans, R. N. J. Complexation of Cu with dissolved organic carbon in municipal solid waste incinerator bottom ash leachates. *Environ. Sci. Technol.* 1999, 33, 1424-1429.

33.   Johnson, C. A.; Kersten, M.; Ziegler, F.; Moor, H. C. Leaching behaviourandsolubility-controlling solid phases of heavy metals in municipal solid waste incinerator ash. *Waste Manage.* 1996, 16, 129-134.

34.   Meima, J. A.; Van der Weijden, R. D.; Eighmy, T. T.; Comans, R. N. J. Carbonation processes in municipal solid waste incinerator bottom ash and their effect on the leaching of copper and molybdenum. *Appl. Geochem.* 2002, 17, 1503-1513.
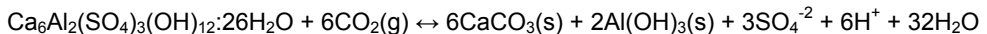
Supporting Information
Chapter 5

Contents:

- Major element leaching
- Linear concentration-pH plots for Cu, Mo and SO$_4$;
- Model predictions for common Cu-carbonates and –hydroxides.

Major element leaching before and after accelerated aging

The pH dependent leaching pattern of Ca is an indicator for the degree of aging (*1,2*). In the fresh bottom ash Ca leaching is adequately described by the solubility of gypsum in the pH range 2-9 and ettringite above pH 9. After treatment, the Ca leaching pattern has clearly shifted towards the theoretical solubility curve of calcite (Figure S1), in particular above pH 7 where calcite is less soluble than both gypsum and ettringite. This difference results from the reaction of gypsum and ettringite with carbon dioxide, during which calcite is produced (see below). Figure S1 also includes the pH dependent leaching pattern of Ca from a MSWI bottom ash sample that has been in outside storage for 1.5 years (data from ref. *1*), showing a stronger similarity with the theoretical solubility curve of calcite than the sample treated by accelerated aging. This observation suggests that the aging process in the treated sample is not complete. The oversaturation of calcite in our leachates ($SI_{calcite} \sim 1.1 - 1.4$ above pH 8) is commonly observed in leachates from incineration residues and natural waters (see ref *1* and references therein).

In the pH range above pH 9, the leaching of SO_4 has strongly increased after treatment (Figure 1). This process can be explained by the reaction between ettringite and dissolved $CO_2(g)$, leading to the formation of calcite and $Al(OH)_3(s)$:

$$Ca_6Al_2(SO_4)_3(OH)_{12}{:}26H_2O + 6CO_2(g) \leftrightarrow 6CaCO_3(s) + 2Al(OH)_3(s) + 3SO_4^{-2} + 6H^+ + 32H_2O$$

The above equation shows that the conversion of ettringite leads to the release of SO_4^{-2}. The released SO_4^{-2} may be controlled by more soluble minerals at high pH such as hydrocalumites (*3*), and may be used to estimate the minimum amounts of reaction products formed after aging. The increase of SO_4^{-2} amounts to 6.83 mM (derived from Figure S1), indicating that 13.66 mM of calcite has formed $\sim$ 13.7 g calcite/kg dry ash (1 mol $SO_4^{-2} \sim$ 2 mol calcite, L/S ratio = 10 L/kg). Similarly, it can be estimated that 3.6 g $Al(OH)_3(s)$/kg has formed. Both in the fresh and the aged sample, the leaching of Al largely follows the pH-dependent solubility behavior characteristic for aluminum (hydr)oxides (Figure S1).

Literature citations (supporting information):

1.   Meima, J. A.; Comans, R. N. J. Geochemical modelling of weathering reactions in MSWI bottom ash. *Environ. Sci. Technol.* 1997, 31, 1269-1276.
2.   Johnson, C. A.; Brandenberger, S.; Baccini, P. Acid neutralizing capacity of municipal waste incinerator bottom ash, *Environ. Sci. Technol.* 1995, 142-147.
3.   Reardon, E. J.; Della Valle, S. Anion sequestering by the formation of anionic clays: lime treatment of fly ash slurries, *Environ. Sci. Technol.* 1997, 31, 1218-1223.
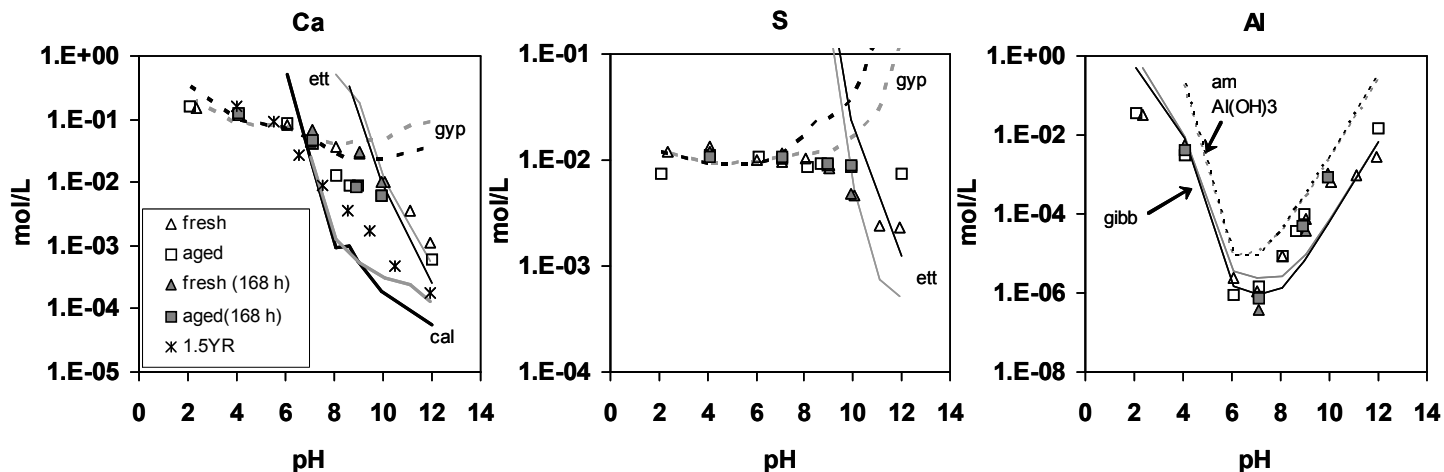
Figure S1. Leached concentrations and model predictions as a function of pH of Ca, SO_4^{-2} and Al from the fresh sample and the sample treated by accelerated aging (fresh = triangles, aged = squares; closed symbols are independent experiments obtained after a longer equilibration time of 168 h). The Ca panel includes the leaching pattern for a naturally aged sample (1.5YR, see text for further explanation). Grey model curves refer to model predictions of the fresh sample, black to the aged samples treated by accelerated aging. Abbreviations of model predictions are ett = ettringite, gyp = gypsum, cal = calcite, gibb = gibbsite, am Al(OH)$_3$ = amorphous Al(OH)$_3$.
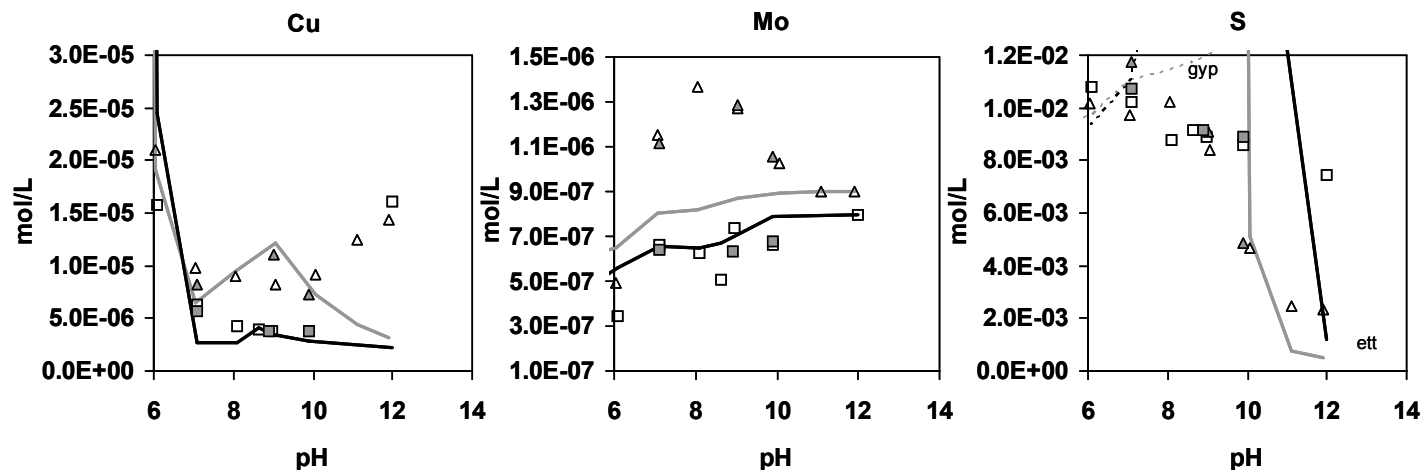
Figure S2: pH versus concentrations of Cu, Mo and SO$_4$ plotted on a linear scale in the pH-range 6 – 12 (fresh = triangles, aged = squares; closed symbols are independent experiments obtained after a longer equilibration time of 168 h). The data is identical to that of Figure 1 in the main text that covers the whole pH range (pH 2 – 12) and in which concentrations are plotted on a log scale to account for the log-scale concentration differences over the full pH range. Grey model curves refer to the fresh sample, black model curves to the aged sample. The model scenarios shown are for Cu: surface complexation to (hydr)oxides, precipitation of Cu(OH)$_2$(s) and complexation of Cu to fulvic acids in solution; For Mo: surface complexation to (hydr)oxides; For SO$_4^{-2}$: solubility of gypsum and ettringite. For detail see main text and (for SO$_4^{-2}$) text on the first pages of this supporting information.
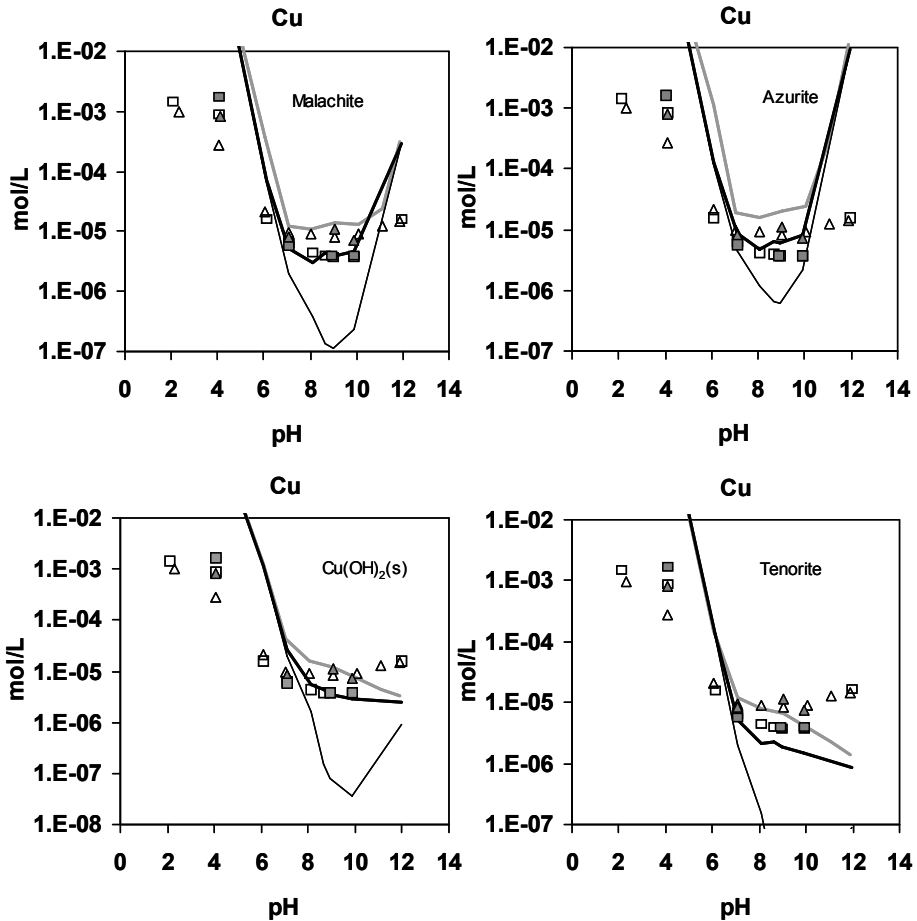
Figure S3: Leached concentrations and model predictions as a function of pH of Cu from the fresh and aged sample (fresh = triangles, aged = squares; closed symbols are independent experiments obtained after a longer equilibration time of 168 h) for different mineral phases. Grey model curves refer to model predictions of the fresh sample, black to the aged samples. Thin black curves illustrate the model scenarios in which interactions with dissolved humic acids (HA) and fulvic acids (FA) were not taken into account, in order to demonstrate the importance of these ligands for copper binding in MSWI bottom ash leachates (for clarity only shown for the aged sample).

Chapter 6

A consistent geochemical modelling approach for the leaching and reactive transport of major and trace elements in MSWI bottom ash

Abstract

To improve the long-term environmental risk assessment of waste applications, a predictive "multi-surface" modelling approach is developed to simultaneously predict the leaching and reactive transport of a broad range of major and trace elements and fulvic acids from MSWI bottom ash. The geochemical part of the model approach incorporates surface complexation/precipitation on iron- aluminium (hydr)oxides, complexation with humic and fulvic acids (HA and FA, respectively) and mineral dissolution/precipitation. In addition, a novel approach is used to describe the dynamic leaching of FA, based on the surface complexation of FA on iron/aluminium (hydr)oxides. To enable reactive transport calculations, the geochemical part of the model is combined with advective/dispersive transport of water and first-order mass transfer between mobile and stagnant zones. Using a single, independently determined set of input parameters, adequate model predictions are obtained for the leaching of a broad range of elements under widely different conditions, as verified with data from the European standardised pH-static and percolation leaching tests (TS 14997 and TS 14405, respectively). The percolation test was operated at different flow velocities and with flow interruptions to enable verification of the local equilibrium assumption. The generally adequate agreement between the model predictions and measurements for MSWI bottom ash shows that the use of equilibrium-based reactive transport models to predict data from dynamic laboratory leaching tests is promising. This finding is supported by the generally low sensitivity of leached concentrations to flow velocity and flow interruptions. Physical non-equilibrium processes are identified for non-reactive soluble salts, and possible sorption-related non-equilibrium processes for the leaching of molybdenum, FA and associated trace metals. Further improvement of the reactive transport model can be achieved by a more mechanistic description of the (dynamic) leaching behaviour of humic substances. Finally, the combination of batch and dynamic leaching test methods, in particular TS 14997/TS 14429 (pH-dependence tests) and TS 14405 (percolation test), in combination with selective chemical extractions and a mechanistically based modelling approach, constitutes a promising set of tools to assess the long-term environmental impact of the application of granular waste materials in the environment.

Introduction

Percolation tests are commonly used instruments to estimate the long-term percolation-dominated release potential from granular waste materials (e.g., NEN 7343 (*1*); TS 14405 (*2*)). For a process-based interpretation of test results and their translation to field situations, sufficient understanding is required of the geochemical and mass transfer processes that control the leaching of contaminants in a percolation regime. Reactive transport modelling is a potentially valuable instrument to identify and describe the dynamic leaching processes of contaminants from waste materials (the "source term") as well as their further rate of transport in soil and groundwater, and may form a basis for the development of realistic regulatory limits.

Municipal Solid Waste Incineration (MSWI) bottom ash is a particularly relevant material to study reactive transport processes, as is it the most significant residual waste stream from MSW incineration and is re-used in many countries as a construction product (*3*). The material is known for its complex physicochemical characteristics and metastable mineralogical composition (*3, 4*) and is considerably enriched in potentially toxic trace elements compared to its parent material (*3*). Although geochemical models have been used successfully to identify the leaching processes in MSWI bottom ash in batch experiments (e.g., refs *5-8*), reports on the application of such models to dynamic MSWI bottom ash systems are, however, relatively scarce (e.g., refs *9-14*).

Dijkstra et al. (*14*) have used a reactive transport model based on equilibrium chemistry to identify processes that control the leaching of major and trace elements from weathered MSWI bottom ash in a percolation test. In that study, local non-equilibrium processes were inferred from the relatively abrupt changes that the modelled leaching curves showed in comparison with the gradual concentration changes observed experimentally (*14*). It was concluded that model predictions could be improved by including both non-equilibrium processes and a model for the reactive transport of dissolved organic carbon (DOC), because of the dominant role of organic ligands in the facilitated transport of metals.

Recent work indicates that the leaching of natural humic substances, in particular fulvic acids (FA) of which DOC in MSWI bottom ash leachates is partially composed,

is the key process responsible for the facilitated leaching of copper and possibly other metals (*15*). In turn, the leaching of FA from MSWI bottom ash is most likely controlled by adsorption of FA to (neoformed) iron/aluminium (hydr)oxides present in the bottom ash matrix (*16*). Based on these insights, conditional surface complexation constants for FA adsorption to iron/aluminium(hydr)oxides have been derived that adequately describe FA leaching in fresh MSWI bottom ash (*16*).

The role of kinetics in the leaching of major and trace elements from MSWI bottom ash has recently been investigated in detail in batch pH-dependent leaching experiments (*8*). It was concluded that even at short equilibration times (~ 48 h) most major and trace elements closely approach equilibrium model curves, in particular at the "natural" pH of the sample (*8*). Although this observation is promising for the application of equilibrium geochemical models to dynamic systems, the validity of the local equilibrium assumption in percolation tests such as TS 14405 (*2*) is yet to be demonstrated.

This paper presents a predictive, "multi-surface" geochemical modelling approach that is based on the above mentioned recent insights in the processes that control the speciation and leaching of elements in MSWI bottom ash. The approach is used to predict the simultaneous leaching of a wide range of major and trace elements (i.e., pH, Na, Al, Fe, Ca, SO_4, Mg, Si, PO_4, CO_3, Cl, Ni, Cu, Zn, Cd, Pb, Mo) and fulvic acids (FA) from MSWI bottom ash under widely different batch and dynamic conditions. The geochemical part of the model includes mineral dissolution/precipitation as well as sorption processes to multiple reactive surfaces, i.e. surface complexation/precipitation on iron- aluminium (hydr)oxides, and complexation of ions with humic and fulvic acids. To enable reactive transport calculations, the geochemical part of the model is extended with one-dimensional, convective/dispersive transport of water combined with first order mass transfer between mobile and stagnant zones ("dual porosity", e.g., ref *17* and references therein). The complete reactive transport model is implemented in the ORCHESTRA modelling environment (*18*).

To parameterize the model, an independently determined set of input parameters is collected from selective chemical extractions (i.e. to determine the amounts and type of reactive surfaces) and low-pH extracts to obtain estimates of the amounts of elements available for leaching. The geochemical (adsorption-) models are applied

without modification and only the published "generic" binding parameters are used, i.e. without parameter fitting.

Using the same set of input parameters, the modelling approach is verified with data collected from two European-wide standardized leaching tests differing in concept and conditions, i.e. the batch pH-static test TS 14997 (*19*) and the European standardized percolation test TS 14405 (*2*). The collected pH dependent leaching data are used to verify whether the geochemical processes that control the leaching are sufficiently described by the geochemical model. Data from the percolation tests, operated with different flow velocities and with flow interruptions, are used to evaluate the validity of the local equilibrium assumption and the robustness of the reactive transport model predictions.

Using the approach outlined above, this study aims to provide a detailed insight in the mechanisms that control the leaching of major and trace elements from MSWI bottom ash in batch and percolation regimes. In addition, this work aims to demonstrate the effectiveness of coupling the present generation of geochemical models with a transport model to predict complex and dynamic leaching scenarios, of which the percolation-dominated leaching of MSWI bottom ash is a representative and relevant case study. Finally, the possible implications that the process-level insights from this study have on the settings of standardized percolation tests such as TS 14405 are briefly discussed.

Materials and methods

MSWI Bottom ash samples

A freshly quenched MSWI bottom ash sample was collected from a Dutch MSW Incinerator plant in early 2004. Prior to the leaching and extraction experiments, the sample was dried at 40 °C and sieved to pass a < 4 mm stainless steel sieve, yielding about 43% of the initial dry sample weight. Sieving was preferred over size-reduction to prevent breaking-up of (weathered) grains and the creation of fresh surfaces. This sample has previously been described by Dijkstra et al. (*16*) in which it is referred to as the "fresh" sample.

Batch pH-static leaching experiments

The batch pH-dependence leaching experiments conducted with this bottom ash sample have been described in detail elsewhere (*16*). In summary, the leaching experiments were carried out largely according to the European standard for the pH-static test TS 14997 (*19*) on individual sub-samples that were each equilibrated for 48 hours, at a specific pH value between pH 2 and 12 (including the native pH of the bottom ash samples that was not adjusted, ~ pH 11.2) and at a liquid to solid (L/S) ratio of 10 L/kg.

Percolation tests with different flow velocities and flow interruption

The percolation tests were performed largely according to TS 14405 (*2*). The columns (borosilicate glass, inner diameter 5 cm) were equipped with 10 μm PTFE filters at the inlet and outlet of the columns. The dry bottom ash was added to the columns in layers of a few cm and packed by shaking and pushing gently with a rod until a filling height of $\pm$ 20 centimetres was reached. Nanopure water of neutral pH was used as the influent solution. The packed columns were water saturated and pre-equilibrated for 72 hours, as prescribed by TS 14405, after which the influent was pumped in up-flow direction. Computer-controlled flow controllers were used assuring a constant flow velocity during the experiments. Fractions were collected automatically at cumulative liquid to solid ratio (L/S) values of 0.2, 0.5, 1, 2, 5 and 10 (L/kg) and a number of intermediate fractions (see below). Effluent fractions were collected in acid-cleaned PE bottles. Tubing conducting the effluent, as well as the effluent collection bottles, was kept under a continuous flow of moistened N_2 to prevent carbonation and oxidation of the leachates. Possible photosynthetic growth (e.g., algae) was prevented by wrapping the column and effluent collection bottles with aluminium foil. Shortly after collection of each effluent fraction, pH, redox potential and conductivity were determined, and sub-samples for chemical analysis were taken and filtered through 0.45 μm membrane filters. The clear filtrates were acidified with concentrated HNO_3 (suprapure) and analyzed by ICP-AES to obtain solution concentrations of Al, As, Ba, Ca, Cd, Co, Cr, Cu, Fe, K, Mg, Mn, Mo, Na, Ni, P, Pb, S, Sb, Se, Si, Sn, Sr, V, and Zn. A carbon analyzer (Shimadzu TOC 5000A) was used to determine dissolved inorganic and organic carbon in non-acidified fractions.

Chloride and sulphate were determined by ion chromatography (IC). It was assumed that total P as measured by ICP-AES equated to PO_4.

In deviation of TS 14405, the column tests were performed at different flow velocities and with flow interruptions during the course of the experiment in order to verify the local equilibrium assumption. The experiment referred to as "standard" was conducted with a flow velocity of 12 mL/h, which approximates the flow rate prescribed by TS 14405. The "fast" experiment was conducted with a four times higher flow rate of 48 mL/h. In both the "standard" and the "fast" experiment, the flow was stopped for 77 hours at L/S ~ 2 and 70 hours at L/S ~ 10. After the flow interruption periods, the pump was started and an "equilibrated" leachate fraction of about 120 mL was collected, which is slightly less than 1 pore volume (~ 160 mL). The relevant characteristics of the column experiments are summarized in Table 1.

Table 1. Characteristics of the percolation tests. The cumulative L/S values printed in italics indicate "equilibrated" fractions after flow interruption (between brackets the duration of flow interruption (h)). The "standard" percolation test is conducted with the flow velocity prescribed by the European percolation test standard TS 14405 (2).

	Standard	Fast
flow rate (ml/h)	12	48
dry weight of bottom ash (g)	562	566
filling height (cm)	20	21
saturated pore volume (mL) [a]	165	178
initial L/S ratio (L/kg) [b]	0.29	0.31
residence time (h) [c]	13.8	3.7
Fraction#	Cumulative L/S (L/kg)	
1[d]	*0.23 (72 h)*	*0.24 (72 h)*
2	0.58	0.66
3	1.15	1.31
4	1.95	2.04
5	*2.16 (77 h)*	*2.23 (77 h)*
6	5.20	5.16
7	9.88	9.57
8	*10.09 (70 h)*	*9.96 (70 h)*

[a] Water volume in the saturated column, determined gravimetrically.

[b] Initial L/S ratio calculated from saturated pore volume and mass of dry bottom ash.

[c] Average residence time of the eluate calculated from the saturated pore volume and flow rate.

[d] Initial equilibration period prescribed by TS 14405 (2).

Geochemical and transport modelling

Geochemical modelling approach

Inorganic speciation and mineral solubility was calculated using thermodynamic data from MINTEQA2 version 4.0 (*20*). Specific and non-specific sorption of protons and ions to humic and fulvic acids (HA and FA, respectively) was modelled with the NICA-Donnan model (*21*) using the set of "generic" binding parameters of Milne et al. (*22*) except for the binding of Fe-III to FA, for which the more recent NICA-Donnan parameters derived by Hiemstra and Van Riemsdijk (*23*) were used. It was assumed that 50% of HA and FA consists of carbon (*24*).

The Generalized Two Layer Model (GTLM) of Dzombak and Morel (*25*) was used to model surface complexation and surface precipitation of ions to Hydrous Ferric Oxide (HFO). Amorphous aluminium (hydr)oxides present in the bottom ash matrix were considered as potentially important sorbent minerals. Following Meima and Comans (*26*), HFO was taken as a surrogate sorbent for these surfaces in the model, as no complete and systematic database for sorption reactions on aluminium (hydr)oxides is currently available. For detail and justification of this approach, the reader is referred to Meima and Comans (*26*). HFO was also used as a surrogate sorbent mineral for crystalline iron (hydr)oxide surfaces, however, site densities were calculated using a lower specific surface area of 100 m^2/g (*27*).

The surface complexation constants of Dzombak and Morel (*25*) were included in the model for H, Ca, Ba, Mg, Mn, Ni, Cu, Zn, Cd, Pb, Sb, Mo, Si, SO$_4$ and PO$_4$. The surface complexation constant for the low affinity site for Pb was considered an underestimate by Dzombak and Morel (*25*), therefore a higher log K value of 1.7 was used to be consistent with the general trend of an approximate 3 log-unit difference between the sorption constants for the high and low affinity sites (*25*). The adsorption of carbonate was modelled using the surface complexation constants derived by Appelo et al. (*28*). For surface precipitation of trace metals to iron- and aluminium (hydr)oxides, surface precipitate solubility constants were adopted from Farley et al. (*29*) for Pb, Cd and Zn.

Surface complexation of FA to iron- and aluminium (hydr)oxides was modelled using the reactions and conditional surface complexation constants derived by Dijkstra et al. (*16*) for the same MSWI bottom ash sample. A molar weight of 1000 g

FA/mol is assumed (*30*). The leaching of HA was not taken into account in the forward model predictions, as HA concentrations were generally not detectable in the leachates over a wide pH range (*16*), and because the underlying processes of HA solid/solution partitioning in MSWI bottom ash are at present not sufficiently known (see results section for discussion).

Component activities were calculated with the Davies equation as ionic strengths in the leachates were up to ~ 0.5 M, at which Debeye-Hückel is not applicable (*31*). A moderately oxidizing environment was assumed (pH + pe = 15), in agreement with measured redox potentials in batch experiments with similar MSWI bottom ash samples (*6*) and in the percolation tests (see results section).

Table 2. Estimated available concentrations of elements and reactive surfaces that serve as input in the geochemical and transport model.

Si [a]	2.45E+00	mol/kg	Zn	5.37E-02	mol/kg
Ca	1.59E+00	mol/kg	Cu	1.07E-02	mol/kg
Al [a]	1.35E+00	mol/kg	Mn	7.18E-03	mol/kg
CO_3	7.00E-01	mol/kg	Ni	1.94E-03	mol/kg
Fe	2.93E-01	mol/kg	Pb	1.31E-03	mol/kg
Mg	1.83E-01	mol/kg	Ba	8.14E-05	mol/kg
Cl	1.47E-01	mol/kg	Cd	3.71E-05	mol/kg
Na	1.47E-01	mol/kg	PO_4 [b]	1.00E-04	mol/kg
SO_4	1.39E-01	mol/kg	Mo	9.01E-06	mol/kg
Fulvic acids [c]	3.67E-04	mol/kg			
Fe+Al (hydr)oxides [d]	2.90E-02	kg/kg			
specific surface area [e]	4.08E+05	m^2/kg			

[a] Derived from reaction stoichiometry, see text.

[b] In the batch calculations fixed to 1E-5 mol/L, see text.

[c] A molar weight is used of 1000 g FA/mol (*30*)

[d] As measured by selective chemical extractions, see ref *16*.

[e] The overall specific surface area is calculated from the weighted contributions of amorphous Fe- and Al (hydr)oxides for which 600 m^2/g is used (*25*) and crystalline Fe-(hydr)oxides for which a specific surface area of 100 m^2/g is used (*27*).

Parameterization of the geochemical model

All geochemical model input parameters, expressed in the appropriate units, are presented in Table 2 and will be explained below. Independent estimates of the amount of reactive surfaces present in the bottom ash matrix, which are required for sorption modelling, were made by selective chemical extractions. Amounts of

"reactive" iron- and aluminium (hydr)oxides in the bottom ash sample, as estimated by selective chemical extraction, were adopted from Dijkstra et al. (*16*). In short, the amounts of amorphous and crystalline iron (hydr)oxides in the bottom ash matrix were estimated by ascorbate and dithionite extractions, respectively, following the protocol of Kostka and Luther III (*32*). The amount of amorphous aluminium (hydr)oxides was estimated by an oxalate extraction according to Blakemore (*33*).

The solid and dissolved organic carbon in the sample and in the leachates was characterized quantitatively in terms of three fractions, i.e. HA, FA and hydrophilic acids (HY) by a batch procedure (*34*) derived from the method currently recommended by the International Humic Substances Society (IHHS) (*35, 36*). Results of this method for the pH dependence test leachates of this bottom ash sample have been discussed in detail by Dijkstra et al. (*16*). Results for the leachates of the percolation tests will be presented in the results section below.

Measurements at pH 2 in the pH-static test (L/S = 10) were used as first estimates of the concentrations of major and trace elements that are active in mineral dissolution/precipitation and sorption processes. It is assumed that cations are fully desorbed from iron- and aluminium (hydr)oxide surfaces (*26*) and that solubility controlling mineral phases are largely dissolved under these conditions. Concentrations measured at this pH value generally represent the maximum over the pH range investigated (pH 2-12). Exceptions are the anionic species MoO_4^{-2} and FA for which concentrations measured at pH 12 were used, assuming complete desorption from iron- and aluminium (hydr)oxides at this pH value (*8, 16*). For carbonate, the total content in the sample was used as input in the model, as low or high pH extracts cannot be used for this purpose due to the degassing of $CO_2(g)$ and precipitation of carbonate minerals, respectively. The total content of carbonate was measured with a carbon analyzer (Shimadzu TOC 5000A). Consequences of the "availability" estimates for the different groups of elements will be further discussed in the results section.

To predict MSWI bottom ash leaching as a function of pH the amounts listed in Table 2 were used as input in the model in combination with the liquid-solid value of 10 L/kg. The model calculates the speciation of all elements simultaneously at fixed pH values between pH 2 and 12 (in steps of 0.1 pH units). The selection of minerals

that were allowed to precipitate during the calculation (Figure 2) is discussed in the results section.

It is important to note that the present modelling approach differs in a number of aspects from the approach followed in the authors' previous studies (for detail see refs *6* and *8*). In short, the most important differences with previous work are:

    [i)] *Solubility controlled elements.* In previous publications, model predictions for solubility controlled elements are calculated according to the "infinite solids approach". In that approach, the leachate composition is calculated in equilibrium with an infinite amount of a selected mineral. Each element/mineral(s) combination requires a separate model run (for detail on this approach see ref *6*). In the present approach, the leachate composition is predicted using finite amounts of minerals that are constrained by the availability estimates listed in Table 2. The leachate composition based on the resulting mineral assemblage is calculated in a single model run.

    [ii)] *Sorption controlled elements.* In previous publications, model predictions for sorption controlled elements are calculated in the presence of total solution concentrations of major elements that compete for the same sorption sites. The total solution concentrations of these elements are fixed to their measured value to fully account for competition for available adsorption sites (for detail on this approach see ref *8*). In the present approach, the solution concentrations of all major and trace elements, whether they are based on solubility and/or sorption reactions, are predicted simultaneously in a single model run.

As the present model predictions are conducted for all solubility and/or sorption controlled elements simultaneously, the model predictions for one element depend on that of all other elements, as well on the parameters listed in Table 2.

Transport model

To predict MSWI bottom ash leaching in a percolation regime, the geochemical part of the model was extended with one-dimensional transport of water. To account for physical non-equilibrium (e.g., as indicated by observed "tailing" of element concentrations, refs *10, 14*) the "dual porosity" approach (e.g., ref *17*) was followed. The dual porosity approach assumes that the liquid phase is partitioned in a mobile

(flowing) and immobile (stagnant) zone. Solute exchange between the mobile and stagnant zone is approximated by a first-order process according to (e.g., ref *17* and references therein):

$$\theta_{im} \, dC_{im}/dt = \alpha \, (C_m - C_{im}) \tag{1}$$

In equation [1], α is the first order mass transfer coefficient (s^{-1}), C_m is the concentration in the mobile zone, and C_{im} is the concentration in the stagnant zone. The parameters θ_{im} and θ_m are the stagnant and mobile portions of the total water filled porosity θ, a fraction of the total volume (-):

$$\theta = \theta_m + \theta_{im} \tag{2}$$
$$\beta = (\theta_m / \, \theta) \tag{3}$$

The parameter β in equation [3] is the ratio between the mobile and total porosity. The relatively simple dual porosity approach has the advantage over more complex diffusion models in that it can be used in situations where little is known about the physical characteristics of the stagnant zones.

The parameter θ was obtained gravimetrically from the saturated pore volume and total volume in the columns (Table 2). The two parameters α and β of equations [2] and [3] were fitted such that an adequate description was obtained for the leaching of chloride (see results section), of which conservative leaching behaviour is assumed. By implementing the fitted dual porosity parameters in the reactive transport model, it is implicitly assumed that the physical transport behaviour of all dissolved components is similar to that of chloride. The fitted values for the parameter α and β are presented and discussed in the results section. The column was represented in the model by 10 cells (5 mobile and 5 stagnant cells). The numerical dispersivity generated by this schematization matches the observed dispersivity of chloride in the first eluate fractions. It is noted that ORCHESTRA enables a correct representation of flow interruption periods, i.e. by pausing the convective flow of water while diffusion processes continue.

TS 14405 prescribes relatively large effluent fractions, which vary in size from one to several pore volumes (e.g., see Table 1, 1 pore volume ~ 0.3 L/S). To enable an

appropriate comparison between transport model results and the collected data in the graphs (Figure 3 and 4), the transport model output (fractions of equal size) was made compatible with the size of the different fractions in the test by averaging the modelled concentrations over the appropriate time intervals (i.e. L/S fractions).

The initial composition of the system was calculated from the "available" concentrations of elements expressed in moles per kg solid material (Table 2) in combination with the liquid-solid ratio in the column (~ L/S 0.3, Table 1). For protons, the initial $H+-OH-$ mass balance was not measured but calculated from the initial pH of the system, which was estimated from the pH of the first fraction of the percolation test. After initialisation, column pH values were not fixed but calculated from the total H^+-OH^- mass balance per cell, which changes in time as a result of convective transport. It was assumed that the initial chemical composition of the system was equal for all mobile and stagnant cells in the column. The influent solution in the model was kept in equilibrium with the atmosphere (pCO_2 = -3.5, pH = 5.67) and contained negligible concentrations of other elements.

Results and discussion

pH-static leaching test data and model results

Measured concentrations and model predictions of a number of important components, i.e. Al, Ca, SO_4, Si, Fe, fulvic acids (FA), Ni, Cu, Zn, Cd, Pb and Mo are shown in pH-concentration diagrams in Figure 1. For the selection of potentially solubility controlling processes in MSWI bottom ash for each of the elements of interest is referred to previous work, in particular Dijkstra et al. (*8*) and references therein. For a detailed discussion on the solubility controlling processes of FA, FA-associated Cu, and Mo is referred to Dijkstra et al. (*16*).

The major components Al, Ca, SO_4 and Si play a major role in governing leachate pH (*6, 37*) and, therefore, an adequate prediction of these components is crucial with respect to pH-prediction by the transport model (see below). The minerals gibbsite ($Al(OH)_3(s)$, gypsum ($CaSO_4.2H_2O)(s)$), calcite ($CaCO_3(s)$), ettringite ($Ca_6Al_2(SO_4)_3(OH)_{12}.26H_2O$) and laumontite ($CaAl_2Si_4O_{12}.4H_2O(s)$) were considered as plausible solubility controlling phases for these elements (ref *8* and references there-
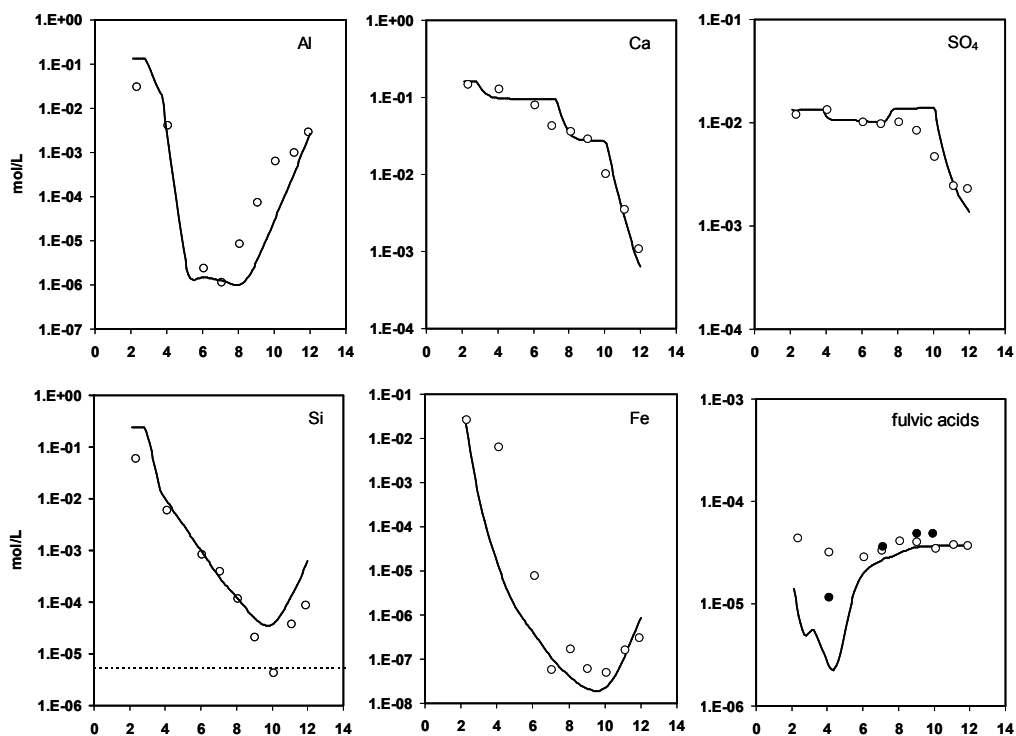
Figure 1. Leached concentrations as a function of pH as measured with the pH-static test (open circles) and model predictions (curves) for Al, Ca, SO_4, Si, Fe, fulvic acids, Cu, Mo, Ni, Cd, Pb, Zn and Mo. The closed circles in the diagrams for fulvic acids and Cu are from independent experiments obtained after a longer equilibration time of 168 h. Horizontal dashed lines represent detection limits.

in) and were allowed to precipitate. For gibbsite the solubility product of Lindsay (*38*) was used, as it generally provided a better description of Al solubility than the more soluble/stable Al (hydr)oxides available in the MINTEQ 4.0 (*20*) database. The laumontite solubility product was adopted from the MINTEQ 3.11 database (*39*). For calcite, a ten times higher solubility product of $10^{-7.48}$ was used according to the generally observed calcite oversaturation of about one order of magnitude in leachates from incineration residues and natural waters (see ref 6 and references therein). The presence of this combination of minerals provides an excellent prediction of the leaching of Al, Ca, SO_4, Si, (Figure 1), and also of carbonate that is not included in Figure 1.
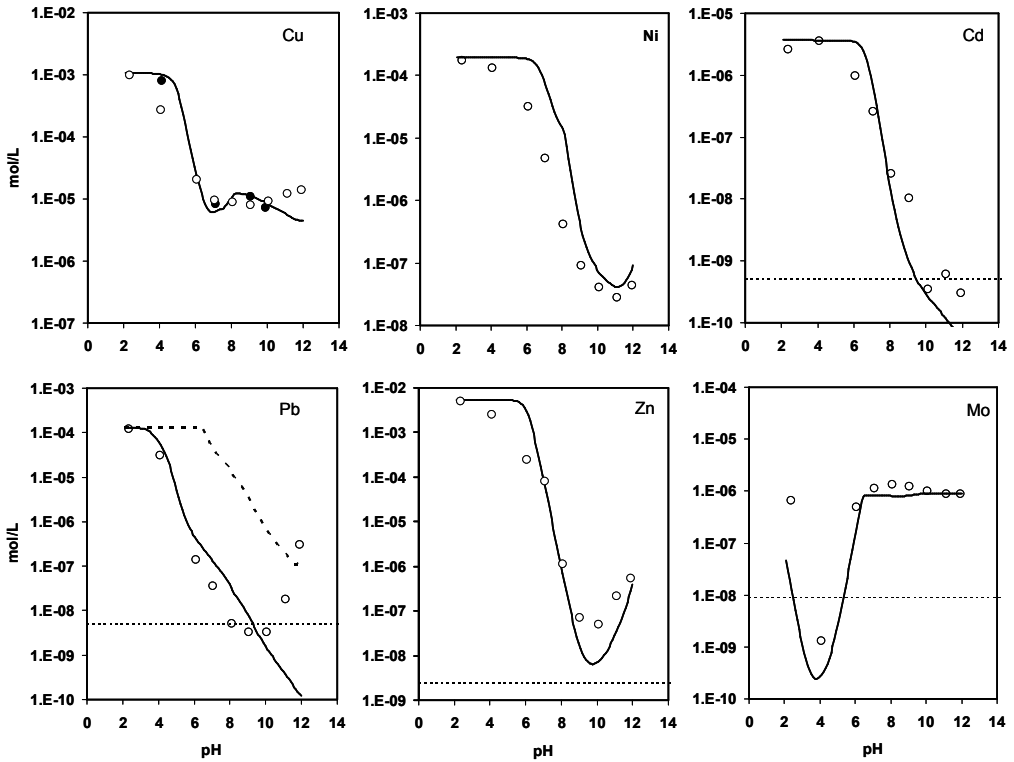
Figure 1 (continued) The dashed curve in the diagram for Pb represents a solubility curve of pure Pb(OH)$_2$(s). See results section for explanation.

The initial estimates of the availability of Al and Si estimated at pH 2, L/S 10, led to inadequate model predictions. Therefore, the present estimate of the availability of Al and Si (as listed in Table 2) are calculated from the stoichiometry of laumontite (CaAl$_2$Si$_4$O$_{12}$.4H$_2$O(s)), based on the measured availability of Ca (Table 2). In this calculation the Ca- consumption by the simultaneous precipitation of calcite (limited by the CO$_3$ availability) and ettringite (limited by the SO$_4$ availability) is accounted for. The calculated amount of Al was insufficient to explain the observed saturation of gibbsite, and therefore a slight excess amount of Al was added such that gibbsite precipitates over the entire pH range of pH 2-12, which agrees with the observed concordance of measured Al concentrations with Al-(hydr)oxide dissolution behaviour (Figure 1). It is important to note that the derived Al- and Si availabilities are still well below their total content as measured by total digestion in the sample (75

145

and 35% of their total content, respectively). Apparently, the availabilities of Si and Al are underestimated using pH 2 extracts, and/or the solubility controlling mechanisms of the Ca/Al/Si in MSWI bottom ash at high pH are still insufficiently understood.

The availability estimate of Ca and SO_4 (Table 2) could in principle be biased by the precipitation of gypsum at low pH (see Figure 1). However, their availability estimated from an additional pH-static experiment conducted at L/S 100 remained virtually unchanged, indicating that gypsum is already close to depletion at L/S 10.

The solubility product for amorphous iron hydroxide of Lindsay (*38*) allows an adequate prediction of the measured Fe-solubility (Figure 1), which is better than those obtained with either the more soluble or more stable iron (hydr)oxides in the MINTEQ 4.0 database. The calculated solubility curves of Al and Fe are considerably influenced by complexation to FA, which follows from the relatively strong affinity of these cations for complexation with dissolved humic substances (*22, 23*). Adequate model predictions are also obtained for Mg (based on brucite solubility) and manganese (based on manganite solubility), of which their pH-concentrations plots for reasons of clarity are not included in Figure 1.

In the study of Dijkstra et al. (*16*), it was shown that the pH-dependent leaching of FA is presumably controlled by sorption of FA to iron- and aluminium (hydr)oxides, a process that could be described adequately with two conditional surface complexation reactions. It appeared that the modelled FA concentrations were sensitive to competitive adsorption of other anionic species in the low pH range, in particular to phosphate (*16*). In the present study, adequate model predictions of phosphate could not be obtained, and therefore the solution concentrations of phosphate were fixed to 10^{-5} M, which agrees with the fairly constant phosphate concentrations measured at pH > 4 (data and model not shown in Figure 1). The resulting model descriptions for FA are adequate (Figure 1). Clearly, phosphate leaching behaviour, due to its competitive influence on FA and other anionic species, is a source of uncertainty that requires further study.

The leaching of Cu is predicted well by surface complexation to iron- and aluminium (hydr)oxides, and by allowing $Cu(OH)_2(s)$ to precipitate as it becomes oversaturated, which occurs at pH > 8. At pH > 6, the leaching of Cu is primarily controlled by the availability and leachability of FA present in the MSWI bottom ash leachates due to the formation of strong Cu-FA complexes (*16*). These interactions

are well predicted by the model (Figure 1). The anionic species MoO_4^{-2} is adequately predicted by (weak) surface complexation at high pH, and the formation of wulfenite ($PbMoO_4$(s)) at low pH (Figure 1).

Leached Ni concentrations were modelled based on surface complexation to iron- and aluminium (hydr)oxides, and by allowing $Ni(OH)_2$(s) to precipitate as it becomes oversaturated (*8*). The solubility product of $Ni(OH)_2$(s) was taken from the previous MINTEQ 3.11 database (*39*), as the present solubility product of this phase (MINTEQ 4.0, ref *20*) led to overestimates by about one order of magnitude. The trend of leached Ni concentrations is well described by the model, in particular around the natural pH (~ pH 11.2). Although predicted Ni concentrations generally overestimate the measurements by up to one order of magnitude, it has been shown that Ni concentrations at pH < 10 continue to increase beyond equilibration times of 48 hours, suggesting slow desorption/dissolution processes (*8*).

Following the work of Meima and Comans (*26*) and Dijkstra et al. (*8*), the leaching of Zn was modelled by surface precipitation to iron- and aluminium (hydr)oxides, leading to adequate model predictions (Figure 1). Measured concentrations of Cd and Pb (Figure 1) are substantially lower than in these previous studies, which is the result of improved measurement techniques (Dijkstra et al. (*8*) use leaching data from 1998). In the previous studies, the leaching of these elements was explained by surface complexation to iron- and aluminium (hydr)oxides (*8, 26*), but preliminary model calculations showed that the present low concentrations cannot be explained solely by this process, at least not using the estimates for available concentrations and reactive surface area of Table 2 (not shown). Therefore, surface precipitation to iron- and aluminium (hydr)oxides was considered for these metals in the model, which led to adequate descriptions for Cd over the complete pH range, and for Pb up to pH 10 (Figure 1). Although neoformed calcite has been suggested to be an important scavenger of trace metals in weathered MSWI bottom ash (*40*), Meima and Comans (*26*) tried to model the leaching of Cd from weathered MSWI bottom ash by surface precipitation and subsequent solid solution formation with calcite and obtained strongly overestimated concentrations. Also attempts to model the leaching of Pb based on this process were unsuccessful (unpublished results). Therefore, based on the present model calculations, surface precipitation of Cd to iron- and aluminium (hydr)oxides seems more likely (Figure 1). The concentrations of Pb around the

natural pH (~ 11.2) correspond better to those predicted by the solubility of pure $Pb(OH)_2(s)$ than by surface precipitation to iron- and aluminium (hydr)oxides, as indicated by the dashed curve in Figure 1. Further research, e.g., by using spectroscopic techniques, is needed to investigate the possible formation of surface precipitates / solid solutions of these metals in MSWI bottom ash. For the present reactive transport model (see results section), the selection of solubility controlling processes for the metals Cu, Pb, Ni, Cd and Zn will be based on the model scenario providing the closest agreement with the data around the natural pH of 11.2 in Figure 1, anticipating on similar pH values of the percolation tests leachates. Therefore, the leaching of Cu, Ni and Pb around the natural pH is assumed to be controlled by the solubility of their respective (hydr)oxides, while for Cd and Zn, surface precipitation to iron- and aluminium (hydr)oxides is assumed to be the controlling process.
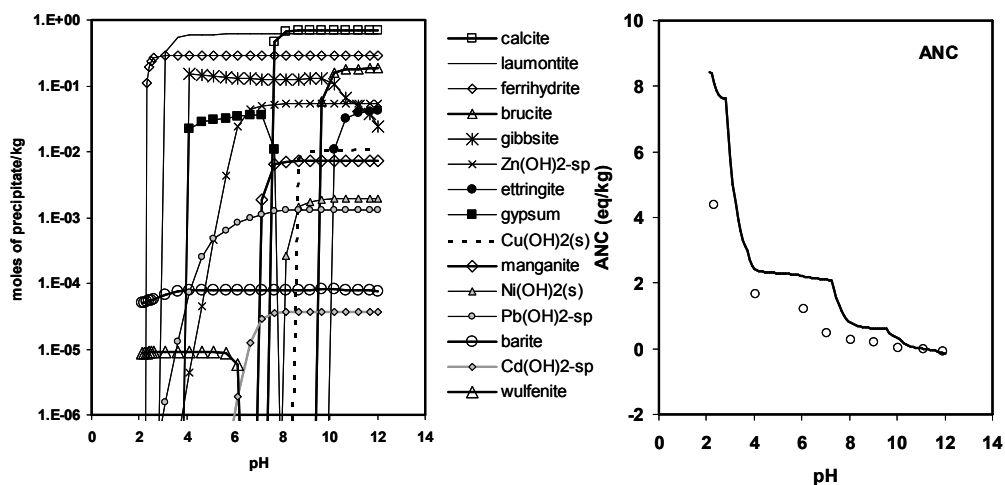
Figure 2. Overview of the mineral phases and surface precipitates (denoted by -sp) that are allowed to precipitate as a function of pH during the model run (left diagram), and the measured versus predicted acid neutralizing behaviour of the material (right diagram). See text for explanation.

Figure 2 (left diagram) provides an overview of the minerals and surface precipitates that are allowed to form during the model run. The right diagram in Figure 2 shows the measured and predicted Acid Neutralizing Capacity (ANC). An adequate prediction of the pH using a reactive transport model depends on how

accurately the acid/base buffering behaviour is described. The shape of the modelled ANC curve is related to the estimated availabilities of cations and anions (Table 2), the mineral phases that are allowed to precipitate (e.g., see the concordance resulting from calcite dissolution in both diagrams of Figure 2) and the amount and type of reactive surfaces in the model. The predicted ANC curve shows strong similarity to the measured ANC behaviour, although the latter is increasingly overestimated towards low pH. It is noted, however, that substantial kinetic effects have been observed for the acid/base consumption of MSWI bottom ash in particular at low pH (*8*).

Percolation tests data and modelling results

Measured responses to flow velocity and flow interruptions

Results of the percolation tests are presented in Figures 3 and 4. The measured pH and conductivity, and leached concentrations of an assumed conservative element, chloride, are presented as a function of the cumulative liquid-to-solid (L/S) ratio in Figure 3. Leached concentrations of Al, Ca, SO_4, Si, Fe, fulvic acids (FA), Ni, Cu, Zn, Cd, Pb and Mo are shown in Figure 4. The charge balance of the leachates was calculated from the chemical analysis results and amounts to 4.2 ± 3%, which is accurate given the complex leachate composition and high salt levels.

The initial pH of the leachates (pH ~ 10.8) increases after a few pore volumes (L/S 0.6, ~ 2 pore volumes) to rather constant values of around pH = 11.2, which is equal to the "natural" pH measured in the pH-static experiment without acid/base dosage. These pH values are in the range typically found for freshly quenched MSWI bottom ash (*6*). No systematic difference is observed between the pH measured in the standard and fast column, and virtually no response of pH on the flow interruptions is recorded. The lower pH value upon flow interruption at L/S 2 in the fast column is probably a measurement error, as a response of strongly pH-dependent elements such as Al is absent (Figure 4).

Measurements of the redox potential resulted in a rather constant relationship of pH + pe = 16 ± 0.5, without observed sensitivity to flow velocity, and with marginal increased values after the flow interruptions (not shown). These values point to a moderately oxidising environment of the leachates (e.g., ref *41*).
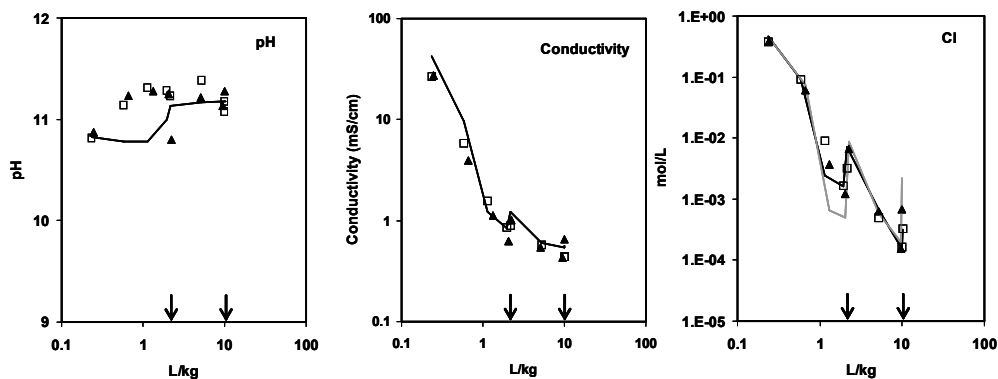
Figure 3. Results of the percolation tests and model predictions for pH, conductivity and the leaching of chloride expressed as a function of cumulative liquid-to-solid ratio (L/kg). Open squares are the data collected at the "standard" flow velocity (as prescribed by the percolation test TS 14405 (2)), closed triangles are de data collected at a four times higher flow velocity ("fast"). The arrows on the x-axis indicate the position of the equilibrated fractions that are collected immediately after flow interruption (at ~ L/S 2.2 and L/S 10, respectively). The solid lines in the diagrams for pH and conductivity represent model predictions. The solid black and grey curves in the diagram for chloride are model descriptions based on the dual porosity approach for the "standard" and "fast" experiment, respectively, calculated by the same parameters.

Values for the Electrical Conductivity (EC) strongly decrease during the first pore volumes as a result of the wash-out of soluble salts. Chloride concentrations decrease almost by three orders of magnitude over the course of the experiment and show a long "tailing" of element concentrations (Figure 1). A considerable increase in chloride concentrations is measured in the eluate fractions directly following flow interruption (Figure 3). This effect is clearly more pronounced in the fast column (a factor of 5 versus a factor of 2 increase, respectively for the fast and standard flow velocity). The response on flow interruptions of assumed conservative elements is a typical indication for physical non-equilibrium processes (*42, 43*), i.e. diffusional mass transfer between mobile and stagnant zones in the column. Such stagnant zones may consist of small pores in particles and/or, on a larger scale, domains in the columns that do not actively take part in the transport process as a result of preferential flow paths. Similar responses to flow velocity and flow interruption were observed for Na and Br (not shown).
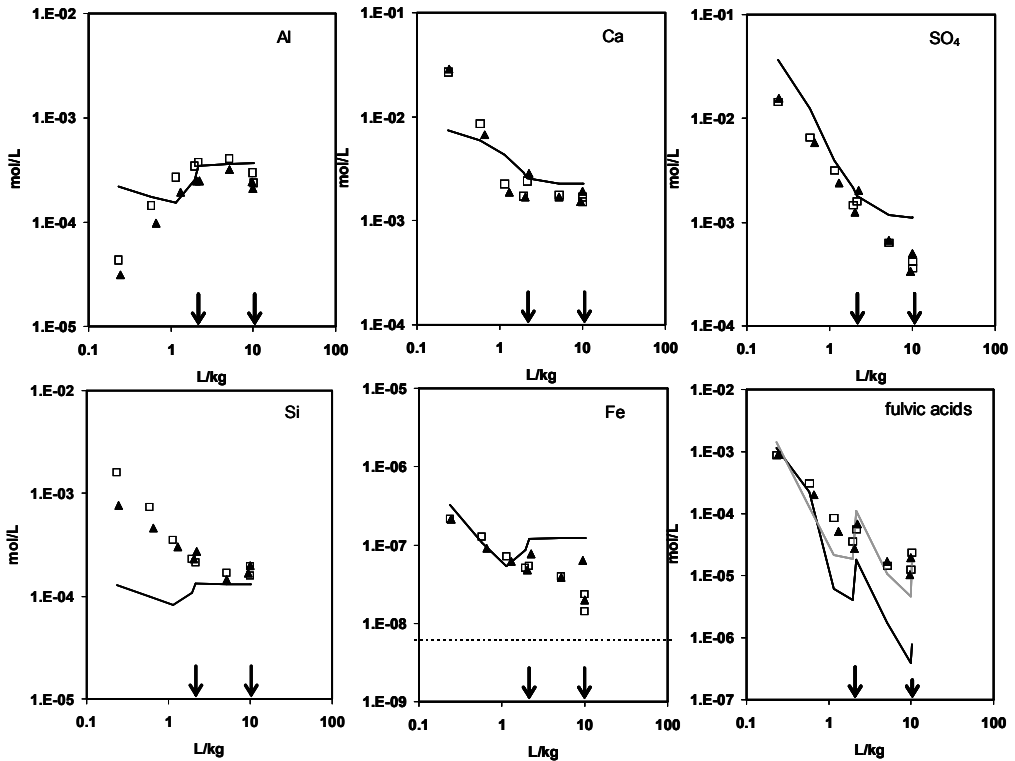
Figure 4 (continued on next page). Results of the percolation tests and model predictions for Al, Ca, SO$_4$, Si, Fe, fulvic acids, Cu, Mo, Ni, Cd, Pb, Zn and Mo expressed as a function of cumulative liquid-to-solid ratio (L/kg). Open squares are the data collected at the "standard" flow velocity (as prescribed by the percolation test TS 14405 (2)), closed triangles are de data collected at a four times higher flow velocity ("fast"). The arrows on the x-axis indicate the fractions collected immediately after flow interruption (at ~ L/S 2.2 and L/S 10, respectively). The solid lines represent model predictions by the reactive transport model.

Overall, response on flow velocity was remarkably small for the leaching of a broad range of elements (Figures 3 and 4). Expressed in cumulatively leached amounts (expressed in mol/kg) after L/S 10, and averaged over all components measured by chemical analysis (35 components) and excluding measurements around detection limit, an 8 ± 14 % higher cumulative leaching is measured in the standard column relative to the fast column. Although responses upon flow interruption on individual column fractions are considerably large (see chloride), the contribution of flow interruptions at L/S 2 and L/S 10 to the overall cumulatively leached amounts after

151

L/S 10 is very small: 3 ± 1 % in the standard column, and a slightly higher 5 ± 2 % in the fast column.
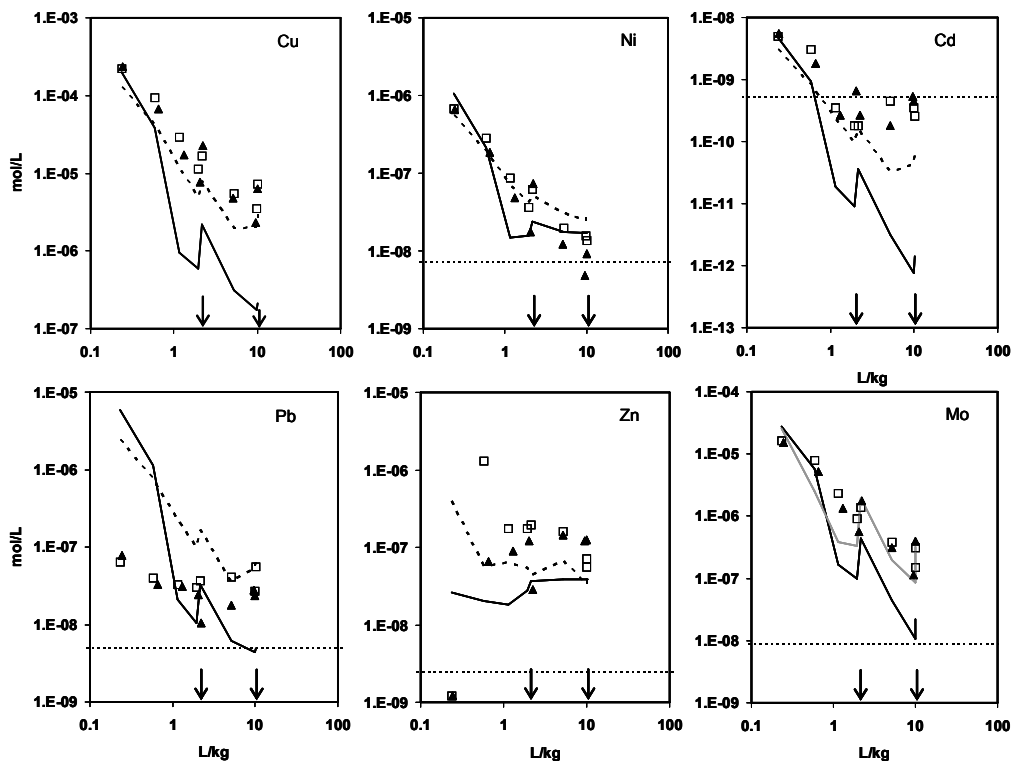
Figure 4 (continued from previous page). The dashed lines in the diagrams for Cu, Ni, Cd, Pb and Zn are model predictions calculated for each data point separately (see section "metals"). Solid grey curves in the diagrams for FA and Mo represent an alternative model scenario in which a different set of kinetic parameters was used (for explanation see section "fulvic acids and molybdenum")

Leaching and composition of DOC in the percolation test leachates

Humic substances (HA and FA) have been shown to be of crucial importance for the understanding of the leaching of Cu and possibly other metals from MSWI bottom ash (*15, 16*). Therefore, the leached DOC concentrations from both percolation tests were characterized in terms of HA, FA and HY (see methods section). The results are presented in Figure 5 and show that about 50% of the leached DOC consists of FA, a percentage that remains fairly constant during the

course of the test. Low concentrations of HA are measured in the first fractions of the percolation tests (Figure 5). The above observations are similar for both flow velocities. In the fast column, the relative proportion of FA in the equilibrated fractions (i.e. after flow interruption at L/S 2.2 and L/S 10) are lower compared to the preceding and subsequent fractions (Figure 5), while total DOC in these fractions have increased by a factor of 2-3, indicating that the release of HY during the flow interruptions is faster than the release of FA.
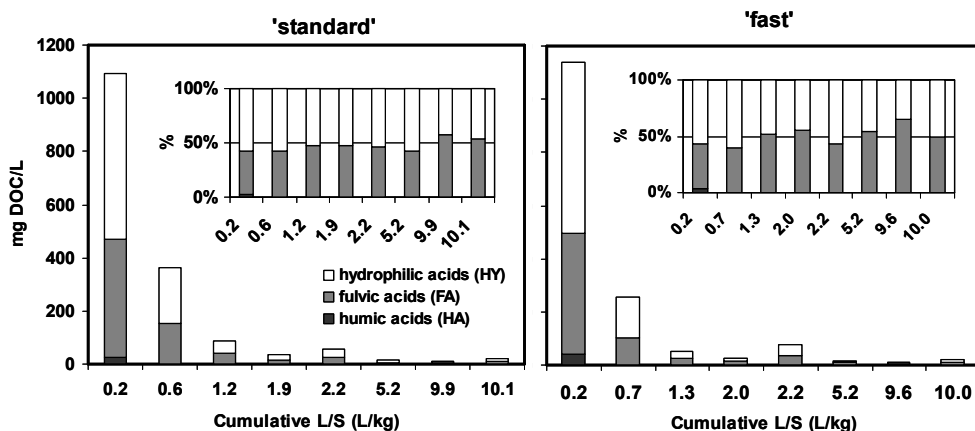
Figure 5. Results of the characterization of organic carbon present in the MSWI bottom ash leachates from the percolation test in terms of hydrophilic acids, fulvic acids, and humic acids, expressed in mg DOC/L as a function of cumulative liquid-to-solid ratio, L/S.

The effect of flow interruptions on the composition of DOC is less pronounced for the standard column (Figure 5). The cumulatively leached amount of FA corresponds to ~ 0.5 g FA/kg bottom ash, which is close to the measured availability in the pH-static experiment of ~ 0.37 g FA/kg (equivalent to 3.7e-4 mol FA/kg in Table 2) as well as to the estimated total FA content in the sample (0.4 g FA/kg, ref *16*). These observations indicate that virtually all FA present in the MSWI bottom ash sample is washed out after L/S = 10, which is in agreement with the observed weak interaction of FA with reactive surfaces present in the bottom ash matrix at high pH (*16*). The low leachability of HA from bottom ash can be attributed to the presence of relatively high amounts of di- and trivalent ions (e.g. Ca, Al and Fe), which have been

shown to reduce the solubility of HA by charge neutralisation and subsequent coagulation (*44, 45*).

Model predictions for the percolation test

Using the same set of input parameters and assumptions as for the batch pH-dependence calculations in the preceding sections, reactive transport calculations are performed to predict the leaching of the elements as measured with the percolation tests. The resulting model curves are included in Figure 3 and 4 (for clarity only shown for the standard flow velocity; model predictions for the "fast" column were quite similar).

Chloride

Physical non-equilibrium processes were included in the reactive transport model by fitting the two parameters α and β of the dual porosity approach (see methods section) to the leaching curve of chloride, assuming non-reactive behaviour of this anion. An excellent fitted transport behaviour for chloride leaching was obtained with α = 5e-8 s^{-1} and β = 0.95 (Figure 3). Note that also the more pronounced effects of flow interruptions in the column operated at the higher flow velocity are adequately predicted when the same parameter values are used (Figure 3).

It is possible to relate the exchange factor α to an effective diffusion coefficient using the size and geometry of the stagnant zone, according to the relationship of Van Genuchten (*46*) cited in Appelo and Postma (*47*). Such a physical interpretation of the values for α and β is complicated as characteristics of the stagnant zones are unknown for this sample and for MSWI bottom ash in general. However, if it is assumed that the stagnant zones consist of micropores within spheres with a radius of 2 mm (i.e. the largest particle size fraction in the sample), an effective diffusion coefficient (D_e) in the order of 10^{-12} - 10^{-13} m^2/s is found (for details of this calculation see ref *47*). This value is similar to that found by Gardner et al. (*10*) for the leaching of conservative elements (Na and Cl) from MSWI fly ash columns.

pH and conductivity

The calculated pH of the column leachate is determined by the estimated initial pH of the material (~ pH 10.8, see methods section) in combination with the assumed set

of minerals and, to a lesser extent, the amount and type of adsorbing surfaces. The same mineral assemblage present at the natural pH in the pH-static experiments is predicted to precipitate in the columns (refer to the minerals present at pH ~ 11.2 in Figure 2), and complete depletion of these minerals from the column is not predicted up to L/S = 10. The pH of the leachates is predicted well, although the time at which the pH increases from 10.8 to pH 11.2 is somewhat overestimated (Figure 3). The calculated eventual pH level of ~ 11.2 is consistent with the equilibrium pH of the assumed mineral assemblage. Although the pH remains quite similar over the duration of the experiment, an adequate prediction of pH in systems with a more variable pH (i.e., in which a large portion of the available buffering capacity is consumed) strongly depends on an accurate prediction of the ANC (Figure 2).

Electrical conductivity (EC) is a bulk parameter that is primarily determined by the major ions present in the leachates. EC was derived from the ionic strength (I) using the relationship I (M) = 0.013 x EC (mS/cm) (*38*), which resulted in an excellent prediction of EC as a function of L/S (Figure 3), indicating that the processes underlying the leaching of major ions are adequately captured by the model.

Major elements

Leached concentrations of the major components Al, Ca, SO$_4$, are generally predicted adequately to excellently based on the input parameters of Table 2 and the processes selected in the section "pH-static leaching test data and model results" (Figure 4). Adequate predictions were also obtained for other major elements not shown in Figure 4, such as Mg, Mn and CO$_3$. Model predictions for Si and Fe are accurate within approximately one order of magnitude. Deviations between model predictions and data for major elements are particularly observed below L/S = 1. These deviations are partly explained by an insufficiently accurate description of the pH during the first pore volumes (e.g., see the concordance in the model predictions for pH in Figure 3 and Al in Figure 4). Deviations may also arise from inaccurate estimates of the available concentrations in Table 2, to which the reactive transport predictions are very sensitive, and/or a still insufficient representation of processes in the model (see Fe and Si).

Fulvic acids and molybdenum

The reactive transport model predicts a virtually conservative wash-out of FA from the column (Figure 4), which follows from the predicted complete desorption at pH values around the natural pH of the sample (~ pH 11.2; see Figure 1). However, FA concentrations are increasingly underestimated by the model towards higher L/S ratios (Figure 4). Figure 4 shows that FA concentrations are described more accurately when using the cumulatively leached amount of FA as input in the model (i.e., 5e-4 mol/kg) instead of the estimated availability (3.67E-4 mol/kg, Table 2), in combination with dual porosity parameters that are different from those for chloride (α = 2.5e-7 s^{-1} and β = 0.75). These modified dual porosity parameters for FA represent a higher release rate and a larger effective stagnant fraction relative to chloride (α = 5e-8 s^{-1} and β = 0.95). Possible explanations for these deviating transport parameters of FA include sorption-related non-equilibrium (e.g., ref *42*) and/or a different physical transport behaviour as a result of an inhomogeneous distribution of the different components within and between the bottom ash particles.

There is a striking similarity between the leaching behaviour of FA and that of other anionic compounds, i.e. phosphate (not shown) and molybdenum (Figure 4). These components show a similar "wash-out" pattern as FA. The components FA and MoO_4^{-2} have in common that rather pronounced leaching kinetics have been observed in batch pH-static leaching experiments at alkaline pH (refs *8* and *16*; see also FA behaviour in Figure 1), while the model predictions indicate virtually 100% desorption in this pH region (Figure 1). The grey solid curve in the diagram for MoO_4^{-2} in Figure 4 indicates that the transport behaviour of this component is adequately described using the same kinetic (i.e. "dual porosity") parameters as derived for FA. These similarities suggest a similar release process for FA and Mo. Further research is required to establish whether the kinetic features observed for these compounds have a chemical (i.e. slow desorption kinetics) or physical nature.

Metals

The reactive transport model prediction for Ni is excellent over the full L/S range, whereas model predictions of Cu and Cd have in common that initial leached concentrations are predicted adequately, but concentrations become increasingly underestimated toward higher L/S ratios. Model predictions for Pb strongly

overestimate the measurements at low L/S and are slightly better at higher L/S where the deviation is approximately one order of magnitude. Rather exceptional behaviour is observed for Zn, of which the concentration in the first fraction was found to be below detection limit. The reasons for this apparently anomalous behaviour are currently unknown. Concentrations towards higher L/S are predicted generally within a factor of 5 - 10.

The dashed curves shown for the trace metals Ni, Cu, Zn Cd and Pb represent model calculations performed for each data point separately, using the measured pH and concentrations of HA, FA and background elements as input in the model (i.e., without transport of water) according to the modelling approach outlined by Dijkstra et al. (*8*). The plausible assumption underlying these curves is that there is no significant removal of their "available" concentration up to L/S 10. These curves provide generally a better match with the measurements of Cu, Ni, Cd and Zn shown in Figure 4, indicating that the model predictions for these metals may be further improved when important parameters are more accurately predicted, in particular the pH and concentrations of FA. In this respect it is important to stress that a model for the leaching of HA was not included in the reactive transport model (see "geochemical modelling approach" in methods section and "synthesis and conclusions" below). The observed and predicted behaviour of the different metals will be explained below on the basis of calculated speciation diagrams.

Figure 6 includes calculated speciation diagrams based on the "dashed" model scenarios for the metals Ni, Cu, Cd, Pb and Zn as shown in Figure 4. The solution speciation is subdivided into "complexed with FA", "complexed with HA", inorganic complexes" and "free ions" (Me^{2+}). The metals Cu, Cd and Pb are predicted to be virtually 100% complexed to leached humic substances (FA and HA) over the full L/S range. The role of metal complexation by these humic substances is particularly pronounced at low L/S ratios, where concentrations of FA and HA are highest. The strong overestimation of Pb, in particular at low L/S, suggests that the solubility controlling processes for this metal are not sufficiently understood (see also Figure 1). Initially, Ni is largely present as FA-Ni complexes, but at higher L/S ratio's, inorganic complexes form the dominant Ni species. This explains the predicted rather invariant concentrations of Ni towards higher L/S, while those of Cu, Cd and Pb closely follow the continuously decreasing concentrations of FA. Leached Zn does not show
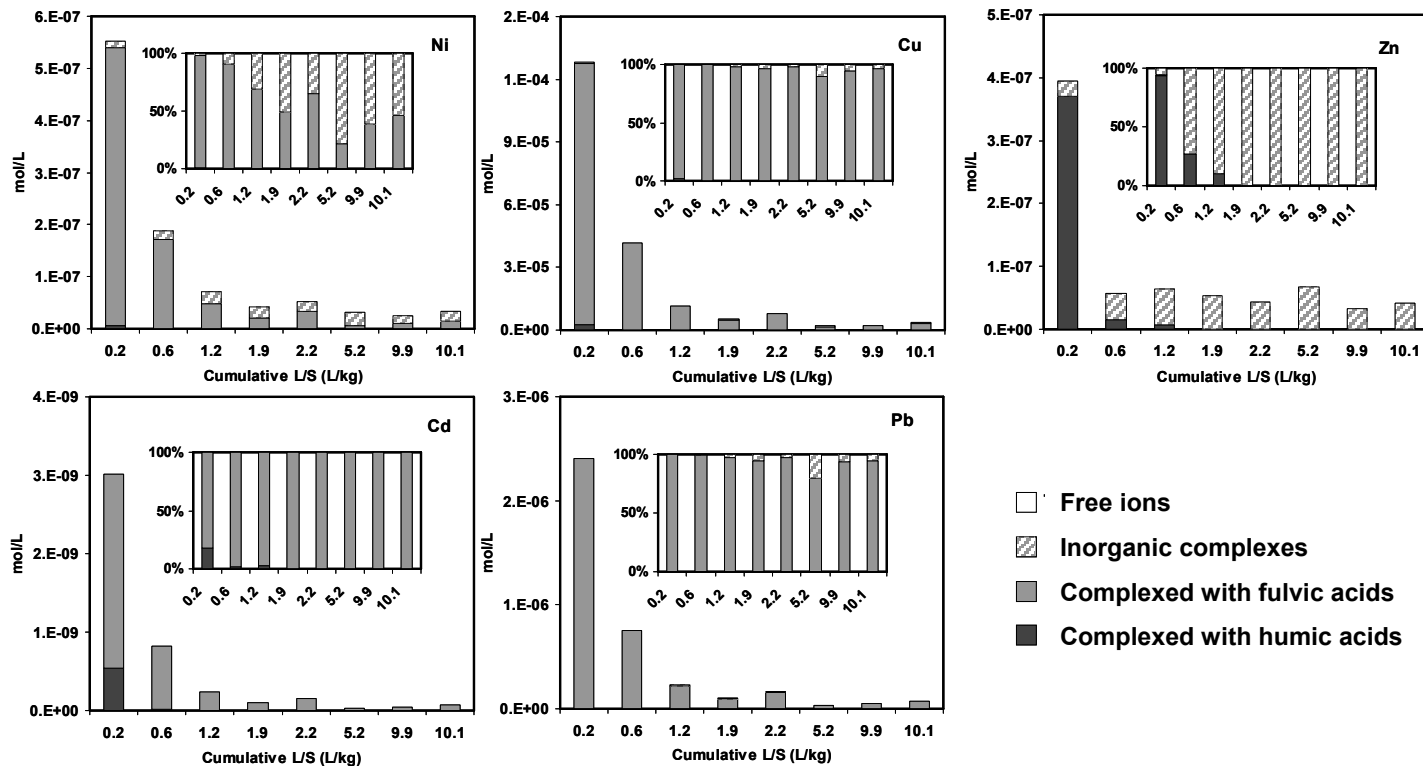
Figure 6. Predicted solution speciation of Ni, Cu, Cd, Zn and Pb. The figure complements the predicted concentrations based on the model scenario indicated by the dashed curves in Figure 4 (see results section for explanation).

significant interaction to FA, but is predicted to form strong complexes with the low concentrations of HA in the first few fractions and, similar to Ni, predominantly inorganic complexes towards higher L/S ratios. In addition to Zn, Cu and Cd are predicted to show significant interaction with the low concentrations of HA measured in the leachates.

The differences in predicted speciation between the metals are the result of different binding affinities for humic substances and the ability to form inorganic complexes, particularly at high pH. For each metal separately, the speciation is also influenced by the relative difference in binding affinity for HA and FA (e.g., see the strong complexation of Zn with HA).

Synthesis and conclusions

Characterization and modelling of processes

The "multi-surface" reactive transport modelling approach presented in this study leads to a strongly improved model prediction and understanding compared to previous reactive transport modelling studies performed on MSWI bottom ash (e.g., refs *9-14*). Novel aspects of the present modelling approach include the characterization of DOC in terms of its reactive components HA and FA as a function of L/S and pH, the inclusion of mechanistic models that predict the binding of metals to these substances, the inclusion of a surface complexation model that predicts FA concentrations, and finally, the combination of these geochemical models with non-equilibrium processes. With the present model set-up and parameterization, the leaching of a broad range of major and trace elements is predicted generally with success over a wide range of conditions (i.e., pH 2-12 at L/S 10 and L/S 0.2- 10 at natural pH), with the same set of independently determined model input parameters in only two single model runs (i.e., a batch and a transport model run).

Within the boundaries of the investigated experimental conditions, the use of equilibrium-based reactive transport models to predict data from dynamic laboratory-leaching tests performed on heterogeneous matrices such as MSWI bottom ash is promising, given the generally adequate agreement between model predictions and data. This conclusion is supported by the generally low sensitivity of leached

concentrations to flow velocity and flow interruptions. In addition, the experimental and modelling approach from this study has led to the identification of physical non-equilibrium processes for non-reactive soluble salts, as well as possible sorption-related non-equilibrium processes for the leaching of molybdenum, FA and associated trace metals.

It should be noted that "equilibrium" with respect to the selected mineral assemblage in this study might not represent "true" thermodynamic equilibrium of the system as a whole (e.g., amorphous phases versus more stable crystalline phases). High temperature products such as MSWI bottom ash are almost by definition thermodynamically unstable, and subject to many dynamic changes such as weathering, including slow mineralogical alterations, and microbial processes (e.g., refs 4 and 6 and references therein). Therefore, also a thermodynamically unstable mineral assemblage may control leaching in the laboratory and/or in the field during a certain time period.

Important input parameters in the modelling approach include the estimates for the "available" concentrations of major and trace elements. In this study pH 2 (metals) or 12 (anions) and L/S 10 extracts were successfully used for this purpose, assuming complete desorption/dissolution. This assumption is justified as close to 100% desorption and/or dissolution is predicted for most components at pH 2 (Figures 1-2). However, a pH 2 extraction apparently leads to an underestimate of the availabilities of important major elements Al and Si (see results section). Moreover, it has been shown that extraction at a pH as low as 0.5 may be needed to estimate the availability of metals in organic rich systems such as soils (*48*). Therefore, further research is necessary to develop a generic approach for the estimation of the "availability" of components in contaminated materials.

Given the predicted strong influence of FA as well as HA on the leaching of heavy metals, further improvement of the (reactive transport) modelling approach can particularly be achieved by a more mechanistic description of the (dynamic) leaching behaviour of these humic substances. Important new insights in the solid/solution partitioning of humic substances have been made by Filius et al. (*49*) and Weng et al. (*45, 50, 51*). These developments are likely to contribute to further identification and modelling of the mechanisms controlling the leaching of these substances from soils and waste materials such as MSWI bottom ash.

Implications for test settings and interpretation

The experimental results presented in this paper, in combination with the successful application of equilibrium geochemical modelling, indicates that the leaching of MSWI bottom ash as measured by TS 14405 occurs largely under local equilibrium conditions. This important observation allows the conclusion that the currently prescribed "standard" flow velocity in TS 14405 is an adequate choice, at least in the case of MSWI bottom ash. Data from previous percolation tests on MSWI bottom ash (dating from 1998) performed at the standard, 4x faster and 4x lower flow velocity support these conclusions as no systematic difference in cumulatively leached concentrations could be identified (unpublished results; data available on request). However, the off-line measurements of leachate pH and possibly also other parameters from in particular the slowest experiment from the 1998 data set were biased by carbonation, complicating a process-based interpretation of the results. In particular at alkaline pH, concentration-pH edges are extremely steep (e.g., see Ca in Figure 2) and inaccuracies in the (off-line) measurement of pH by only tenths of a pH-unit would strongly bias the identification of the processes controlling leaching. A lower flow velocity than "standard" is, therefore, not recommended as the longer time periods to collect a leachate fraction may induce such experimental artefacts. In any case, a careful preservation of the leachates as performed in this study is recommended to prevent interactions with the atmosphere (carbonation and/or oxidation).

The flow interruptions during and at the end of the experiments are at present not prescribed by TS 14405. Although these flow interruptions did not substantially contribute to the cumulatively leached amounts at L/S 10, this procedure may be recommended to identify possible non-equilibrium conditions when these are suspected (see also ref *42*). The currently prescribed initial equilibration period in TS 14405 is functional, as it promotes the levelling of concentration gradients after the column has been saturated with water. These gradients originate from the instantaneous dissolution of soluble salts travelling at the same velocity as the wetting front. As field residence times are much longer than column residence times, the initial equilibration period is expected to represent the actual leaching processes in the field more accurately (apart from density-driven flow that may occur in extreme salt-

rich materials). In addition, the assumption of an initially homogeneous distribution of components over the column (see "transport model" in methods section) is better justified when the initial concentration gradients are levelled.

Although cumulatively leached amounts are not substantially influenced by flow velocity and/or flow interruption, non-equilibrium processes have been shown in this study to affect the leaching of soluble salts, as well as reactive organic ligands and associated trace metals. These processes are shown to become increasingly important for the understanding and prediction of element concentrations towards higher L/S ratios (i.e. time periods). Therefore, the application of the present modelling approach to long-term field scenarios requires a careful examination and description of the hydrology at the field site (e.g., refs *52, 53*). In addition, long-term model predictions for specific field-scale applications may require the model to be expanded with additional processes such as carbonation and redox reactions (see also refs *54, 55*).

Finally, this study demonstrates that European standardized test methods for waste materials (pH-dependent tests TS 14497 and TS 14429 (*19, 56*) and percolation test TS 14405 (*2*)) strengthen each other for the characterization of leaching processes in granular waste materials over a wide range of conditions that can be met in the field. The combination of standardized leaching test methods with selective chemical extractions and a mechanistically based modelling approach constitutes a promising set of tools to assess the long-term environmental impact of the application of granular waste materials in the environment.

Acknowledgements

References

1. NEN (Standardization Agency of the Netherlands), 1995. *Leaching characteristics of solid earthy and stony building and waste materials - Leaching tests - Determination of the leaching of inorganic components from granular materials with the column test*, NEN 7343:1995.

2. CEN/TC292, 2004. *Characterization of waste - Leaching behaviour tests - Up-flow percolation test (under specified conditions)*, CEN/TS 14405:2004.

3. Chandler, A. J.; Eighmy, T. T.; Hartlen, J.; Hjelmar, O.; Kosson, D. S.; Sawell, S.E.; Van der Sloot, H. A.; Vehlow, J. *Municipal solid waste incinerator residues*. Elsevier Science B.V., Amsterdam, The Netherlands, 1997.

4. Zevenbergen, C.; Vander Wood, T.; Bradley, J. P.; Van der Broeck, P. F. C. W.; Orbons, A. J.; van Reeuwijk, L. P. Morphological and chemical properties of MSWI bottom ash with respect to the glassy constituents. *Hazard. Waste Hazard. Mater.* 1994, 11, 371–383.

5. Johnson, C. A.; Kersten, M.; Ziegler, F.; Moor, H. C. Leaching behaviour and solubility-controlling solid phases of heavy metals in municipal solid waste incinerator ash. *Waste Manage.* 1996, 16, 129-134.

6. Meima, J. A.; Comans, R. N. J. Geochemical modelling of weathering reactions in MSWI bottom ash. *Environ. Sci. Technol.* 1997, 31, 1269-1276.

7. Meima, J. A.; Comans, R. N. J. The leaching of trace elements from municipal solid waste incinerator bottom ash at different stages of weathering. *Appl. Geochem.* 1999, 14, 159-171.

8. Dijkstra, J. J.; Van der Sloot, H. A.; Comans, R. N. J. The leaching of major and trace elements from MSWI bottom ash as a function of pH and time. *Appl. Geochem.* 2006, 21, 335-351.

9. Bävermann, C.; Sapiej, A.; Moreno, L.; Neretnieks, I. Serial batch tests performed on municipal solid waste incineration bottom ash and electric arc furnace slag in combination with computer modelling. *Waste Manage. Res.* 1997, 15, 55-71.

10. Gardner, K. H.; Theis, T. L.; Iyer, R. An experimental and analytical approach to understanding the dynamic leaching from municipal solid waste combustion residue. *Environ. Eng. Sci.* 2002, 19, 89-100.

11. Baranger, P.; Azaroual, M.; Freyssinet, P.; Lanini, S.; Piantone, P. Weathering of a MSW bottom ash heap: a modelling approach. *Waste Manage.* 2002, 22, 173-179.

12. Mostbauer, P., Lechner, P. *Weathering of MSWI bottom ash in laboratory test cells and under field conditions – effect on metal and metalloid mobility*. Proceedings of the sixth international

conference on the environmental and technical implications of construction with alternative materials, WASCON 2006, Belgrade, 2006, pp. 323-333.

13. Yan, J.; Bäverman, C.; Moreno, L.; Neretnieks, I. Neutralising processes of municipal solid waste incineration bottom ash in a flow-through system. *Sci. Total Environ.* 1999, 227, 1-11.

14. Dijkstra, J. J.; Van der Sloot, H. A.; Comans, R. N. J. Process identification and model development of contaminant transport in MSWI bottom ash. *Waste Manage.* 2002, 22, 531-541.

15. Van Zomeren, A.; Comans, R. N. J. Contribution of natural organic matter to copper leaching from municipal solid waste incinerator bottom ash. *Environ. Sci. Technol.* 2004, 38, 3927-3932.

16. Dijkstra, J. J.; Van Zomeren, A.; Meeussen, J. C. L.; Comans, R. N. J. Effect of Accelerated Aging of MSWI Bottom Ash on the Leaching Mechanisms of Copper and Molybdenum. *Environ. Sci. Technol.* 2006, 40, 4481-4487.

17. Toride, N.; Leij, F. J.; Van Genuchten, M. T. *The CXTFIT Code for Estimating Transport Parameters from Laboratory or Field Tracer Experiments*, Version 2.1. Research report no. 137, U.S. Salinity Laboratory, USDA, ARS, Riverside CA, USA, 1999.

18. Meeussen, J. C. L. ORCHESTRA: An object-oriented framework for implementing chemical equilibrium models. *Environ. Sci. Technol.* 2003, 37, 1175-1182.

19. CEN/TC292, 2006. *Characterization of waste - Leaching behaviour tests - Influence of pH on leaching with continuous pH-control*, CEN/TS 14997:2006.

20. US-EPA, *MINTEQA2/PRODEFA2, A Geochemical assessment model for environmental systems: user manual supplement for version 4.0.* National Exposure Research Laboratory, Ecosystems Research Division, Athens, GA, 1999.

21. Kinniburgh, D. G.; Van Riemsdijk, W. H.; Koopal, L. K.; Borkovec, M.; Benedetti, M. F.; Avena, M. J. Ion binding to natural organic matter: competition, heterogeneity, stoichiometry and thermodynamic consistency. *Colloids Surf A* 1999, 151, 147-166

22. Milne, C. J.; Kinniburgh, D. G.; Van Riemsdijk, W. H.; Tipping, E. Generic NICA-Donnan model parameters for metal-ion binding by humic substances. *Environ. Sci. Technol.* 2003, 37, 958-971.

23. Hiemstra, T.; Van Riemsdijk, W. H. Biogeochemical speciation of Fe in ocean water. *Marine Chem.* 2006, 102, 181-197.

24. De Wit, J. C. M. *Proton and metal ion binding by humic substances;* Ph.D. Thesis, Wageningen University, Department Soil Quality, 1992.

25. Dzombak, D. A.; Morel, F. M. M. *Surface complexation modeling: hydrous ferric oxide*; John Wiley & Sons: New York, 1990.

26. Meima, J. A.; Comans, R. N. J. Application of surface complexation/precipitation modelling to contaminant leaching from weathered municipal solid waste incinerator bottom ash. *Environ. Sci. Technol.* 1998, 32, 688-693.

27. Hiemstra, T.; De Wit, J. C. M.; Van Riemsdijk, W. H. Multisite proton adsorption modeling at the solid/solution interface of (hydr)oxides: a new approach, II. application to varous important (hydr)oxides. *J. Colloid Interface Sci.* 1989, 133, 105-117.

28. Appelo, C. A. J.; Van der Weiden, M. J. J.; Tournassat, C.; Charlet, L. Surface complexation of ferrous iron and carbonate on ferrihydrite and the mobilization of arsenic. *Environ. Sci. Technol.* 2002, 36, 3096-3103.

29. Farley, K. J.; Dzombak, D. A.; Morel, F. M. M. A surface precipitation model for the sorption of cations on metal oxides. *J. Colloid Interface Sci.* 1985, 106, 226-242.

30. Filius, J. D.; Lumsdon, D. G.; Meeussen, J. C. L.; Hiemstra, T.; Van Riemsdijk, W. H. Adsorption of fulvic acid on goethite. *Geochim. Cosmochim. Acta* 2000, 64, 51-60.

31. Stumm, W.; Morgan, J. J.; Aquatic Chemistry, *An Introduction Emphasizing Chemical Equilibria in Natural Waters*, 2nd ed. John Wiley & Sons: New York, 1981.

32. Kostka, J. E.; Luther III, G. W. Partitioning and speciation of solid phase iron in saltmarsh sediments. *Geochim. Cosmochim. Acta* 1994, 58, 1701-1710.

33. Blakemore, L. C.; Searle, P. L.; Daly, B. K. *Methods for chemical analysis of soils*. Science report 80; NZ Soil Bureau: Lower Hutt, New Zealand, 1987.

34. Van Zomeren, A.; Comans, R. N. J. Measurement of humic and fulvic acid concentrations and dissolution properties by a rapid batch procedure. *Environ. Sci. Technol.*, submitted.

35. Thurman, E. M.; Malcolm, R. L. Preparative isolation of aquatic humic substances. *Environ. Sci. Technol.* 1981, 15, 463-466.

36. Swift, R. S. Organic matter characterization. In: Methods of soil analysis. Part 3. Chemical methods (ed. D.L.Sparks), pp. 1011-1069. Soil Sci. Soc. Am., Madison, WI, U.S.A., 1996.

37. Johnson, C. A.; Brandenberger, S.; Baccini, P. Acid neutralizing capacity of municipal waste incinerator bottom ash. *Environ. Sci. Technol.* 1995, 29, 142-147.

38. Lindsay, W. L. *Chemical equilibria in soils*. John Wiley & Sons, New York, 1979.

39. Allison, J. D.; Brown, D. S.; Novo-gradac, K. J. *MINTEQA2/PRODEFA2, Geochemical assessment model for environmental systems: version 3.11 databases and version 3.0 user's manual*; Environmental Research Laboratory, U.S.-EPA: Athens, GA, 1991.

40. Piantone, P.; Bodenan, F.; Chatelet-Snidaro, L. Mineralogical study of secondary mineral phases from weathered MSWI bottom ash: implications for the modelling and trapping of heavy metals. *Appl. Geochem.* 2004, 19, 1891-1904.

41.   Brookins, D. G. *Eh-pH diagrams for geochemistry.* Springer-Verlag, Berlin Heidelberg, 1988.

42.   Brusseau, M. L.; Rao, P. S. C.; Jessup, R. E.; Davidson, J. M. Flow interruption: a method for investigating sorption nonequilibrium. *J. Contam. Hydrol.* 1989, 4, 223-240.

43.   Koch, S.; Flühler, H. Non-reactive solute transport with micropore diffusion in aggregated porous media determined by a flow-interruption method. *J. Contam. Hydrol.* 1993, 14, 39-54.

44.   Temminghoff, E. J. M.; Van der Zee, S. E. A. T. M.; De Haan, F. A. M. Effects of dissolved organic matter on the mobility of copper in a contaminated sandy soil. *Eur. J. Soil Sci.* 1998, 49, 617-628.

45.   Weng, L.; Temminghoff, E. J. M.; Van Riemsdijk, W. H. Interpretation of humic acid coagulation and soluble soil organic matter using a calculated electrostatic potential. *Eur. J. Soil Sci.* 2002, 53, 575-587.

46.   Van Genuchten, M. T. A general approach for modeling solute transport in structured soils. *IAH Memoirs* 1985, 17, 513-526.

47.   Appelo, C. A. J.; Postma, D. Geochemistry, groundwater and pollution. 2nd edition, Balkema, Rotterdam, The Netherlands, 2005.

48.   Dijkstra, J. J.; Meeussen, J. C. L.; Comans, R. N. J. Leaching of heavy metals from contaminated soils: an experimental and modeling study. *Environ. Sci. Technol.* 2004, 38, 4390-4395.

49.   Filius, J. D.; Meeussen, J. C. L.; Lumsdon, D. G.; Hiemstra, T.; Van Riemsdijk, W. H. Modelling the adsorption of fulvic acid by goethite. *Geochim. Cosmochim. Acta* 2003, 67, 1463-1474.

50.   Weng, L.; Van Riemsdijk, W. H.; Hiemstra, T. Adsorption free energy of variable-charge nanoparticles to a charged surface in relation to the change of the average chemical state of the particles. *Langmuir* 2006, 22, 389-397.

51.   Weng, L.; Van Riemsdijk, W. H; Koopal, L.; Hiemstra, T. Adsorption of humic substances on goethite: comparison between humic acids and fulvic acids. *Environ. Sci. Technol.* 2006, in press.

52.   Johnson, C. A.; Richner, G. A.; Vitvar, T.; Schittli, N.; Eberhard, M. Hydrological and geochemical factors affecting leachate composition in municipal solid waste incinerator bottom ash. Part I: The hydrology of landfill Lostorf, Switzerland. *J. Contam. Hydrol.* 1998, 33, 361-376.

53.   Johnson, C. A.; Kaeppeli, M.; Brandenberger, S.; Ulrich, A.; Baumann, W. Hydrological and geochemical factors affecting leachate composition in municipal

solid waste incinerator bottom ash. Part II: The geochemistry of leachate from landfill Lostorf, Switzerland. *J. Contam. Hydrol.* 1999, 40, 239-259.

54.   CEN/TC292, 2006. *Characterisation of waste - Methodology guideline for the determination of the leaching behaviour of waste under specified conditions*, EN 12920:2006.

55.   Kosson, D. S.; Van der Sloot, H. A.; Sanchez, F.; Garrabrants, A. C. An integrated framework for evaluating leaching in waste management and utilization of secondary materials. *Environ. Eng. Sci.* 2002, 19, 159-204.

56.   CEN/TC292, 2005. *Characterization of waste - Leaching behaviour tests - Influence of pH on leaching with initial acid/base addition*, CEN/TS 14429:2005.

Summary

Waste materials often contain increased levels of potentially toxic trace elements compared to natural materials such as soils. In many countries, the recycling of waste materials in the environment, such as in construction works, is regulated by environmental criteria that aim to ensure long-term environmental protection. These criteria are increasingly based on the potential "leaching" of contaminants, i.e. the release of contaminants from the solid phase to the water phase with which the material may be in contact (e.g., percolating rainwater). The extent to which contaminants are susceptible for leaching processes depends on many chemical and physical factors, such as the specific chemical form of the contaminant ("chemical speciation") and transport processes such as convection and diffusion. To better understand the environmental risks associated with the application of waste materials in the environment, it is important to gain a fundamental understanding of the underlying speciation and transport processes that control the leaching of contaminants, as well as the fate of these contaminants in soil and groundwater.

The complexity of speciation in combination with transport processes (referred to as "reactive transport") make that the identification of the major controlling processes responsible for observed leaching phenomena is generally not straightforward. However, hypotheses with respect to possible involved processes can often be translated in (computer) models that simulate these processes. The verification of predictions made by such models against experimental data may lead to either confirmation or rejection of the underlying hypotheses. The latter may result in modification and/or expansion of the model, until the system is sufficiently understood and adequate model predictions are obtained. Used in this way, models form valuable instruments in the scientific process of gaining knowledge, and contribute to the identification of the dominant processes that control the behaviour of contaminants in the situation under study. Since processes on a molecular scale have a general validity, models of that are based on these processes ("mechanistic" models) are more suitable for these purposes and of a wider applicability than an empirical models. Once a model, based on gained fundamental insights in leaching processes, sufficiently describes observed leaching phenomena under a wide range of

conditions, it may be used for different practical purposes. Among these are the quality improvement of (recycled) waste materials with respect to their leaching properties and the development of realistic regulatory limits for the safe application of waste materials in the environment.

The aim of this thesis is to develop a generally applicable, mechanistic geochemical modelling approach with which dynamic leaching and reactive transport processes in "contaminated materials" can be predicted. The term "contaminated materials" ultimately refers to any natural or waste material that may potentially release contaminants by leaching. In this thesis, Municipal Solid Waste Incinerator (MSWI) bottom ash, the major residue that remains from the incineration of municipal solid waste, and contaminated soils are studied as relevant and representative cases of such materials. This thesis focuses on the leaching of inorganic contaminants, although the principles of the approach do also apply to organic contaminants that fall beyond the scope of this work.

The approach consists of a number of successive steps. The first step consists of the identification of the (major) processes that control the leaching of contaminants from the material under study. In this step, geochemical model calculations are performed and compared to experimental data in order to verify hypotheses on the underlying leaching processes. As leached concentrations of elements generally vary by orders of magnitude as a function of pH, data generated by batch pH-static experiments (leaching experiments conducted at constant pH values) over a wide range of pH (e.g., pH 2 to pH 12) provide a sensitive verification of such hypotheses. Depending on the outcome of the verification the model may need to be modified and/or further expanded with additional relevant processes, until the model calculations provide an adequate representation of the measurements. In the next step, the resulting geochemical model is coupled with a model for transport processes. Based on the processes identified in the previous step, the time- dependent leaching of contaminants in dynamic (reactive transport) systems is predicted and verified against experimental data from column experiments. Similar to the previous step, the verification of model predictions may lead to modification and/or further expansion of the reactive transport model.

The general applicability and (long- term) predictive value of models strongly depends on the way the model is parameterized, i.e. with respect to the used

thermodynamic parameters and estimates of material- specific properties/input parameters (e.g., the actual amounts of "reactive surfaces" to which contaminants can bind, such as iron (hydr)oxide minerals and natural organic matter). Therefore, the approach described in this thesis aims for consistency between the hypothesized processes, the selection of (sorption) models to simulate these processes, necessary model input parameters, and experimental methods to determine these parameters. Wherever sorption to a reactive surface is suspected to be an important process, mechanistic sorption models are selected, with a preference for models for which "generic" parameter sets have been derived. The selected models and parameter sets are applied without modification (i.e. without parameter fitting). Whenever sorption models are taken into account, information is needed on the amount of the specific surfaces present in the sample under study. This information is collected using independent, carefully selected experimental procedures that aim to estimate the concentrations of the specific type of reactive surface of interest. Examples of processes that are important for contaminant mobility in soil and waste systems and are treated in the above described way include the adsorption of ions to iron (hydr)oxides and natural organic matter.

The successive steps of the modelling approach as outlined above are reflected in the different chapters. The point of departure is described in **chapter 2**. For the case of weathered MSWI bottom ash, the at that time available knowledge of processes that control the leaching of contaminants in batch systems is used to predict experimental leaching data obtained from (dynamic) column experiments. This evaluation leads to the identification of potentially important processes on the basis of which the modelling approach can be further improved in the forthcoming chapters. The first step was to use batch pH-static leaching data to verify that heavy metal concentrations as a function of pH could be described adequately with a surface complexation model for sorption to hydrous ferric oxide (HFO) and amorphous Al-(hydr)oxides. The next step was to perform reactive transport simulations, which led to predictions of leached heavy metal concentrations generally within one order of magnitude. Non-equilibrium leaching processes were inferred from the generally more abrupt changes of the reactive transport model predictions compared to the measurements. It was concluded that processes that have to be taken into account for

further model development are the influence of non-equilibrium effects and the facilitated transport of heavy metals by dissolved organic matter.

In **chapter 3**, it is investigated to what extent the batch modelling approach followed in the preceding chapter is also applicable to identify and describe the processes that control the pH-dependent leaching of the metals Ni, Cu, Zn, Cd and Pb from contaminated soils. As soils contain relatively high amounts of natural organic matter compared to MSWI bottom ash, the modelling approach used in the preceding chapter is extended with a model for the adsorption of ions to dissolved and particulate organic matter. The approach is also extended with a model for the non-specific sorption to clay surfaces. The resulting model predictions of heavy metal leaching appeared generally adequate, and sometimes excellent. Results from speciation calculations were consistent with the well-recognized importance of organic matter as the dominant reactive solid phase in soils. Further modelling challenges are to include a model for the pH-dependent leaching of DOC from soils as well as to predict soil pH and buffering processes.

In **chapter 4**, the leaching of a wide range of major and trace elements from MSWI bottom ash is studied as a function of equilibration time, over a wide range of pH under pH-controlled conditions. Based on recent insights and assumptions on the composition of dissolved organic carbon (DOC) in MSWI bottom ash leachates, a similar "multi-surface" geochemical modelling approach as developed in the preceding chapter for contaminated soils is used to improve the interpretation of MSWI bottom ash leaching test results and to investigate whether "equilibrium" is attained during the time scale of the batch pH-static leaching experiments. Depending on the element of interest and setpoint-pH value, net concentration increases or decreases as a function of equilibration time were observed up to one order of magnitude. In addition, different concentration-time trends (increase or decrease) are observed in different pH ranges. Although the majority of the elements do not reach steady state, leached concentrations over a wide pH range have been shown to closely approach "equilibrium" model curves within an equilibration time of 168 hours. The major result from this chapter is that the different effects that leaching kinetics may have on the pH dependent leaching patterns have been identified for a wide range of elements, and can generally be explained in a mechanistic way.

Chapter 5 aims to provide a mechanistic insight into the beneficial effects of accelerated aging of MSWI bottom ash using the "multi-surface" geochemical modelling approach developed in the preceding chapters on the leaching of copper and molybdenum. Experimental observations and model calculations in literature and in the previous chapters have shown that the leaching of DOC is likely to be the key process responsible for the generally observed enhanced leaching of copper and possibly other metals. Therefore, a novel experimental method is used to characterize DOC quantitatively in terms of humic, fulvic and hydrophilic acids over a wide pH range in order to identify the processes controlling the solid/liquid partitioning of these reactive ligands and their role in the effects of aging on contaminant leaching. Based on the experimental and model results, a new approach is developed to model the pH-dependent leaching of fulvic acids from MSWI bottom ash. The results of this chapter show that accelerated aging results in enhanced adsorption of FA to (neoformed) iron/aluminium (hydr)oxides, leading to a significant decrease in the leaching of FA and associated Cu. Accelerated aging was also found to reduce the leaching of Mo, which is also attributed to enhanced adsorption to (neoformed) iron/aluminium (hydr)oxides. These findings provide important new insights that may help to improve accelerated aging technology of MSWI bottom ash.

In the final **chapter 6**, the insights and model developments of the preceding chapters are combined into a novel predictive modelling approach in which the leaching of a broad range of major and trace elements from MSWI bottom ash is predicted simultaneously, based on a single set of model input parameters. The approach is applicable to both batch and dynamic systems, as verified experimentally with data from pH-static and dynamic (column) experiments. To address the possible influence of non-equilibrium processes, the column experiments are operated at different flow velocities and with flow interruption periods. The generally adequate agreement between the model predictions and measurements for MSWI bottom ash shows that the use of equilibrium-based reactive transport models to predict data from dynamic laboratory leaching tests is promising. This finding is supported by the generally low sensitivity of leached concentrations to flow velocity and flow interruptions. The experimental and modelling results indicate physical non-equilibrium processes for non-reactive soluble salts and possible sorption-related non-

equilibrium processes for the leaching of molybdenum, FA and associated trace metals.

The reactive transport modelling approach, as presented in the final chapter, leads to strongly improved model predictions and understanding compared to previous reactive transport modelling studies performed on MSWI bottom ash in literature so far. Novel aspects of the modelling approach outlined in this final chapter compared to that of the initial chapter 2 include the characterization of DOC in terms of its reactive components HA and FA as a function of L/S (liquid-to-solid ratio) and pH, the inclusion of mechanistic models that predict the binding of metals to these substances, the inclusion of a surface complexation model that predicts FA concentrations, and the combination of these geochemical models with non-equilibrium processes. Further improvement of the modelling approach can be achieved by a more mechanistic description of the (dynamic) leaching behaviour of humic substances. In addition, this chapter makes clear that further research is necessary to develop a generic approach for the estimation of the "availability" of components in different types of contaminated materials.

It is shown that the consistent geochemical modelling approach as developed in this thesis allows the identification and prediction of contaminant leaching and reactive transport processes from contaminated materials of very different origin and with different physical and chemical characteristics. This is demonstrated with a number of fresh and weathered MSWI bottom ash samples from different Dutch MSW incineration plants (chapters 2, 4, 5 and 6), and soils from various locations with different contamination histories (chapter 3). Although the prospect for a wide applicability is promising, the major challenge for the future is the verification of the approach against data from (long-term) field applications.

Samenvatting

Afvalstoffen bevatten in veel gevallen verhoogde concentraties van potentieel toxische spoorelementen vergeleken met natuurlijke materialen zoals bodems. Daarom is in veel landen het hergebruik van afvalstoffen, bijvoorbeeld als bouwmateriaal, gebonden aan regelgeving die de veiligheid van dergelijke toepassingen op de korte en langere termijn dient te waarborgen. Deze regelgeving is steeds vaker gebaseerd op de potentiële "uitloging"van verontreinigingen, d.w.z. de afgifte van verontreinigingen uit een materiaal naar de waterfase waarmee dat materiaal in contact is (bijvoorbeeld regenwater). De mate waarin verontreinigingen die in een materiaal zitten vatbaar zijn voor uitloogprocessen hangt af van vele chemische en fysische factoren, zoals de specifieke chemische vorm van de verontreiniging (aangeduid met de term "speciatie") en transportprocessen zoals convectie en diffusie.

Om de milieurisico's die samenhangen met het hergebruik van afvalstoffen beter te begrijpen, is het belangrijk dat er fundamentele kennis wordt vergaard op het gebied van de onderliggende speciatie en transportprocessen die de uitloging van verontreinigingen controleren, alswel van het verdere gedrag van uitgeloogde verontreinigingen in bodem en grondwater.

De complexiteit van speciatie in combinatie met transportprocessen (aangeduid met de term "reactief transport") zorgt er voor dat het identificeren van de belangrijkste processen die de uitloging veroorzaken in het algemeen niet eenvoudig is. Echter, hypothesen met betrekking tot de mogelijke processen die een rol spelen, kunnen vaak worden vertaald naar (computer)modellen die de betreffende processen kunnen simuleren. Verificatie van de modelvoorspellingen met behulp van meetgegevens kan leiden tot bevestiging of verwerping van de onderliggende hypothesen. Dit laatste kan leiden tot aanpassing en/of uitbreiding van het model, totdat het systeem voldoende wordt begrepen en goede modelvoorspellingen worden verkregen. Wanneer modellen op deze manier worden gebruikt vormen zij waardevolle instrumenten in het wetenschappelijke proces van kennisontwikkeling, en dragen zij bij aan het identificeren van de dominante processen die de uitloging controleren in specifieke situaties. Omdat processen op moleculaire schaal algemeen geldend zijn, zijn modellen die daarop zijn gebaseerd ("mechanistische" modellen)

geschikter voor de boven beschreven doelen en hebben een breder toepassingsbereik dan empirische modellen. Wanneer een model, gebaseerd op fundamentele inzichten in processen, eenmaal de waargenomen uitloging over een breed bereik van omstandigheden goed kan verklaren, dan kan het worden gebruikt voor diverse praktische doeleinden. Dit varieert van kwaliteitsverbetering van (hergebruikte) afvalstoffen met betrekking tot de uitloogeigenschappen, tot het ontwikkelen van realistische regelgeving voor het veilige hergebruik van afvalstoffen in het milieu.

Het doel van dit proefschrift is om een algemeen toepasbare, "mechanistische" geochemische modelbenadering te ontwikkelen, waarmee dynamische uitloog- en transportprocessen kunnen worden voorspeld in "verontreinigde materialen". Onder de term "verontreinigde materialen" wordt in dit verband elk natuurlijk of afvalmateriaal verstaan waaruit potentieel verontreinigingen uit kunnen logen. In dit proefschrift worden twee relevante en representatieve voorbeelden van dergelijke materialen bestudeerd, te weten Afval Verbrandings Installatie (AVI) bodemas, het belangrijkste residu dat achterblijft bij de verbranding van huisvuil, en verontreinigde bodems. Dit proefschrift spitst zich toe op anorganische verontreinigingen, hoewel de principes van de benadering ook toepasbaar zijn op organische verontreinigingen, hetgeen buiten de scope van dit onderzoek valt.

De benadering bestaat uit een aantal opeenvolgende stappen. De eerste stap bestaat uit het identificeren van de (belangrijkste) processen die de uitloging van verontreinigingen controleren uit het betreffende materiaal dat wordt onderzocht. In deze stap worden geochemische modelberekeningen uitgevoerd en vergeleken met meetgegevens om hypothesen te verifiëren met betrekking tot de onderliggende uitloogprocessen. Omdat uitgeloogde concentraties van verontreinigingen orden van grootte kunnen variëren als functie van de zuurgraad (pH), vormen meetgegevens van pH-stat proeven (proeven waarbij de pH constant wordt gehouden) over een breed pH traject (bijvoorbeeld pH 2 – pH 12) een gevoelige verificatie van deze hypothesen. Afhankelijk van de uitkomst van deze verificatiestap behoeft het model aanpassing of uitbreiding, totdat de modelberekeningen de metingen goed kunnen beschrijven. In de volgende stap wordt het resulterende model gekoppeld met een model voor transportprocessen. Gebaseerd op de geïdentificeerde uitloogprocessen uit de vorige stap worden vervolgens voorspellingen gedaan over de uitloging van verontreinigingen in een (dynamisch) reactief transport systeem. De resultaten van de

modelberekeningen worden getoetst aan meetgegevens gegenereerd met kolomproeven. Evenals in de vorige stap kan deze verificatie leiden tot aanpassing of uitbreiding van het reactief transportmodel.

De algemene toepasbaarheid en (lange termijn) voorspellende waarde van modellen hangt sterk af van de wijze waarop het model wordt geparameteriseerd, in het bijzonder met betrekking tot de gekozen (thermodynamische) parameters en schattingen voor materiaalspecifieke eigenschappen (bijvoorbeeld de gehalten aan "reactieve oppervlakken" waar verontreinigingen aan kunnen binden, zoals ijzer(hydr)oxide mineralen en natuurlijke organische stof). De benadering die in dit proefschrift wordt beschreven streeft daarom naar consistentie tussen de veronderstelde processen die de uitloging controleren, de selectie van mechanistische modellen die deze processen simuleren, benodigde input- parameters voor deze modellen en experimentele procedures om waarden voor deze input- parameters te schatten. Wanneer sorptie van verontreinigingen aan een bepaald type reactief oppervlak belangrijk wordt verondersteld, wordt voor dit proces een mechanistisch model geselecteerd, met een voorkeur voor modellen waarvoor "generieke" parametersets zijn afgeleid. De geselecteerde modellen en parameter sets worden in dit proefschrift zonder aanpassingen gebruikt (d.w.z. zonder "fitten" van parameters). Wanneer sorptiemodellen worden gebruikt, is er informatie nodig over de hoeveelheid van het specifieke type reactieve oppervlak in het monster dat wordt onderzocht. Dit type informatie wordt verzameld met zorgvuldig geselecteerde experimentele procedures die tot doel hebben de concentraties van specifieke typen reactieve oppervlakken te schatten. Voorbeelden van processen die belangrijk zijn voor de mobiliteit van verontreinigingen in bodem- en afvalstoffenmilieus en op de boven beschreven wijze worden behandeld zijn o.a. de adsorptie van verontreinigingen aan ijzer (hydr)oxiden en natuurlijke organische stof.

De opeenvolgende stappen van de modelbenadering worden weerspiegeld in de verschillende hoofdstukken. Het vertrekpunt wordt beschreven in **hoofdstuk 2**. Voor verweerde (verouderde) AVI- bodemas wordt de tot dan toe beschikbare kennis over uitloogprocessen van verontreinigingen in batch systemen gebruikt voor het voorspellen van uitlooggegevens die verzameld zijn met kolomexperimenten. Deze evaluatie leidt tot de identificatie van processen op basis waarvan de modelbenadering kan worden aangepast of uitgebreid in de hiernavolgende hoofdstukken. De eerste

stap daarbij was het gebruik van pH-afhankelijke uitlooggegevens om te toetsen in hoeverre concentraties van zware metalen als functie van pH kunnen worden beschreven op basis van een model gebaseerd op surface complexatie aan ijzer- en aluminium (hydr)oxiden. De volgende stap bestond uit het uitvoeren van reactief transportberekeningen, hetgeen leidde tot voorspellingen van gemeten concentraties van zware metalen binnen een nauwkeurigheid van ongeveer een orde van grootte. Niet-evenwichtsprocessen werden verantwoordelijk geacht voor de in het algemeen abruptere veranderingen van de voorspelde concentraties, vergeleken met de geleidelijker veranderingen van de gemeten concentraties. Er werd geconcludeerd dat de invloed van niet-evenwichtsprocessen en het gefaciliteerde transport van zware metalen door complexatie met opgeloste organische stof processen zijn waarmee rekening gehouden dient te worden voor verdere modelontwikkeling.

In **hoofdstuk 3** wordt onderzocht in hoeverre de modelbenadering die in het voorgaande hoofdstuk is gebruikt, ook toepasbaar is voor het identificeren en beschrijven van de processen die de pH-afhankelijke uitloging controleren van de metalen Ni, Cu, Zn, Cd en Pb uit verontreinigde bodems. Omdat bodems relatief hoge concentraties natuurlijke organische stof bevatten vergeleken met AVI-bodemas, is de modelbenadering uit het vorige hoofdstuk uitgebreid met een model voor de adsorptie van ionen aan vaste en opgeloste organische stof. Het model is tevens uitgebreid met een model voor de niet-specifieke adsorptie aan kleioppervlakken. De resulterende modelberekeningen bleken in het algemeen een goede tot zeer goede voorspellingen te leiden. De resultaten van de speciatieberekeningen bleken consistent te zijn met de algemeen geaccepteerde opvatting dat organische stof de dominante reactieve fase is voor zware metalen in bodems. Verdere modelontwikkeling is nodig om de pH- afhankelijke uitloging van DOC te kunnen voorspellen, alsmede de bodem-pH en bufferprocessen.

In **hoofdstuk 4** wordt de uitloging van een breed pakket van hoofd- en spoorelementen uit AVI- bodemas bestudeerd als functie van evenwichtstijd, over een breed pH-traject door middel van pH-stat proeven. Gebaseerd op recente inzichten en aannames over de samenstelling van opgeloste organische stof in AVI- bodemas uitloogoplossingen, wordt dezelfde modelbenadering toegepast als gebruikt in het voorgaande hoofdstuk voor verontreinigde bodems. Dit hoofdstuk heeft tot doel om de interpretatie van uitloogtesten voor AVI- bodemas te verbeteren, en om te

onderzoeken of een toestand van "evenwicht" wordt bereikt gedurende op een tijdschaal typisch voor laboratorium (uitloog-)proeven. Afhankelijk van het element en de opgelegde pH waarde in de pH-stat proeven, werden netto toenames of afnames van de concentraties als functie van de tijd tot een orde van grootte waargenomen op een tijdschaal van 168 uur. Bovendien werden verschillende concentratie-tijd trends waargenomen in verschillende pH-trajecten (toe- of afnames). Hoewel de meerderheid van de elementen geen steady state bereikten, bleken uitgeloogde concentraties over een breed pH-traject de modelcurven (berekend op basis van chemisch evenwicht) dicht te benaderen binnen de onderzochte evenwichtstijd (168 uur). Het belangrijkste resultaat van dit hoofdstuk is dat de verschillende effecten die uitloog- kinetiek kan hebben op de pH-afhankelijke uitloogcurven voor een brede range van elementen zijn geïdentificeerd; bovendien kunnen deze effecten in veel gevallen op mechanistische wijze worden verklaard.

Hoofdstuk 5 heeft tot doel om procesmatig inzicht te verschaffen in de gunstige effecten die kunstmatige verwering (veroudering) van AVI- bodemas heeft op de uitloging van koper en molybdeen, door middel van de modelbenadering zoals die is ontwikkeld in de voorgaande hoofdstukken. Experimenteel en modelmatig is in de voorgaande hoofdstukken en in de literatuur aangetoond dat opgeloste organische stof (DOC, dissolved organic carbon) waarschijnlijk het belangrijkste proces is dat de verhoogde uitloging van koper en mogelijk andere metalen veroorzaakt. In dit hoofdstuk is een nieuwe methodiek gebruikt om DOC kwantitatief te karakteriseren in termen van humus- fulvo- en hydrofiele zuren over een breed pH- traject, met als doel om de processen te identificeren die de oplosbaarheid van deze reactieve liganden veroorzaken en de rol te onderzoeken die zij hebben bij de effecten van kunstmatige veroudering. Daartoe wordt ondermeer een nieuwe benadering ontwikkeld en toegepast om de pH-afhankelijke uitloging van fulvozuren te beschrijven. De resultaten van dit hoofdstuk laten zien dat kunstmatige veroudering leidt tot een verhoogde binding van fulvozuren aan (nieuw gevormde) ijzer- en aluminium (hydr)oxiden in de vaste matrix van de AVI-bodemas. De versterkte binding van fulvozuur aan de vaste matrix leidt vervolgens tot een lagere uitloging van het koper dat aan de fulvozuren is gebonden. Kunstmatige veroudering leidt ook tot een verlaagde uitloging van molybdeen, hetgeen eveneens wordt toegeschreven aan toegenomen adsorptie aan ijzer- en aluminium (hydr)oxiden. Deze bevindingen

verschaffen belangrijke inzichten voor het verder ontwikkelen van de technologie voor kwaliteitsverbetering van AVI-bodemas door kunstmatige veroudering.

In het laatste hoofdstuk, **hoofdstuk 6**, worden de modelontwikkelingen en inzichten uit de voorgaande hoofdstukken gecombineerd tot een nieuwe modelbenadering waarmee de uitloging van een breed pakket van hoofd- en spoorelementen uit bodemas tegelijk kan worden voorspeld, gebaseerd op een enkele set van (onafhankelijk bepaalde) input parameters. De benadering is toepasbaar op zowel batch- als transportsystemen, hetgeen blijkt uit verificatie van de modelbenadering met meetgegevens uit pH-stat en kolomproeven. Om eventuele invloeden van niet-evenwichtsprocessen te detecteren zijn de kolomproeven uitgevoerd bij verschillende snelheden en met flow-interrupties. De over het algemeen goede overeenkomst tussen modelresultaten en metingen voor AVI-bodemas laat zien dat het gebruik van modellen die op chemisch evenwicht zijn gebaseerd veel perspectief biedt. Deze bevinding wordt ondersteund door de relatieve ongevoeligheid van de gemeten uitgeloogde concentraties van veel elementen voor de stroomsnelheid en de flow-interrupties. De waarnemingen duiden voorts op de invloed van fysische niet-evenwichtsprocessen op het uitloogpatroon van niet-reactieve zouten. Daarnaast zijn er aanwijzingen voor mogelijk sorptie-gerelateerd niet-evenwicht voor molybdeen, fulvozuren en de daar aan gebonden metalen.

De modelbenadering zoals die in het laatste hoofdstuk is gepresenteerd leidt tot een sterk verbeterde beschrijving en verdergaande inzichten in vergelijking met eerdere reactief-transportstudies die zijn uitgevoerd voor AVI-bodemas. Nieuwe aspecten van de modelbenadering zoals die in het laatste hoofdstuk is gepresenteerd in vergelijking met het eerste hoofdstuk (hoofdstuk 2) zijn onder andere de karakterisering van DOC in termen van de reactieve fracties (humus- en fulvozuren) als functie van pH en L/S (vloeistof- vaste stof verhouding), het gebruik van mechanistische modellen die de binding van metalen aan deze fracties kan beschrijven, het ontwikkelen en gebruik van een surface- complexatiemodel waarmee de uitloging van fulvozuren kan worden beschreven, en het combineren van deze modellen met niet-evenwichtsprocessen. Verdere ontwikkeling en verbetering van de modelbenadering kan worden bereikt door de (dynamische) uitloging van humus- en fulvozuren te beschrijven op een meer mechanistische wijze dan in hoofdstuk 6 is gedaan. Bovendien blijkt uit het laatste hoofdstuk dat er meer onderzoek nodig is naar

een algemeen toepasbare methode om de "beschikbaarheid" van componenten in verschillende (verontreinigde) materialen te schatten.

De in dit proefschrift ontwikkelde modelbenadering is toepasbaar gebleken voor het identificeren en voorspellen van uitloog- en transportprocessen in zeer verschillende verontreinigde materialen, onder andere verse en verouderde AVI-bodemas monsters afkomstig uit verschillende Afval Verbrandings Installaties (AVI's) (hoofdstuk 2, 4, 5 en 6) en bodems van verschillende Nederlandse locaties met verschillende verontreinigingsgraad en –historie (hoofdstuk 3). Hoewel er een goed perspectief is op een brede toepasbaarheid, vormt de toepassing van de benadering op veldsituaties en verificatie door middel van (lange termijn) meetgegevens in het veld de belangrijkste uitdaging voor de toekomst.

Dankwoord

Veel mensen hebben op de één of andere manier bijgedragen aan de totstandkoming van dit proefschrift. Graag wil ik hier van de gelegenheid gebruik maken om een aantal mensen in het bijzonder te bedanken.

Om te beginnen mijn beide promotoren. Rob, in de eerste plaats wil ik mijn dank uitspreken voor het verzorgen van de middelen en de mogelijkheid om te gaan èn te blijven promoveren. Ik heb de vrijheid waarbinnen ik mijn onderzoek heb mogen invullen en uitvoeren als heel leerzaam en plezierig ervaren. Daarnaast heb ik veel waardering voor de constructieve en uiterst nauwgezette wijze waarop je mijn manuscripten van commentaar hebt voorzien. Natuurlijk dient ook de immer gezellige sfeer niet onvermeld te blijven waarin we soms vele uren cq. dagen hebben besteed aan het uitwerken van (ogenschijnlijke!) details in manuscripten; een soort gezamenlijke hobby die ook zeker lonend is gebleken! Willem, bij dezen wil ik je graag bedanken voor het vertrouwen dat je in me stelde toen je me tijdens mijn afstudeerperiode in contact bracht met mijn huidige werkgever. Ik herinner me nog goed dat je me bij mijn buluitreiking blij verraste met de mededeling dat ik als promovendus was aangenomen bij ECN. Tussendoor hebben we elkaar zo nu en dan gesproken en dat was altijd plezierig en inspirerend.

Hans (van der Sloot), van jou heb ik geleerd om de verbanden te zien tussen het uitlooggedrag van ogenschijnlijk zeer verschillende materialen. Ik vind het bewonderenswaardig hoe je meestal direct een concrete toepassing ziet voor "verse" onderzoeksresultaten. Bovendien is het een eer dat je die resultaten in (bijna) alle uithoeken van de wereld onder de aandacht brengt. Bedankt ook voor het immer snelle en tegelijk kritisch lezen van mijn manuscripten, dit ondanks je drukke bezigheden.

Hans (Meeussen), sinds we alweer enige jaren geleden collega's zijn geworden heb je een belangrijke invloed gehad op mijn promotieonderzoek door mij vertrouwd te maken met Orchestra, een instrument waarmee de mogelijkheden om complexe systemen te modelleren mijns inziens een heel stuk zijn vergroot. Dank voor je hulp bij het opzetten van allerlei, soms zeer lastige, (transport)berekeningen en je nuchtere en kritische blik op mijn manuscripten.

(Ex-) kamer- en lotgenoten André en Wouter: knap dat jullie altijd je geduld hebben kunnen bewaren tijdens het aanhoren van mijn (zinnige danwel onzinnige) gedachtespinsels! Het scheelt enorm als je vrijuit met elkaar van gedachten kunt wisselen over je onderzoek, het gebruikelijke promotieleed samen kunt relativeren of gebruik kunt maken van elkaars kennis. Voor mij zijn er daarom geen geschiktere paranimfen denkbaar dan jullie.

Dirk, Esther, Petra en Remco: jullie ben ik veel dank verschuldigd voor het uitvoeren van veruit het grootste deel van de proeven. Petje af voor de nauwkeurigheid daarbij, want zelf ben ik, zoals jullie misschien wel weten, niet overdreven ruim bedeeld met de voor experimenteel werk benodigde motorische en organisatorische kwaliteiten. Ook wil ik iedereen van de chemisch-analytische groep bedanken voor het uitvoeren van de analyses met grote nauwkeurigheid en precisie.

Huidige en ex- collega's Anette, Arjan, Chanelle, Daniëlle, Gerard, Gerlinde, Hein, Jantine, Patrick, Paul, René: de gezelligheid en de vele grappen en grollen geven het wetenschappelijke gebeuren veel meer kleur dan de buitenwacht doorgaans vermoedt!

Mamma, helaas voor jou ben ik je niet opgevolgd in de muziek, hoewel de term "Orchestra" die zo vaak in dit boekje voorkomt anders doet vermoeden. Dank voor de vele oppasdagen, waardoor ik in de gelegenheid was om aan dit boekje te werken. Het doet me veel verdriet dat Pappa het moment waar hij zo naar uitkeek niet meer heeft mogen meemaken. Wat zou hij trots geweest zijn.

Myn leaf Lyske, mijn gepromoveer heeft veel langer geduurd dan je lief was. Desondanks was dit proefschrift zonder jouw voortdurende aanmoediging, planning en praktische hulp nog lang niet af geweest, en misschien zelfs niet af gekomen. Lieuwe en Jitske, jullie komst was voor mij de drijfveer om het proefschrift eindelijk te gaan afronden. Samen met jullie broertje(s) en/of zusje(s) die op komst zijn gaan we de komende tijd volop van het leven genieten!

Joris
Alkmaar, maart 2007

CASTING AND GATHERING

Years and years ago, these sounds took sides:

On the left bank, a green silk tapered cast
Went whispering through the air, saying *hush*
And *lush*, entirely free, no matter whether
It swished above the hayfield or the river.

On the right bank, like a speeded-up corncrake,
A sharp ratcheting went on and on
Cutting across the stillness as another
Fisherman gathered line-lengths off his reel.

I am still standing there, awake and dreamy,
I have grown older and I can see them both
Moving their arms and rods, working away,
Each one absorbed, proofed by the sounds he 's making.

One sound is saying, "You are not worth tuppence,
But neither is anybody. Watch it! Be severe."
The other says, "Go with it! Give and swerve.
You are everything you feel beside the river."

I love hushed air. I trust contrariness.
Years and years go past and I do not move
For I see that when one man casts, the other gathers
And then *vice versa*, without changing sides.

SEAMUS HEANY
("Seeing things", 1991)

Curriculum vitae

Joris Jasper Dijkstra werd op 2 juli 1973 geboren te Leeuwarden. Na het behalen van zijn HAVO diploma in 1991 (Slauerhoff College, Leeuwarden) ging hij de HBO opleiding Milieukunde volgen aan het Van Hall Instituut, destijds gevestigd te Groningen. In 1993/1994 liep hij stage bij de Provincie Fryslân, bureau bodemsanering, waar hij een aanvullend programma van eisen heeft opgesteld voor oriënterend bodemonderzoek op voormalige bedrijfsterreinen. Vervolgens werd in 1994 een stage uitgevoerd aan de Universiteit van Udine (Italië), waar hij heeft meegewerkt aan micrometeorologisch onderzoek naar de droge depositie van gassen boven met landbouwgewassen begroeide oppervlakken. Zijn afstudeerproject heeft hij uitgevoerd aan Rice University (Houston, Texas, VS) in 1995. Hier verrichtte hij onderzoek naar de opname en afbraak van het explosief TNT door de waterhyacint (*Eichhornia crassipes*). Na zijn afstuderen zette hij zijn studie voort aan Wageningen Universiteit in de richting Bodem, Water en Atmosfeer. Hij studeerde in 1998 af als bodemkundige, met specialisatie bodemscheikunde. Voor zijn afstudeerproject deed hij onderzoek naar de adsorptie van zwakke organische zuren en sulfaat aan het ijzermineraal goethiet. In maart 1998 werd hij aangesteld als promovendus bij de groep Risicobeoordeling Milieuverontreiniging van het Energieonderzoek Centrum Nederland (ECN) te Petten. In mei 2001 volgde een aanstelling voor onbepaalde tijd als wetenschappelijk medewerker. Hij is getrouwd met Lydia van Mourik en samen hebben zij twee kinderen, Lieuwe (2003) en Jitske (2005).

Publications in international journals

Dijkstra, J. J., van Zomeren, A., Meeussen, J. C. L. & Comans, R. N. J. 2006. Effect of accelerated aging of MSWI bottom ash on the leaching mechanisms of copper and molybdenum. *Environmental Science and Technology*, 40, 4481-4487.

Astrup, T., Dijkstra, J. J., Comans, R. N. J., van der Sloot, H. A. & Christensen, T. H. 2006. Geochemical modeling of leaching from MSWI air pollution control residues. *Environmental Science and Technology*, 40, 3551-3557.

Dijkstra, J. J., van der Sloot, H. A. & Comans, R. N. J. 2006. The leaching of major and trace elements from MSWI bottom ash as a function of pH and time. *Applied geochemistry*, 21, 335-351.

Dijkstra, J. J., Meeussen, J. C. L. & Comans, R. N. J. 2004. Leaching of heavy metals from contaminated soils: an experimental and modeling study. *Environmental Science and Technology*, 38, 4390-4395.

Dijkstra, J. J., van der Sloot, H. A. & Comans, R. N. J. 2002. Process identification and model development of contaminant transport in MSWI bottom ash. *Waste Management*, 22, 531-541.

Dijkstra, J. J., Meeussen, J. C. L., Van der Sloot, H. A., & Comans, R. N. J., 2007. A consistent geochemical modelling approach for the leaching and reactive transport of major and trace elements in MSWI bottom ash. Submitted to *Applied Geochemistry*.

Schipper, P. N. M., Comans, R. N. J., Dijkstra, J. J. & Vergouwen, L. 2007. Runoff and windblown vehicle spray from road surfaces: risks and measures for soil and water. *Water Science and Technology*, in press.

Selected other publications and reports

Eikelboom, R. T., Van der Sloot, H. A. & Dijkstra, J. J. 2004. Horizontale meetmethoden voor uitloging van bouwmaterialen naar grond- en oppervlaktewater. *H₂O*, 25/26, 35-38.

Schipper, P. N. M., Dijkstra, J. J., Teunissen, R. J. M. & Comans, R. N. J. 2003. Hoe bevorder je het kwalitatieve functioneren van een wadi? *Bodem*, 5, 176-179.

Verschoor, A. J., Lijzen, J. P. A., van den Broek, H. H., Cleven, R. F. M. J., Comans, R. N. J., Dijkstra, J. J., and Vermij, P. 2006. Kritische emissiewaarden voor bouwstoffen; Milieuhygiënische onderbouwing en consequenties voor bouwmaterialen. RIVM rapport 711701043/2006.

Dijkstra, J. J., Van der Sloot, H. A., Spanka, G., and Thielen, G. 2005. How to judge release of dangerous substances from construction products to soil and groundwater? ECN-C-05-045.

Steketee, J. J., Dijkstra, J. J., and Van der Sloot, H. A. 2005. Optimalisatie en normalisatie zuurstofloze kolomproef. TAUW Rapportnummer R001-4342757JJS-SKB-VO2-NL.

Dijkstra, J. J., De Nie, D., and Van der Sloot, H. A. 2005. Nut en noodzaak van acceptatiecriteria voor kobalt, tin, vanadium, broom, wolfraam en cyanide (vrij en totaal) als onderscheidend acceptatiecriterium op stortplaatsen. ECN-C--05-027.

Van der Sloot, H. A. and Dijkstra, J. J. 2004. Development of horizontally standardized leaching tests for construction materials: a material based or released based approach? ECN-C-04-060.

Comans, R. N. J. and Dijkstra, J. J. 2004. Geochemisch onderzoek naar de kwaliteitsverbetering van AVI-bodemas door kunstmatige veroudering in een pilotproef. ECN-CX-04-129.

Steketee, J. J., Nijboer, M. H., Takens, R. C., Dijkstra, J. J., and Comans, R. N. J. 2003. Beslissingsondersteundend systeem vastlegging van zware metalen in de verzadigde zone van de bodem. TAUW Rapportnummer R003-3897036JJS-C03-D.

Dijkstra, J. J. and Comans, R. N. J. 2003. Ontwikkeling van de vastleggingsindicator en de stabiliteitsindicator. ECN-C-03-04.

Van der Sloot, H. A., Rietra, R. P. J. J., Dijkstra, J. J., and Hoede, D. 2001. Evaluation of the chromium speciation in Israeli coal fly ashes. ECN-C--01-094. Energy Research centre of the Netherlands, Petten, The Netherlands.

Schipper, P. N. M. and Dijkstra, J. J. 2001. Kwaliteitsaspecten bij infiltratie van hemelwater: richtlijnen bovengrondse infiltratievoorzieningen op basis van geochemisch onderzoek. Grontmij 13/99025242/PS.

Schipper, P. N. M., Dijkstra, J. J., and Comans, R. N. J. 2001. Geochemisch onderzoek sandwichconstructie; een fysisch-chemische benadering naast het bouwstoffenbesluit. Grontmij 13/99015267-2.

Selected presentations and conference contributions

Dijkstra, J. J., Meeussen, J. C. L., van der Sloot, H. A., and Comans, R. N. J. Local equilibrium makes column test protocol TS14405 suitable for model predictions. In: Illic, M, Goumans, J. J. J. M., Miletic, S., Heynen, J. J. M., and Senden, G. J. (Eds.), WASCON 2006 Conference proceedings, pp. 345-348, Belgrade, Serbia & Montenegro, 2006.

Van der Sloot, H. A., van Zomeren, A., Dijkstra, J. J., Meeussen, J. C. L., Comans, R. N. J., and Scharff, H. Prediction of the leaching behaviour of waste mixtures by chemical speciation modelling based on a limited set of key parameters. Tenth International waste management and landfill symposium, Sardinia, Italy, 3-7 October, 2005 (ECN-RX-05-166).

Comans, R. N. J. and Dijkstra, J. J. Leaching of contaminants from natural and waste materials: approach and applications. International workshop on water movement and reactive transport modeling in roads. University of New Hampshire, Recycled Materials Resource Center, Portsmouth, New Hampshire (USA), February 21-24, 2004.

Dijkstra, J. J., Meeussen, J. C. L., van der Sloot, H. A., and Comans, R. N. J. Modelling speciation and transport in MSWI bottom ash. In: Ortiz de Urbina, G. and Goumans, J. J. J. M. (Eds) WASCON 2003 Conference proceedings, pp. 667-672, San Sebastian, Spain, 2003.

Comans, R. N. J., Dijkstra, J. J., and Meeussen, J. C. L. Geochemical modelling of contaminant leaching, mobility and fixation in soil: approach and applications. In: Ortiz de Urbina, G. and Goumans, J. J. J. M. (Eds). WASCON 2003 Conference proceedings, pp. 673-677, San Sebastian, Spain, 2003.

Van der Sloot, H. A., Seignette, P., Comans, R. N. J., van Zomeren, A., Dijkstra, J. J., Meeussen, J. C. L., Kosson, D. S., and Hjelmar, O. Evaluation of environmental aspects of alternative materials using an integrated approach assisted by a database/expert system. Advances in Waste Management and Recycling, Dundee, Scotland, 9-11 September, 2003 (ECN-RX-03-031).

Dijkstra, J. J. and Comans, R. N. J. Development of an easy-to-use tool for groundwater risk assessment: an application of geochemical modelling. In: Halm, D. and Grathwohl, P. (Eds). Proceedings of the 2nd international workshop on Groundwater Risk Assessment at COntaminated Sites (GRACOS), Tübingen, Germany, 2003. Tübinger Geowissenschaftliche Arbeiten [C69], pp. 169-172, University of Tübingen, 2003.

Dijkstra, J. J. and Comans, R. N. J. Reactive Transport Modelling of Contaminants in MSWI Bottom Ash and Contaminated Soils. In: Halm, D. and Grathwohl, P. (Eds). Proceedings of the 1st international workshop on Groundwater Risk Assessment at COntaminated Sites (GRACOS), Tübingen, Germany, 2002. Tübinger Geowissenschaftliche Arbeiten [C61], pp. 32-36, University of Tübingen, 2002.

Dijkstra, J. J., and Comans, R. N. J. Process identification and model development of contaminant transport in MSWI bottom ash. WASCON 2000, Harrogate, United Kingdom, 2000.

Cover: Close-up (distance 1 m) of a soil surface that has been heated and altered by geothermal processes: an "intermediate" between soils and MSWI bottom ash? Photo taken near Hveragerdi, Iceland (JD).